# Current status of the space weather study using the GMDN

K. Munakata (Shinshu University)

SHINSHU UNIVERSITY

## On behalf of the Global Muon Detector Network (GMDN) collaboration

**Results obtained by using the GMDN is reviewed in our recent paper…**
**Rockenbach+ Space Sci. Rev., 182, 2014**

**40-years data from a single MD at Nagoya are analyzed in…**
**Munakata+ ApJ, 791, 2014**

# Ground-based detectors

## use atmosphere as an active component

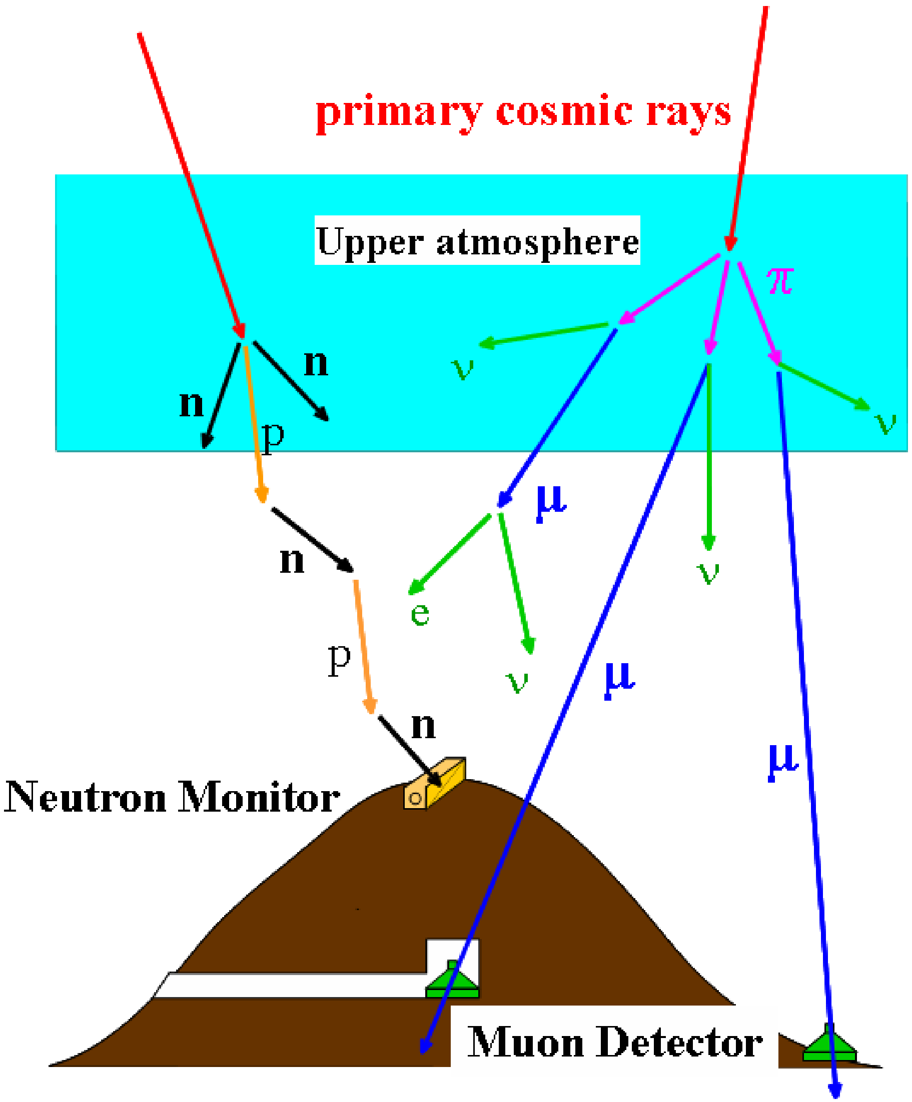


- Two types of observation:
  - **Neutron Monitors**
    Typical energy of primary:
    **~10 GeV** for (Galactic) CRs
  - **Muon Detectors**
    Typical energy of primary:
    **~50 GeV** for (Galactic) CRs
    (surface muon detector)
- Because of a large forward momentum transfer in the high energy interaction, incident direction of muons well preserves the incident direction of primary CRs.
- This makes multi-directional observation of primary CRs possible even with a single detector.

# Muon detector (multi-directional)

## Nagoya, São Martinho, Hobart

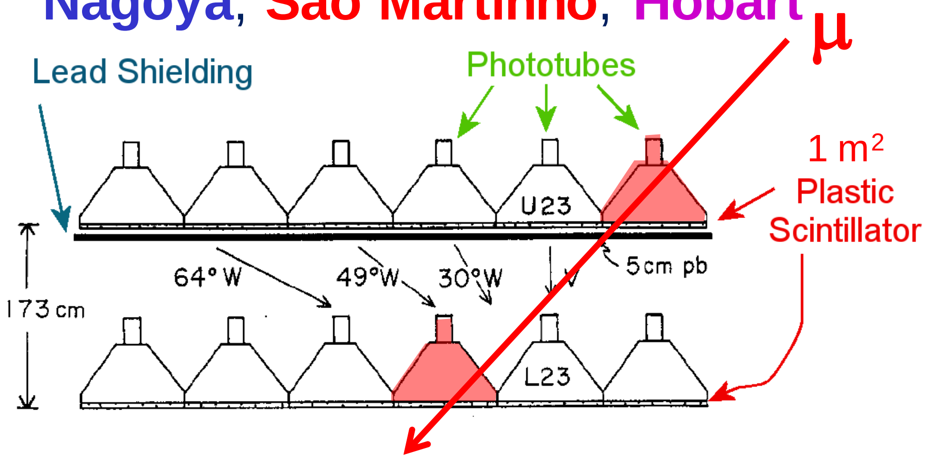


## Kuwait

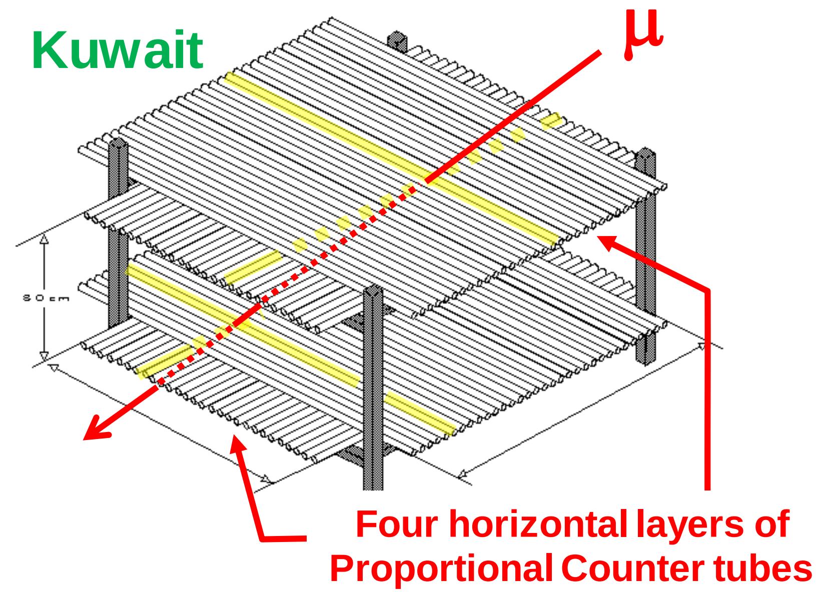


## 2D significance map

**of % deviation from 24h trailing average**

(1 hour data of 09:30UT 12/14 2006)

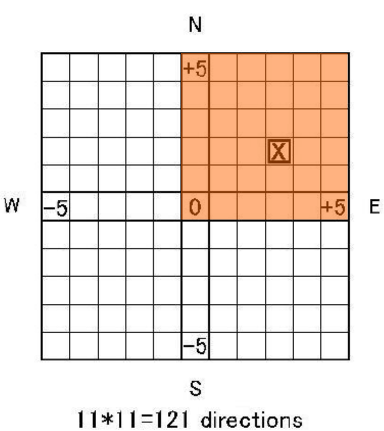


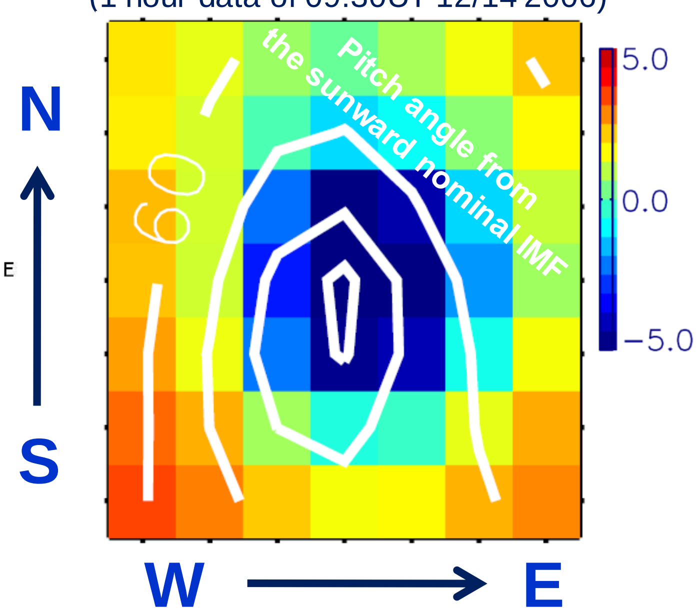


- **Incident direction identified by the combination between upper & lower detectors.**
- **60 conventional combinations in GMDN for analyzing global anisotropy.**
- **2D singnificance maps for observing the local anisotropy like "loss-cone".**

...n Detect...

...artol.udel.edu/spacew...
...shu-u.ac.jp/crest/ ...f...

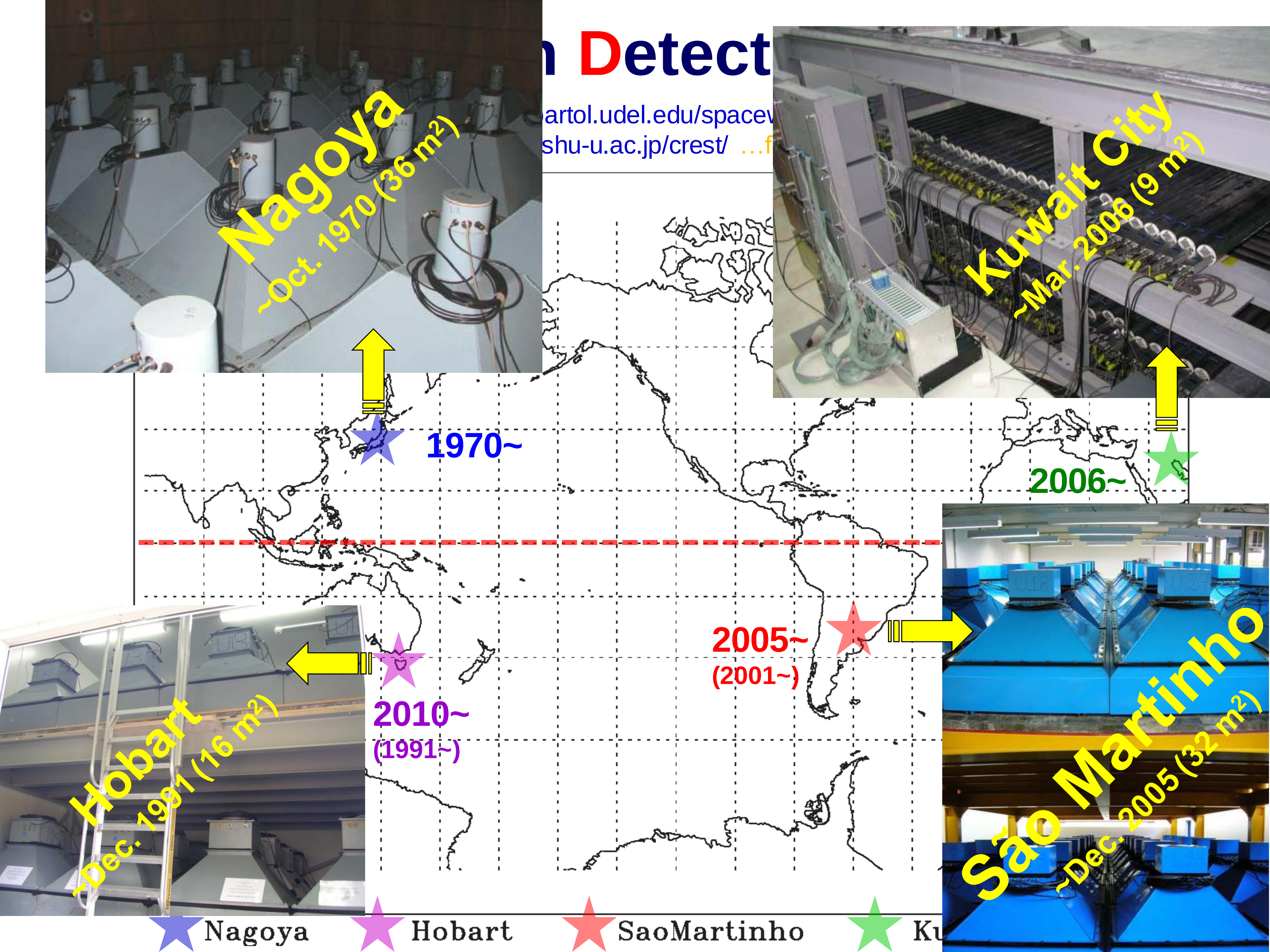

# Asymptotic viewing directions of GMDN

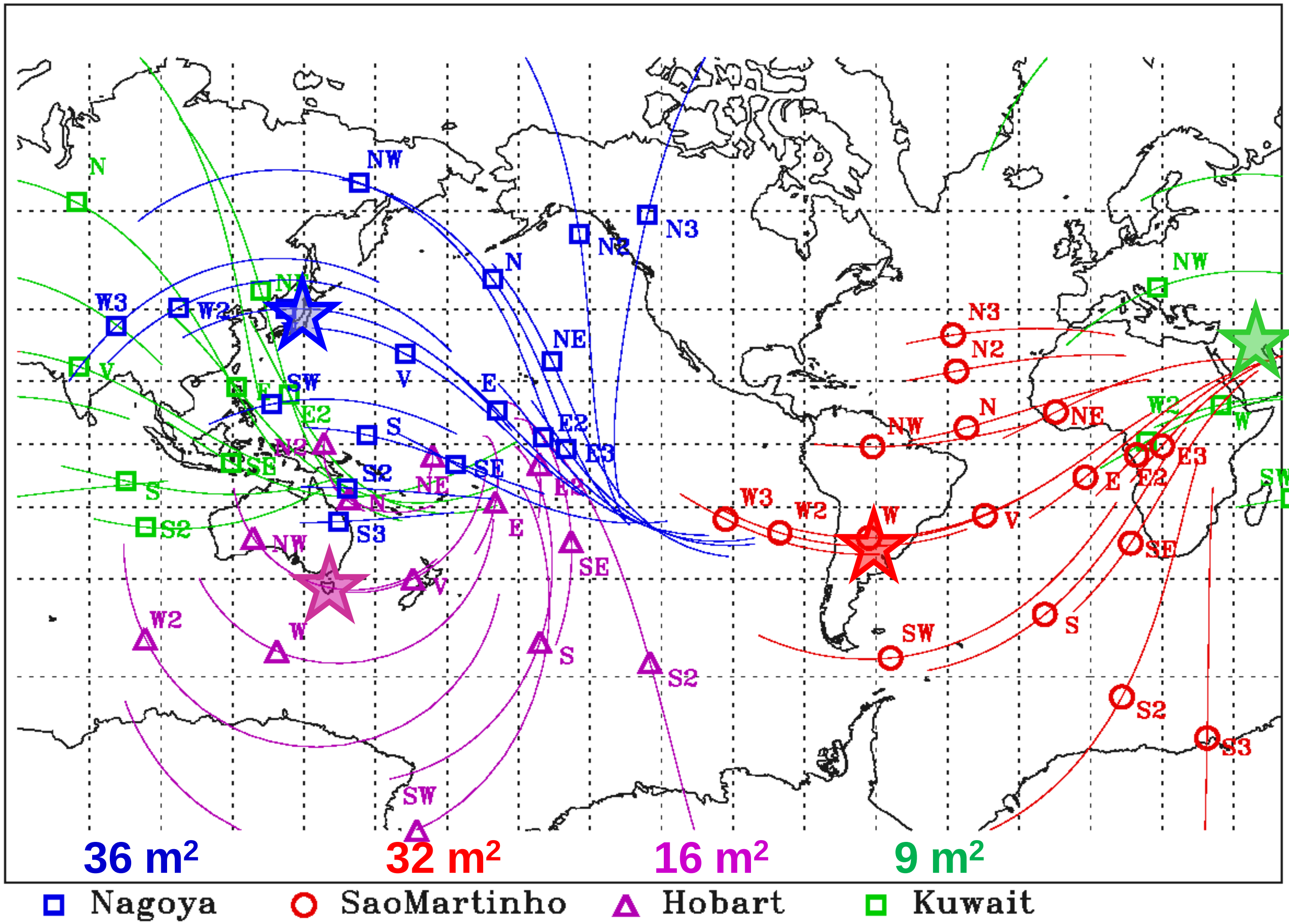


- ☆ indicates the location of the detector.
- ○□△ display the asymptotic viewing directions of median energy CRs corrected for the geomagnetic bending.
- Thin lines indicate the spread of viewing direction for the central 80 % of the energy response to primary CRs.

GMDN is described in Okazaki+ ApJ, 682, 693, 2008

# CR transport equation

$$U(\mathbf{r},p,t)dp = 4\pi p^2 f_0(\mathbf{r},p,t)dp$$

**: CR density**
(omnidirectional intensity)

SW convection   diffusion

$$\frac{\partial U}{\partial t} + \nabla\cdot\left(\frac{2+\gamma}{3}U\mathbf{V}_{SW} - \boldsymbol{\kappa}\cdot\nabla U\right) = -\frac{\partial}{\partial p}\left(\frac{1}{3}p\mathbf{V}_{SW}\cdot\nabla U\right)$$

Adiabatic cooling

$$\mathbf{S}(\mathbf{r},p,t)$$

**: streaming**

$$\boldsymbol{\xi}(\mathbf{r},p,t) = -\mathbf{S}/(\frac{1}{3}vU)$$

**: anisotropy**

$$\mathbf{G} \equiv \nabla U/U = \frac{v}{3}\boldsymbol{\kappa}^{-1}\cdot\left\{\frac{2+\gamma}{v}(\mathbf{V}_{SW} - \mathbf{v}_E) + \boldsymbol{\xi}\right\}$$

**$\therefore$ Anisotropy ( $\boldsymbol{\xi}$ ) tells us the spatial gradient ( $\mathbf{G}$ ) which reflects the magnetic field geometry in space**

# What "CR wind" tells us?

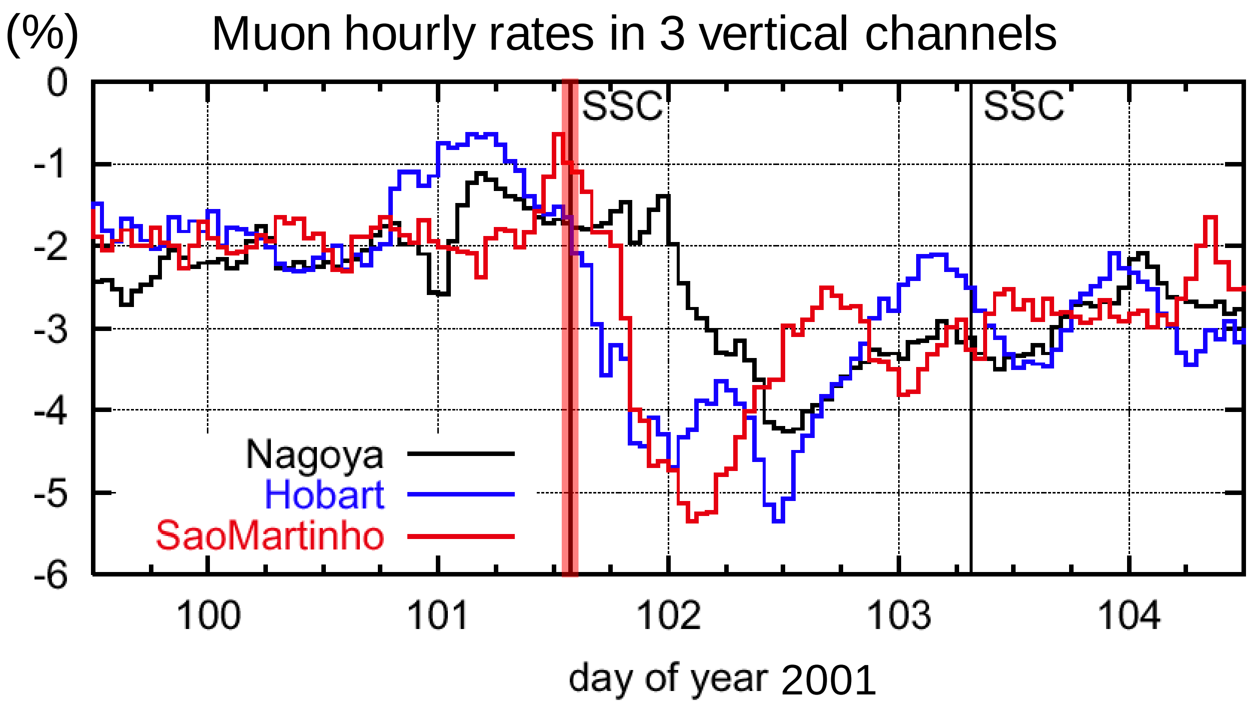


- **CR density decrease (Forbush Decrease).**
- **Strong CR streaming (wind) is associated.**
- **Need to measure density & streaming separately.**
- **Only global network can make such a precise measurement .**

Can deduce 3D distribution from the CR gradient (**G**) from the anisotropy

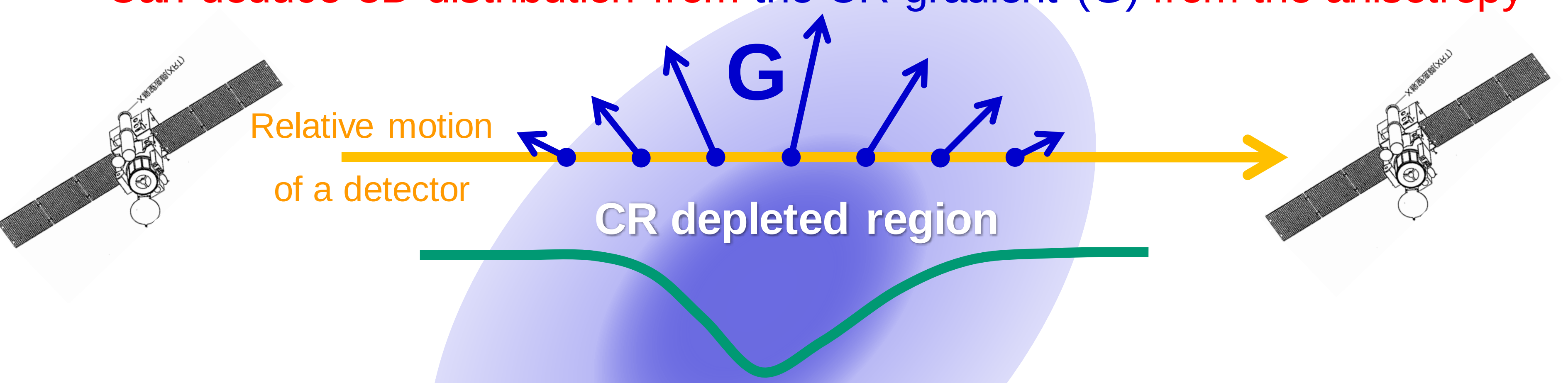


Single telescope tells us only 1D distribution along the orbit

# October 29, 2003 CME event

**Cosmic ray**

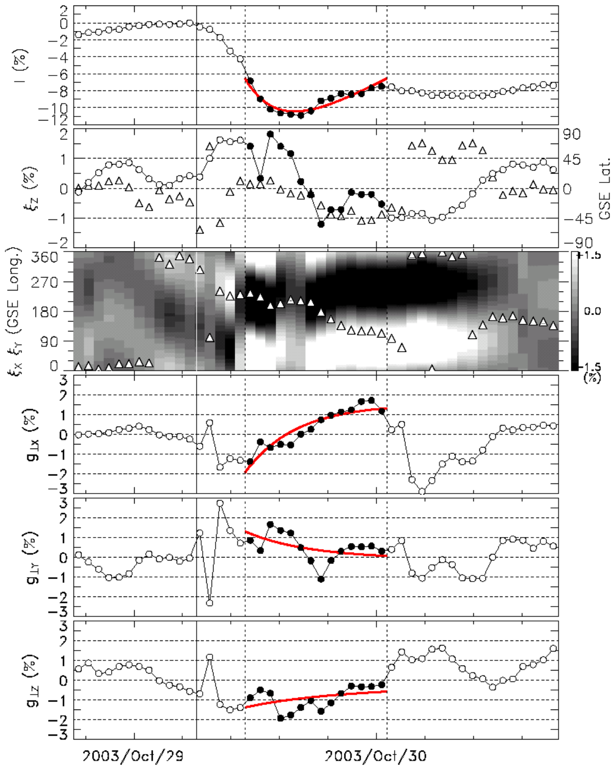


**ACE B&V**

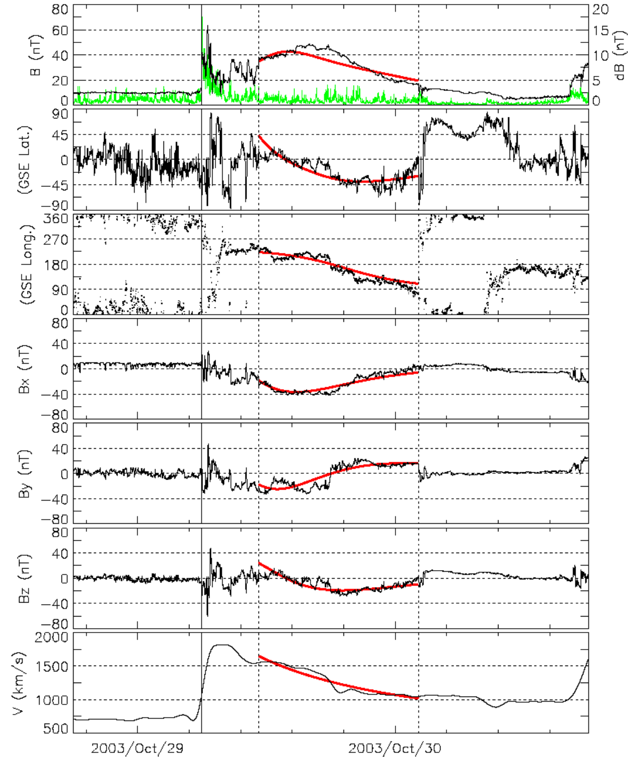


**IPS**

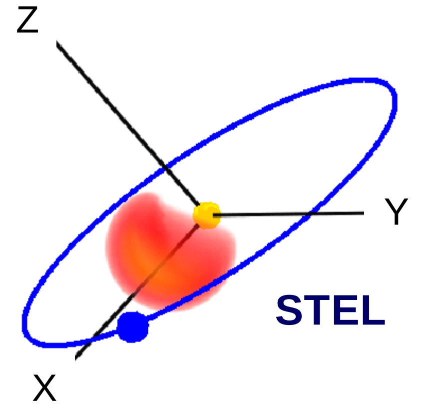


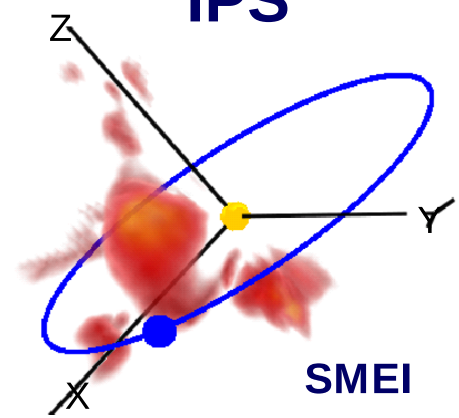


**Tokumaru+, JGR 112, 2007**

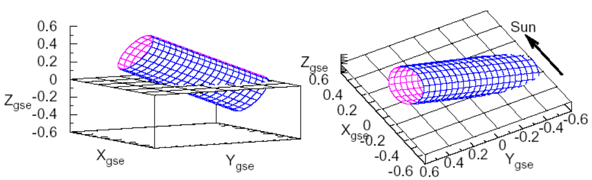


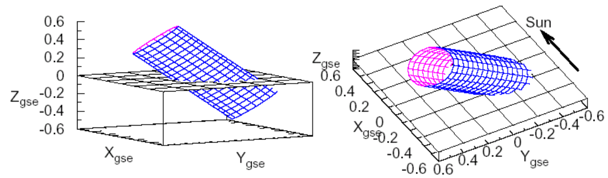


**Kuwabara+, GRL, 31, 2004 JGR, 114, 2009**

| | Cosmic Ray | | | | Magnetic Flux Rope | | | | |
|---|---|---|---|---|---|---|---|---|---|
| Event Date | $\theta$ | $\phi$ | $R(t_c)$ | $\mathbf{P}_c$ | $\theta$ | $\phi$ | $R(t_c)$ | $\mathbf{P}_c$ | |
| Apr/05/2001 | 7 | 56 | 0.109 | -0.004, 0.013,-0.067 | 29 | 277 | 0.175 | 0.000,-0.073,-0.131 | |
| Apr/11/2001 | 66 | 12 | 0.060 | 0.000,-0.002,-0.000 | | | | | |
| Apr/28/2001 | 26 | 283 | 0.097 | 0.001,-0.009,-0.018 | | | | | |
| Nov/06/2001 | 38 | 273 | 0.074 | 0.000,-0.023,-0.030 | | | | | |
| Oct/29/2003 | 35 | 78 | 0.215 | 0.000,-0.066, 0.091 | 46 | 56 | 0.222 | 0.000,-0.080, 0.064 | ○ |
| Jul/27/2004 | 5 | 303 | 0.096 | 0.000,-0.004,-0.032 | 16 | 296 | 0.136 | 0.000,-0.004,-0.012 | ○ |
| Nov/09/2004 | 44 | 187 | 0.065 | 0.001,-0.038,-0.004 | 36 | 195 | 0.060 | 0.000,-0.036,-0.013 | ○ |
| Jan/22/2005 | 7 | 337 | 0.049 | 0.000,-0.003,-0.007 | 51 | 212 | 0.237 | 0.000,-0.170,-0.074 | |

# Cosmic ray precursors

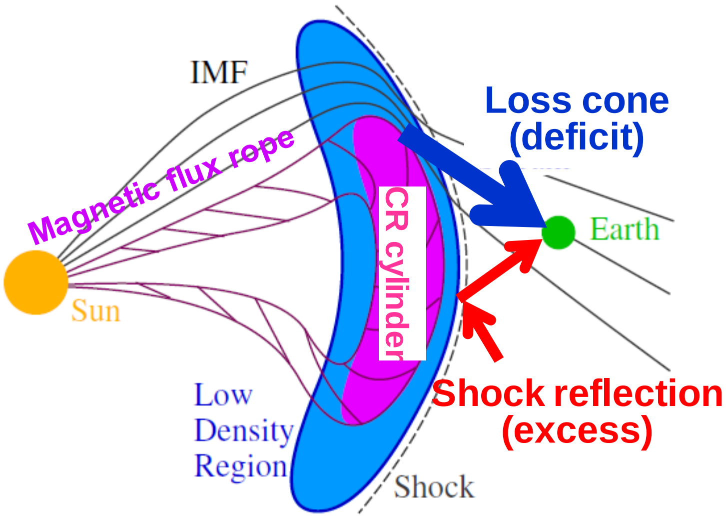


**With the improved network coverage 133 (74%) of 181 storms in 2001-07 analyzed**

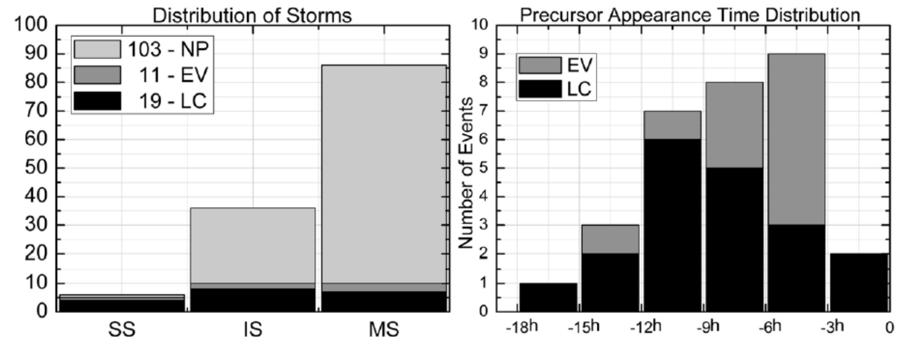


86 %  30 %  15 %

**Dst (nT)=  -250  -100  -50**

**Rockenbach+ GRL, 38, 2011**

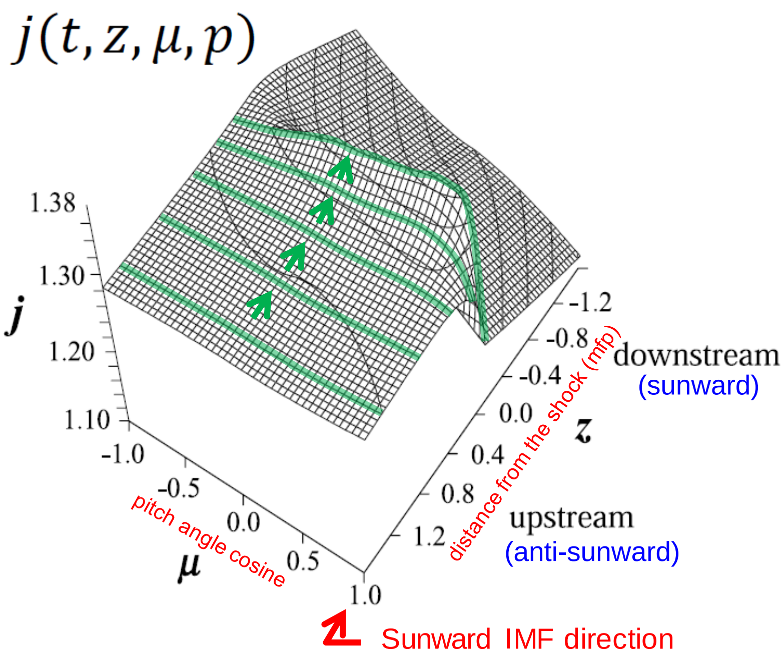


**Leerungnavarat+ ApJ, 593, 2003**

- **CRs from the depleted region travel to the upstream Earth with the speed of light overtaking the shock ahead.**
- **The precursor is seen as the deficit intensity of CRs arriving from the sunward IMF. Loss-cone (LC) precursor.**
- **CRs reflected and accelerated by the approaching shock are also observed as an excess intensity. precursory excess.**
- **GMDN with better sky coverage is capable for detecting more precursors.**

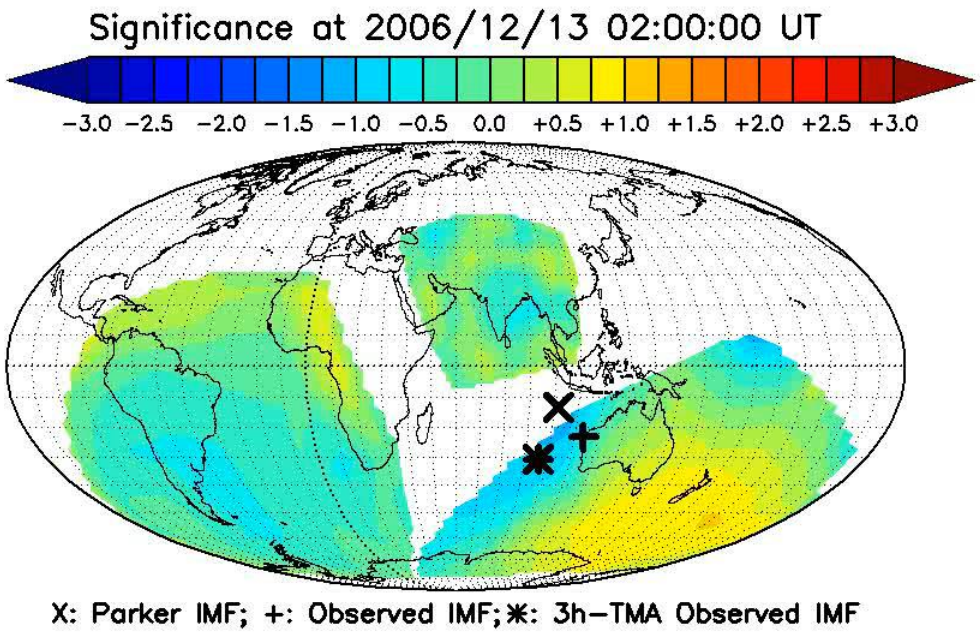

Significance at 2006/12/13 02:00:00 UT
−3.0 −2.5 −2.0 −1.5 −1.0 −0.5 0.0 +0.5 +1.0 +1.5 +2.0 +2.5 +3.0
X: Parker IMF; +: Observed IMF; ✱: 3h−TMA Observed IMF


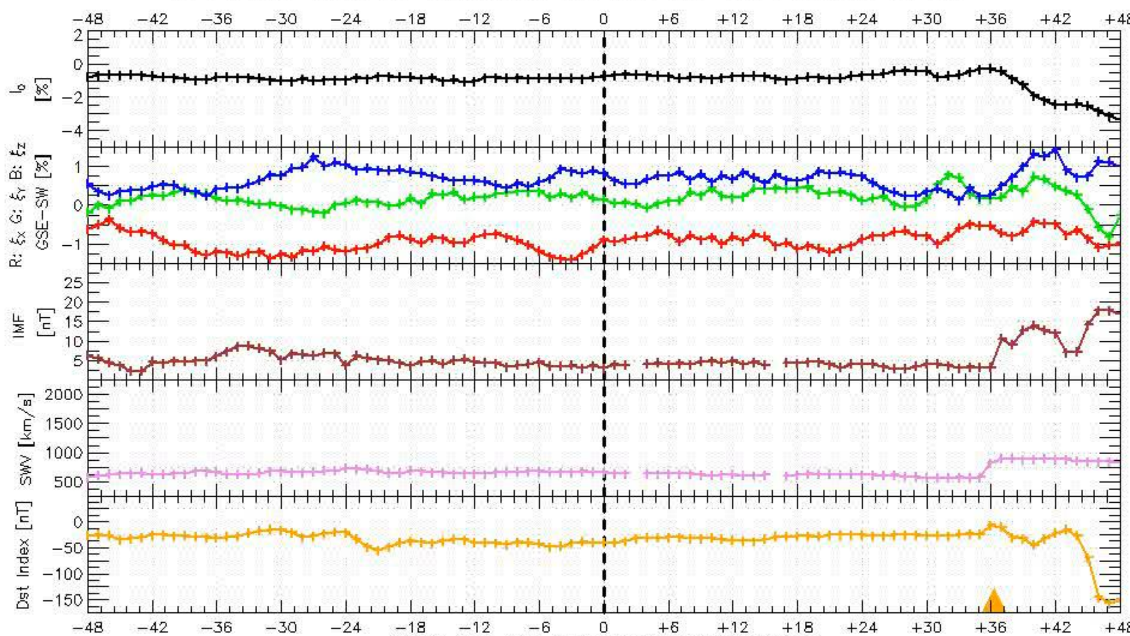

I0 [%]
R: ξX G: ξY B: ξZ GSE−SW [%]
IMF [nT]
SWV [km/s]
Dst Index [nT]
Time in hours, Zero means: 2006/12/13 02:00:00 UT

# Best-fit analysis of LC precursor

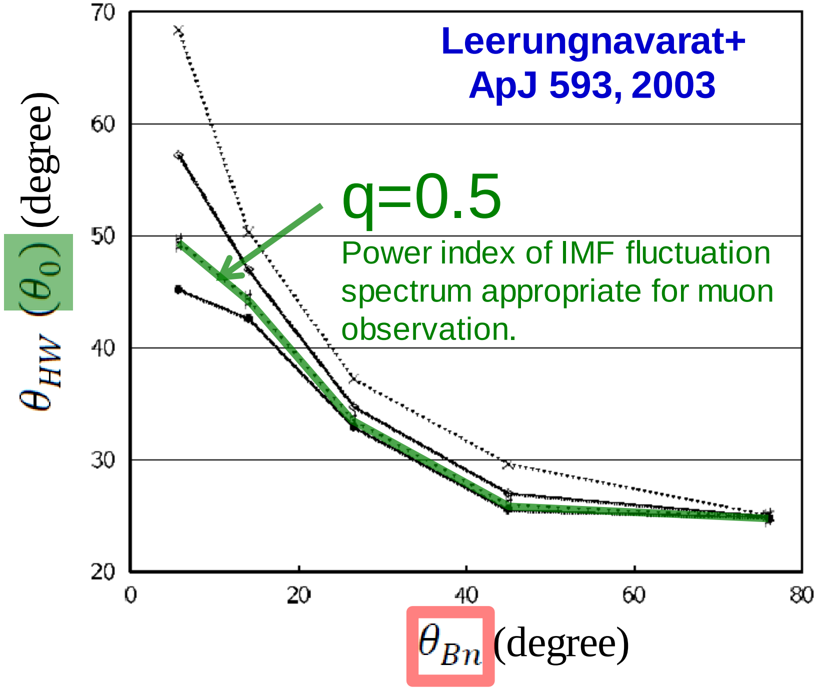


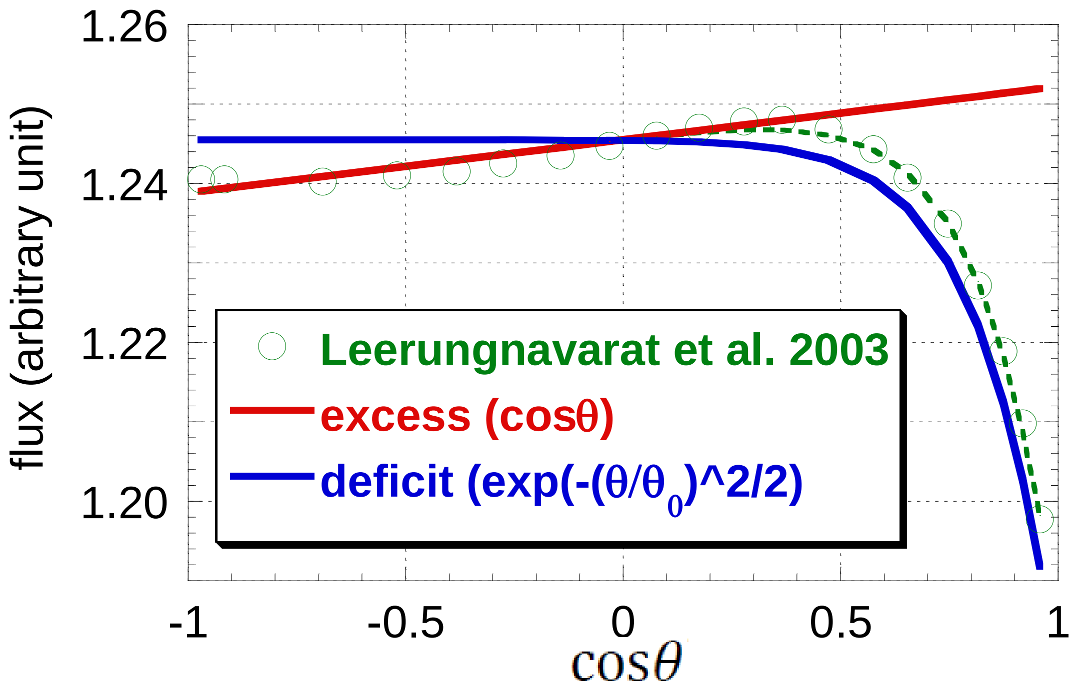


( $\theta$ : **pitch angle measured from the sunward IMF direction**)

$$j(z(t),\mu,p) = C_{LC}(z(t))\left(\frac{p}{30}\right)^{-1}\exp\left(-\frac{\theta^2}{2\theta_0{}^2}\right) + C_{EX}(z(t))(1+\cos\theta)/2$$

**Loss-cone (deficit)**

**Loss-cone width (constant)**
**Related to shock-field angle $\theta_{Bn}$**

**Shock reflection (excess)**

**Fushishita+ ApJ 715 2010**

# A “gap” in the present GMDN

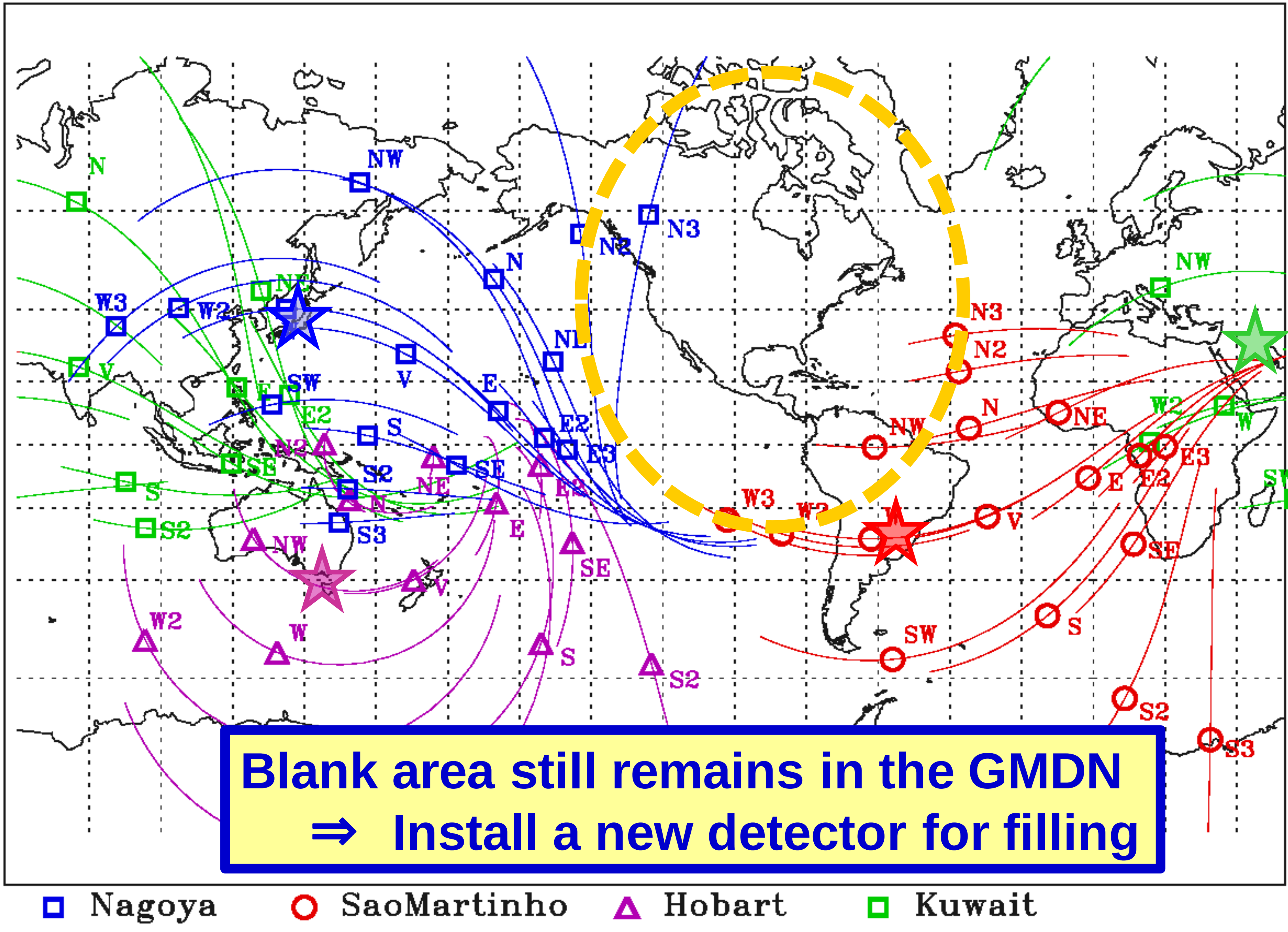


**Blank area still remains in the GMDN**
**⇒ Install a new detector for filling**

# New muon detector in Mexico

(**SciCRT** @Mt. Sierra Negra) Nagai+ Astroparticle Phys. 59 2014

**19.0°N, 97.3 °W**

**4,600 m a.s.l. (590 hPa)**

**Geomag. Cut-off (V) = 7.9 GV**

**Expected muon count rate:**

**$2.7\times10^6$ cph (750 Hz)**

## Now in test operation

Installed in April, 2013

Observation hut

# Before

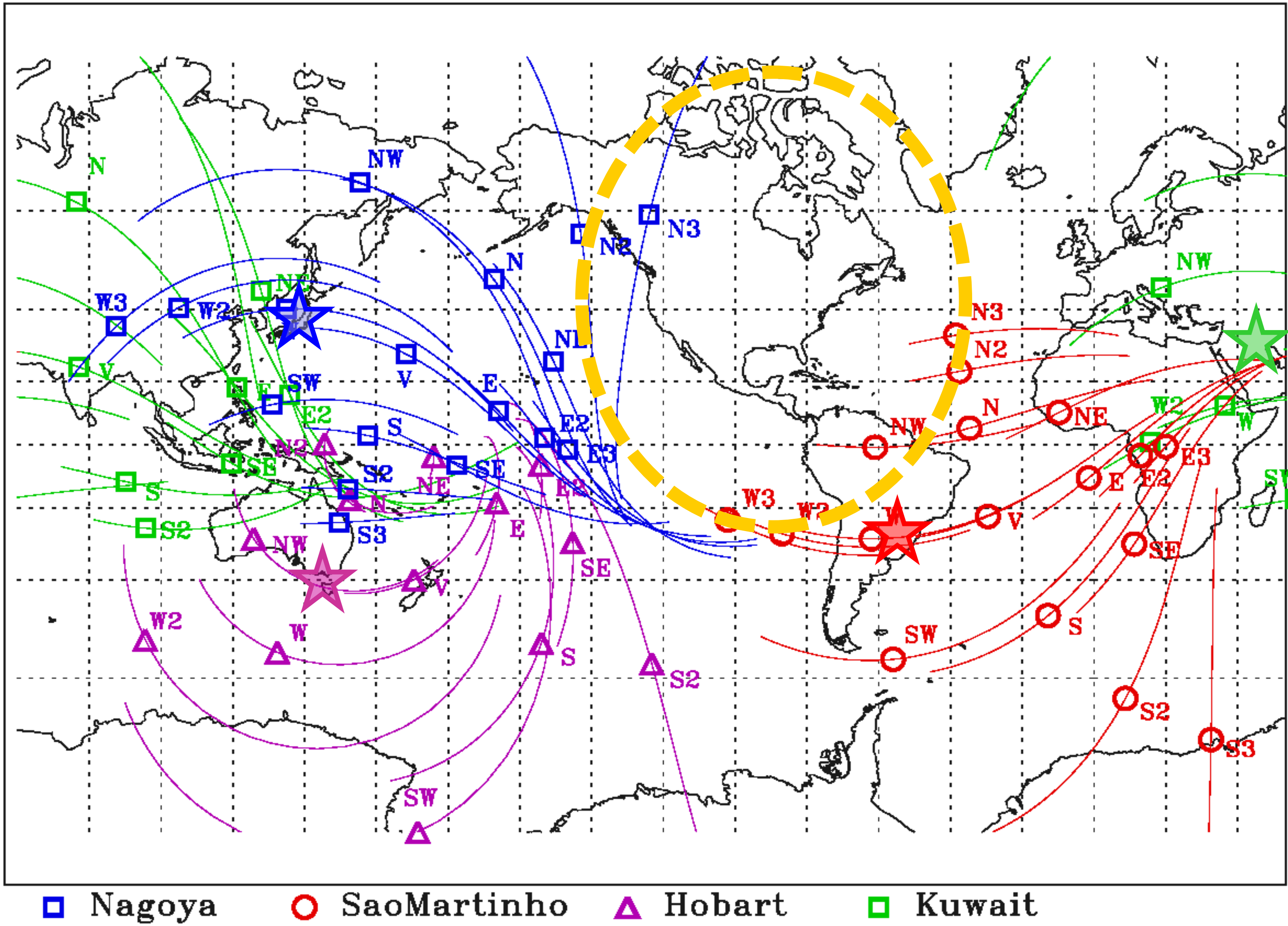

# After

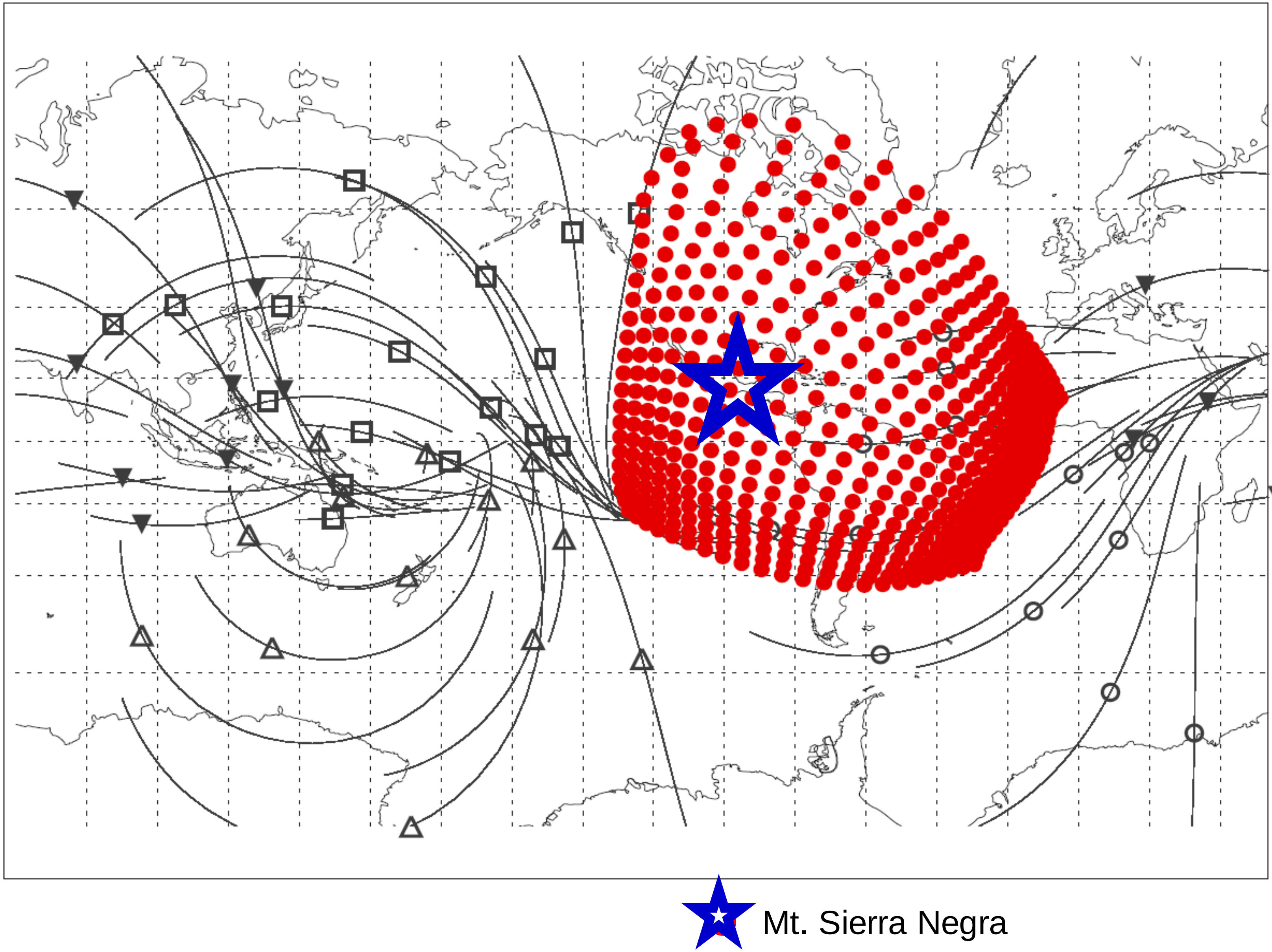

# Summary

- **GMDN is currently a network of four detectors and capable for measuring CR anisotropy precisely.**
- **We deduce the 3D geometry of MFR from the CR anisotropy.**
- **We also observe CR precursors for the potential space weather forecast.**

**GMDN is rooted in the international collaboration.**
**Anybody willing to join us would be welcome!**

**Contact: kmuna00@shinshu-u.ac.jp**

# Thank you
# for your attention!

# Duty cycle of the GMDN (in %)

| | 2006 | 2007 | 2008 | 2009 | 2010 | 2011 | 2012 | 2013 | 2014 |
|---|---|---|---|---|---|---|---|---|---|
| **Nagoya (Japan)** | 95.5 | 97.8 | 98.5 | 98.0 | 96.1 | 97.4 | 98.7 | 92.2 | 98.0 |
| **Hobart (Australia)** | 93.6 | 94.3 | 95.1 | 99.7 | **89.1** | 99.9 | 100.0 | 99.9 | 99.5 |
| **São Martinho (Brazil)** | 94.7 | 99.1 | 99.6 | 99.8 | 98.4 | 100.0 | 97.6 | 98.7 | 97.6 |
| **Kuwait City (Kuwait)** | **75.9** | 98.7 | 99.1 | 93.6 | 97.4 | 99.5 | 99.5 | 98.9 | 100.0 |
| **4 station obs.** | **62.3** | **94.2** | **92.5** | **91.2** | **81.7** | **96.8** | **95.9** | **90.8** | **95.1** |

# Deriving anisotropy vector

$I_{i,j}^{obs}(t)$ : **pressure corrected count rate in the j th directional channel of the i th detector**

$$I_{i,j}^{cal}(t) = I^0(t) + \xi_x^{\mathrm{GEO}}(t)\left(c_{1\ i,j}^{1}\cos\omega t_i - s_{1\ i,j}^{1}\sin\omega t_i\right)$$
$$+\ \xi_y^{\mathrm{GEO}}(t)\left(s_{1\ i,j}^{1}\cos\omega t_i + s_{1\ i,j}^{1}\sin\omega t_i\right) + \xi_z^{\mathrm{GEO}}(t)\,c_{1\ i,j}^{0}$$

$c_{1\ i,j}^{1}$ $s_{1\ i,j}^{1}$

coupling coefficients

$$c_{n\ i,j}^{m} = \frac{1}{\bar{I}_{i,j}}\int_{p_{c;\,i,j}}^{\infty}\int_{\Omega_{i,j}}\int_{S_{i,j}} Y \cdot G(p)\cdot P_n^m(\cos\theta_{or})\cdot\cos m(\phi_{or}-\phi_{st})\,dS\,d\Omega\,dp$$

$$s_{n\ i,j}^{m} = \frac{1}{\bar{I}_{i,j}}\int_{p_{c;\,i,j}}^{\infty}\int_{\Omega_{i,j}}\int_{S_{i,j}} Y \cdot G(p)\cdot P_n^m(\cos\theta_{or})\cdot\sin m(\phi_{or}-\phi_{st})\,dS\,d\Omega\,dp$$

$Y(p;\ x_i,\theta_j,E_{th}^{\mu})$ : response function

**We derive** $I^0(t), \xi_x^{\mathrm{GEO}}(t), \xi_y^{\mathrm{GEO}}(t), \xi_z^{\mathrm{GEO}}(t)$ **minimizing ….**

$$\sum_{i,j}\left|I_{i,j}^{obs}(t) - I_{i,j}^{cal}(t)\right|^2 / \sigma_{i,j}^2$$

# CME on Oct. 29, 2003

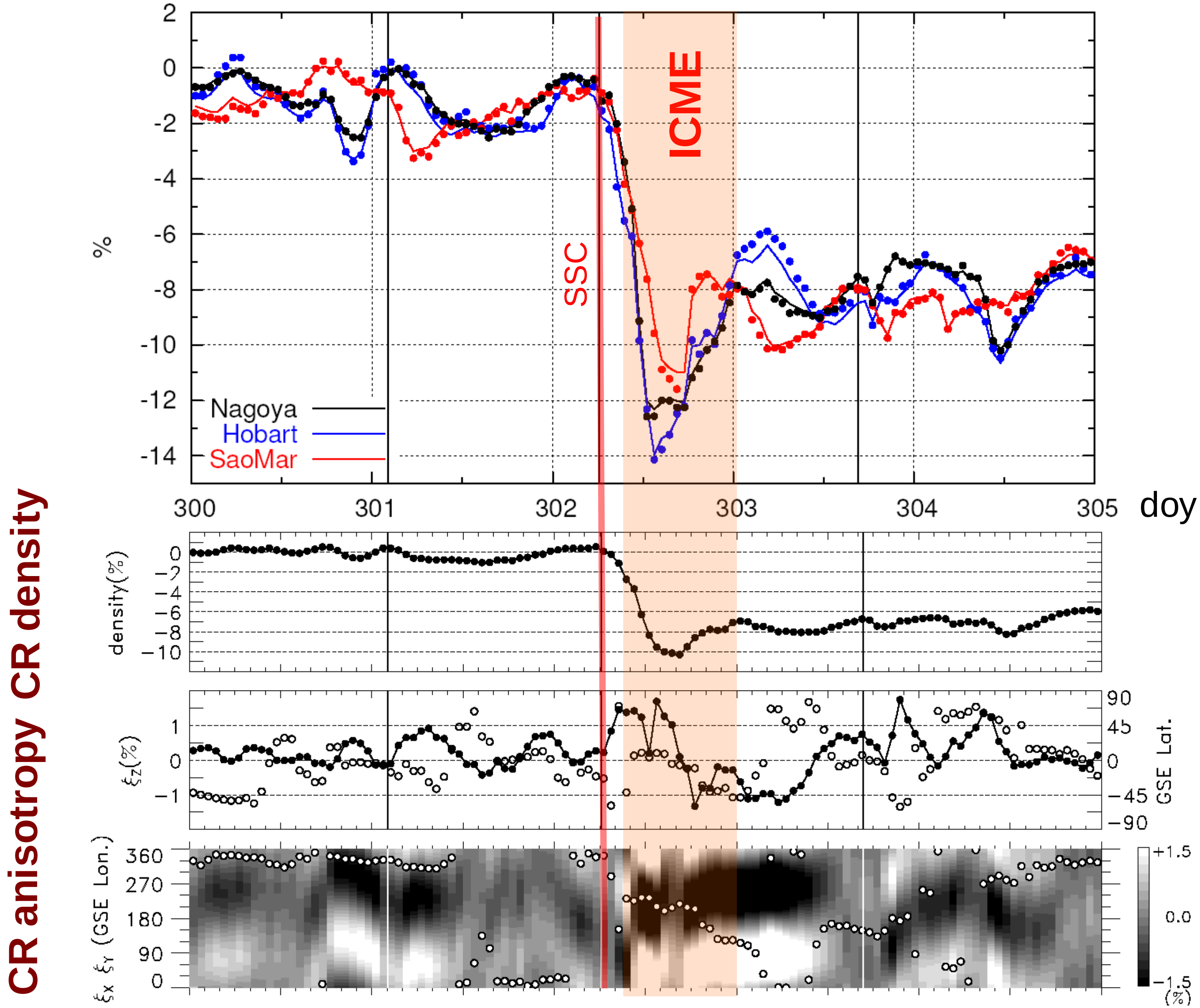

# CR diffusion into MFR

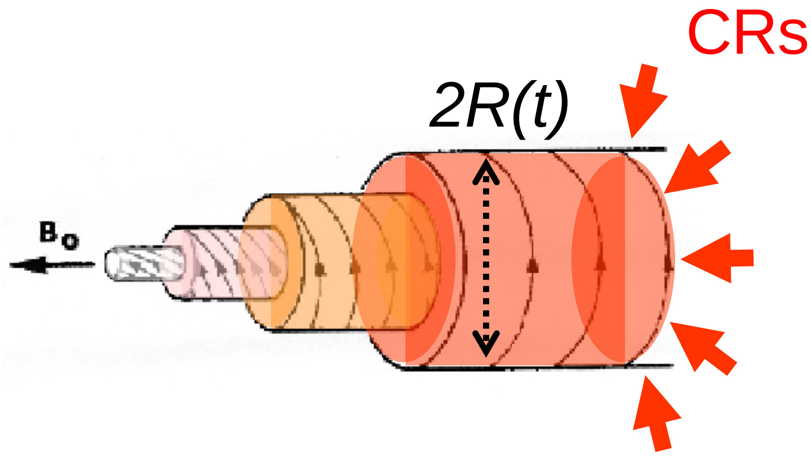


**CRs can penetrate into MFR only by the cross-field diffusion**

**$\kappa_\perp$ also can be evaluated from CR data during MFR**

Self-similar expansion of MFR

$$R(t) = R_0(t/t_0), \quad v(r,t) = v_0(r/R_0)/(t/t_0)$$

$$\kappa_\perp(t) = \kappa_0 v_0 R(t),$$

$$f \propto p^{-(2+\gamma)}$$

$$\frac{\partial f}{\partial s} = \kappa_0\left(\frac{\partial^2 f}{\partial x^2} + \frac{1}{x}\frac{\partial f}{\partial x}\right) - \frac{2(2+\gamma)}{3} f$$

$$x = r/R_0 \quad (0 \le x \le 1)$$

$$s = \log\tau, \quad \tau = t/(R_0^{\ 2}/\kappa_0) \quad (\tau \ge 0)$$

Cross-field diffusion — Adiabatic cooling

**Dimensionless parameter $\kappa_0$ determines $\kappa_\perp$**

# CRs in Magnetic Flux Rope

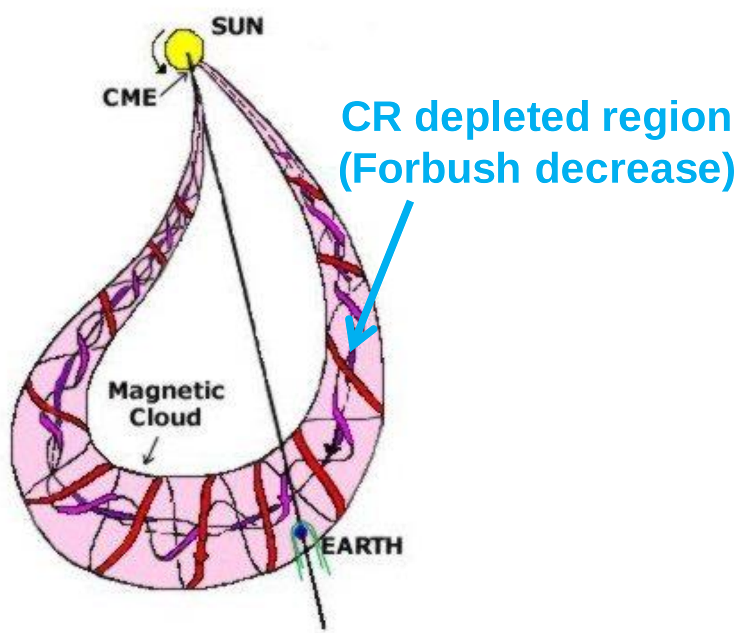


- **CR depleted region** is formed in an expanding MFR into which CRs can penetrate only through the **cross-filed diffusion**.
- CR density gradient **G pointing away from the MFR center** can be deduced from the diamagnetic drift streaming (**Bieber & Evenson, GRL, 25, 1998**).

$$R_L \mathbf{G} = \mathbf{b} \times \boldsymbol{\xi}_\perp$$

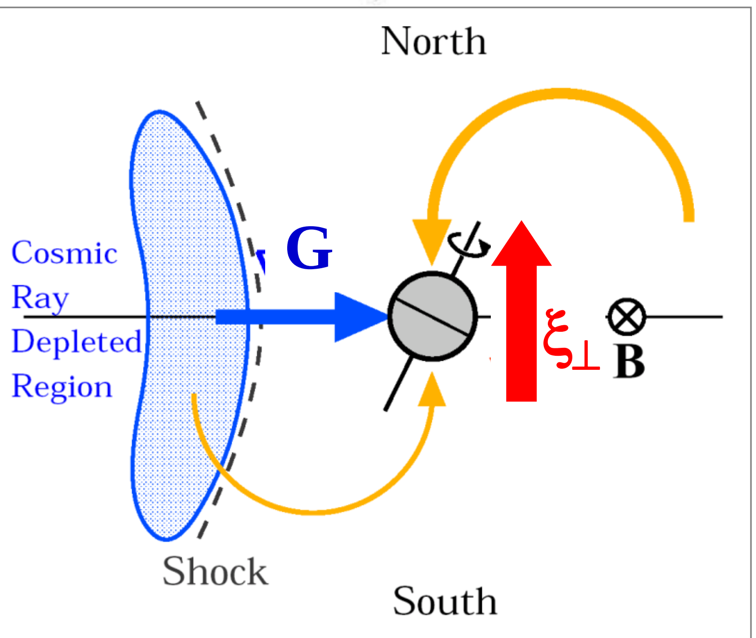


- We deduce **MFR geometry** from the CR density gradient by assuming **an infinite straight cylinder** as a local part of MFR.

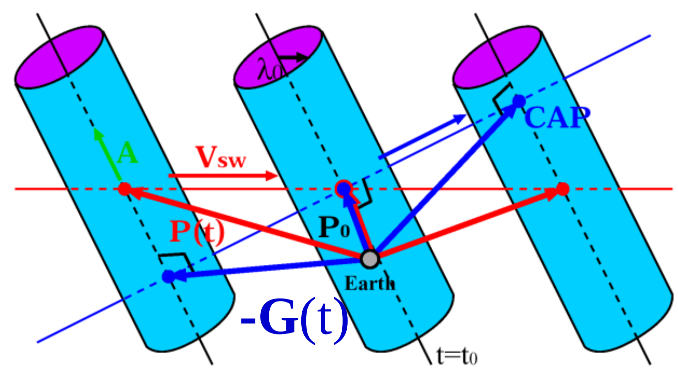

# Cosmic ray precursors

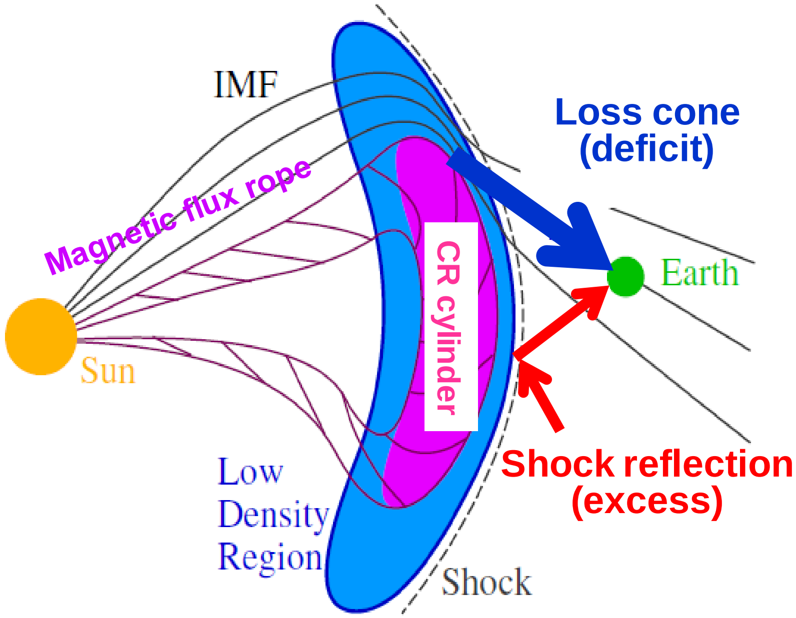


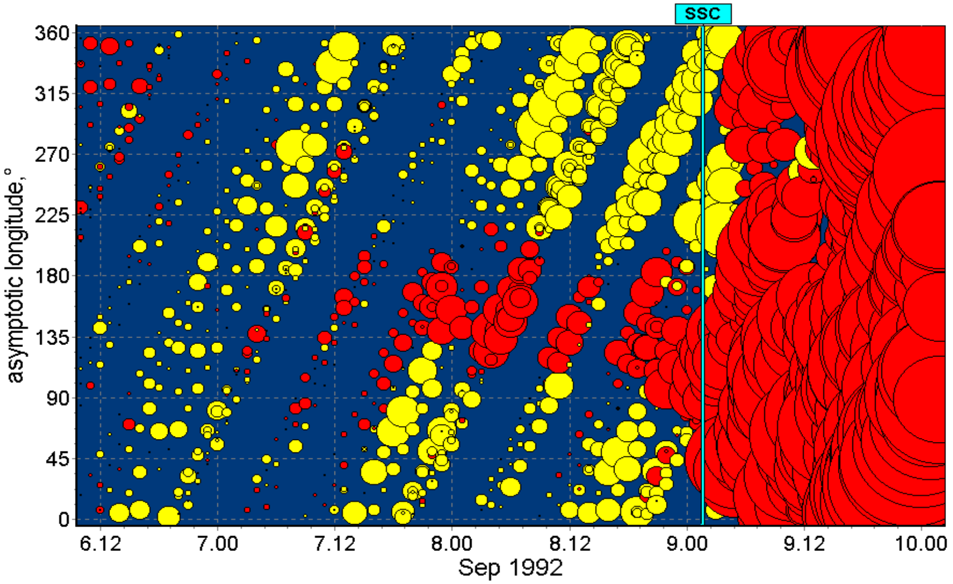


Dorman+ Proc. 28th ICRC, 2003

- **CRs from the depleted region travel to the upstream Earth with the speed of light overtaking the shock ahead.**
- **The precursor is seen as the deficit intensity of CRs arriving from the sunward IMF.**
  **loss-cone (LC) precursor**
- **For detecting LC precursor, we need a detector viewing the sunward IMF direction during a period preceding the SSC.**
- **CRs reflected and accelerated by approaching shock are also observed as a precursor of excess intensity.**
  **precursory excess**

# December, 2006 CME

## X3.4 flare onset 02:38UT on 12/13


Fig. 1.—Difference images of the CME and the source region at different times. EIT difference images at 195 Å are shown within the white circles. A transition layer is visible around the CME front, indicating the existence of a shock (*middle and right*). Adapted from the LASCO CME catalog at http://cdaw.gsfc.nasa.gov. [*This figure is available as an mpeg animation in the electronic edition of the Journal.*]

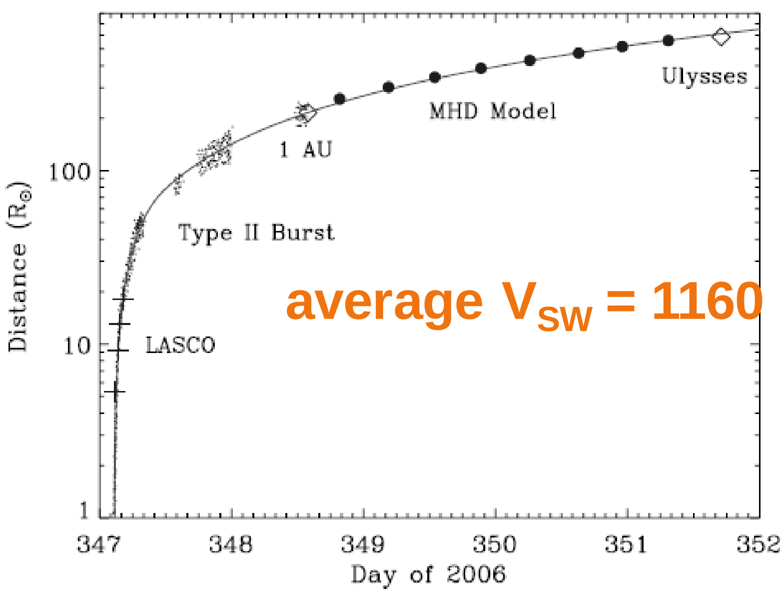


**average $V_{SW}$ = 1160 km/s**

Fig. 10.—Height-time profile (*solid line*) of shock propagation determined from the frequency drift of the type II bands (*dots*) and shock parameters measured at 1 AU (where $R_\odot$ is the solar radius). Plus signs denote the LASCO data. Diamonds indicate the shock arrival times at 1 AU and *Ulysses*. Between 1 AU and *Ulysses* are the shock arrival times (*filled circles*) at 1.2, 1.4, 1.6, 1.8, 2.0, 2.2, 2.4, and 2.6 AU predicted by the MHD model. [*See the electronic edition of the Journal for a color version of this figure.*]

**Liu+, ApJ 689, 2008**

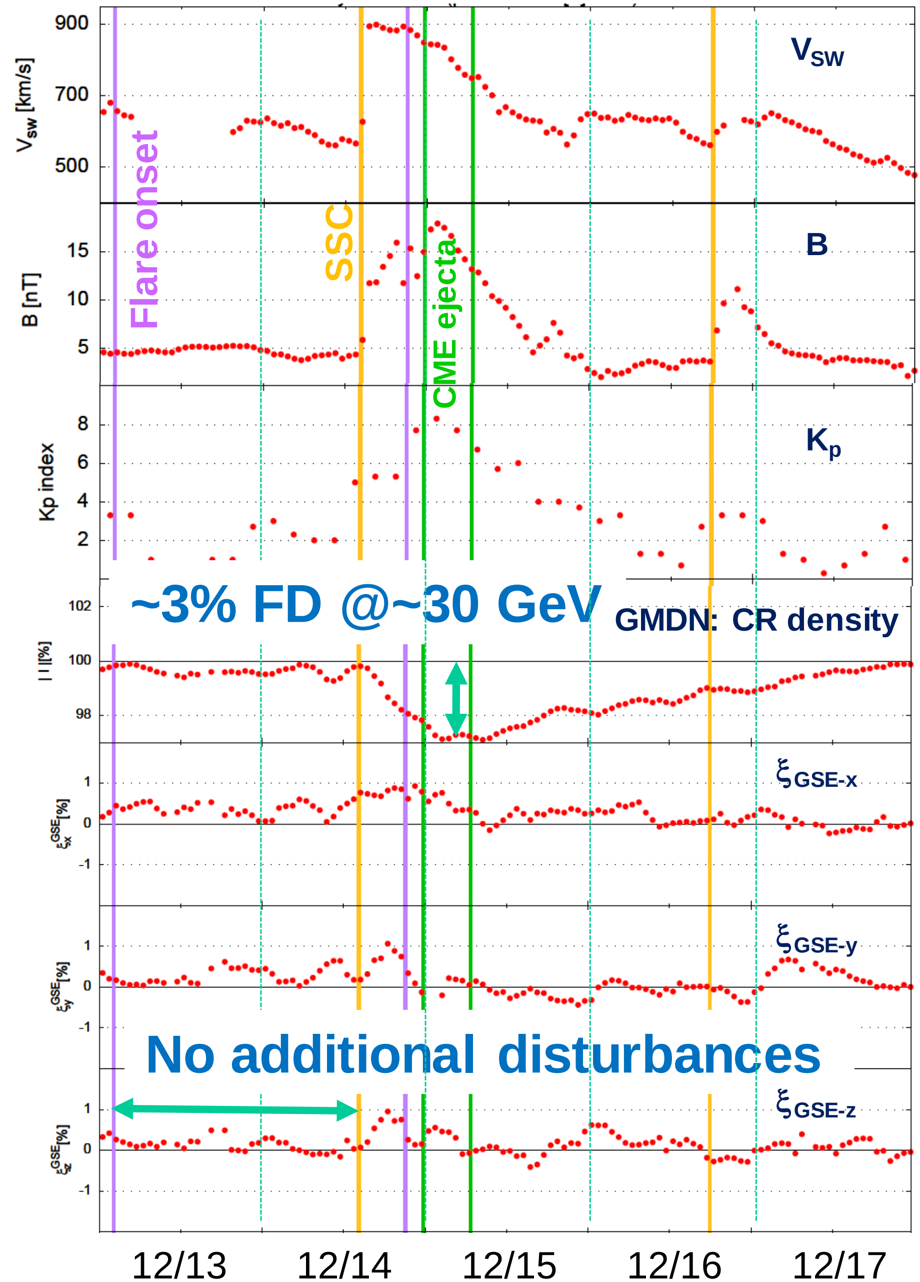

# IMF direction in Field Of Views

## before December 2006 event

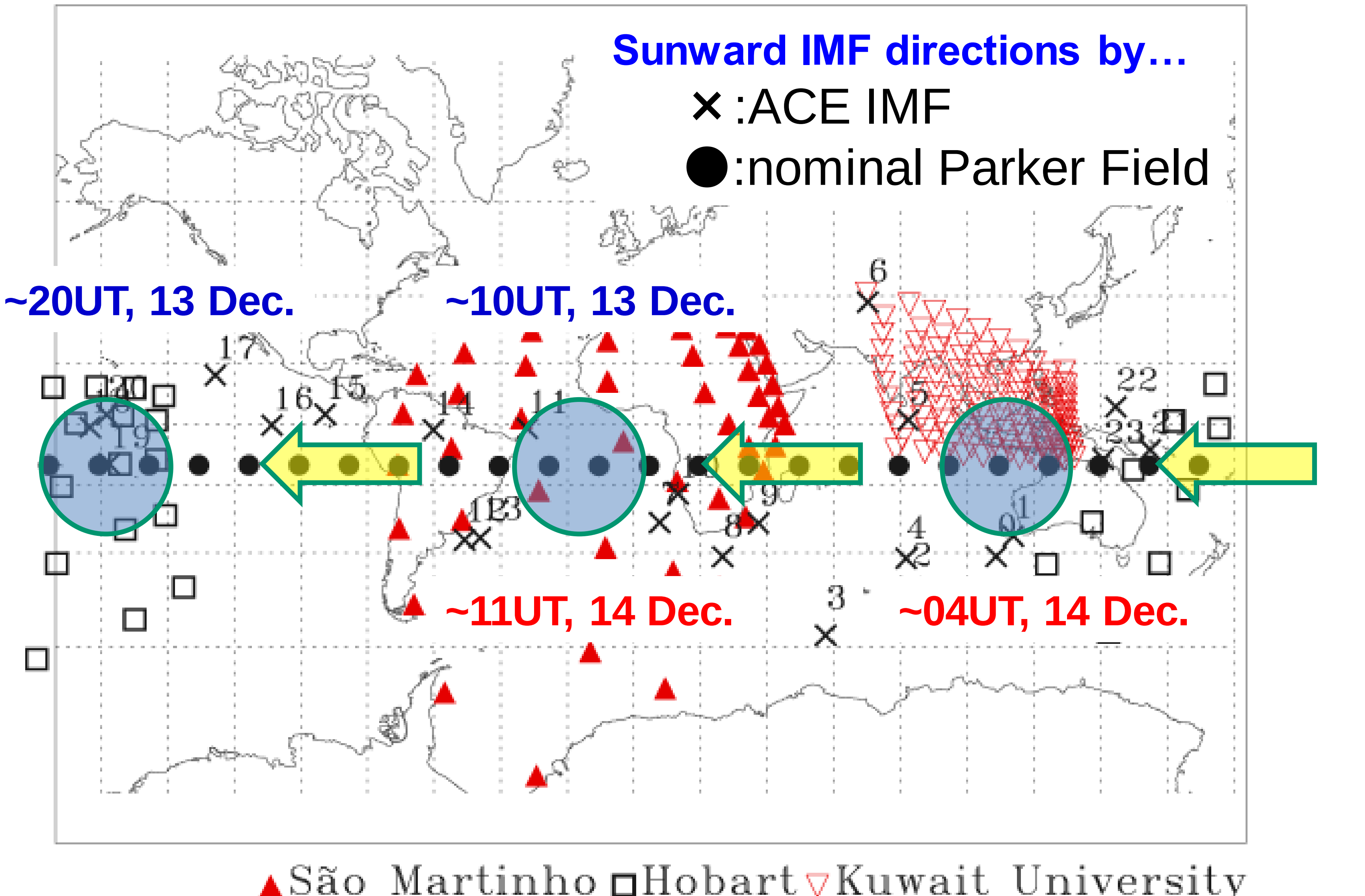

# Observed 2D maps

## São Martinho

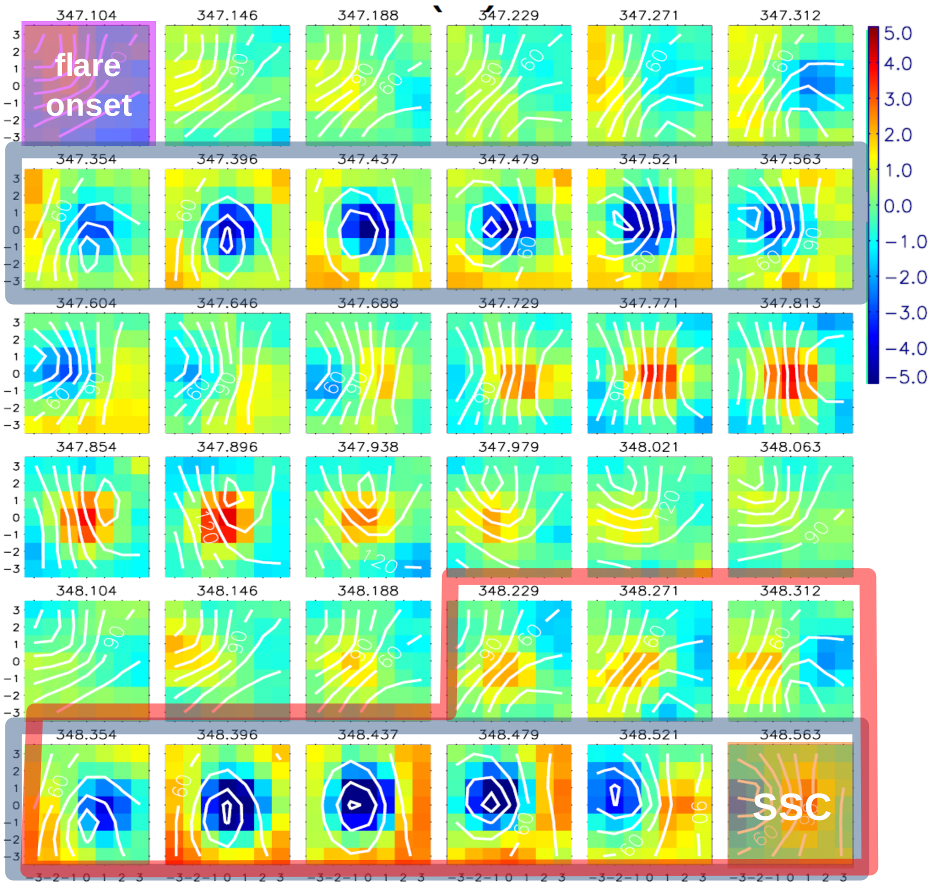


## Hobart

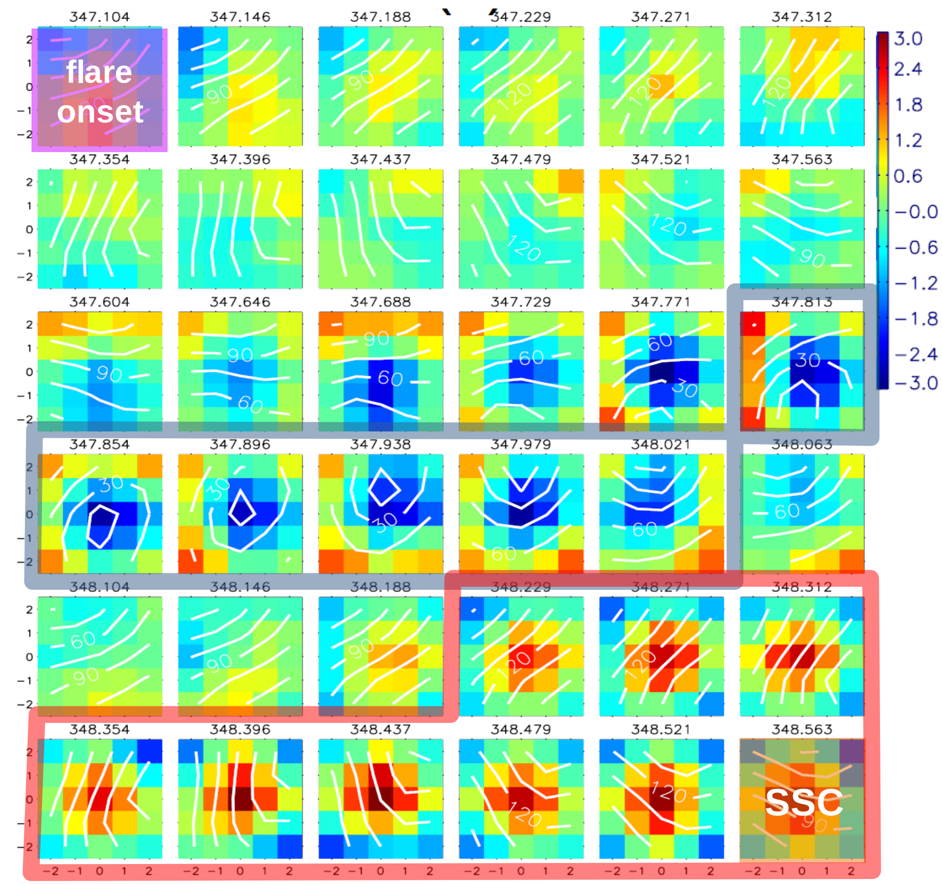


## Kuwait

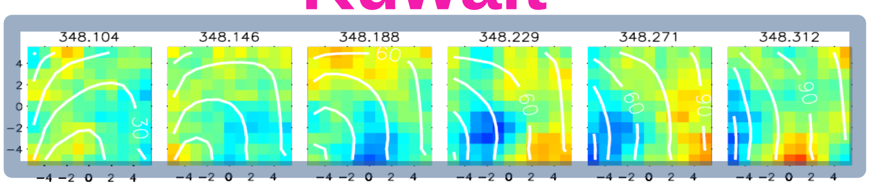


**Fushishita+, ApJ 715, 2010**

# Best-fit parameters

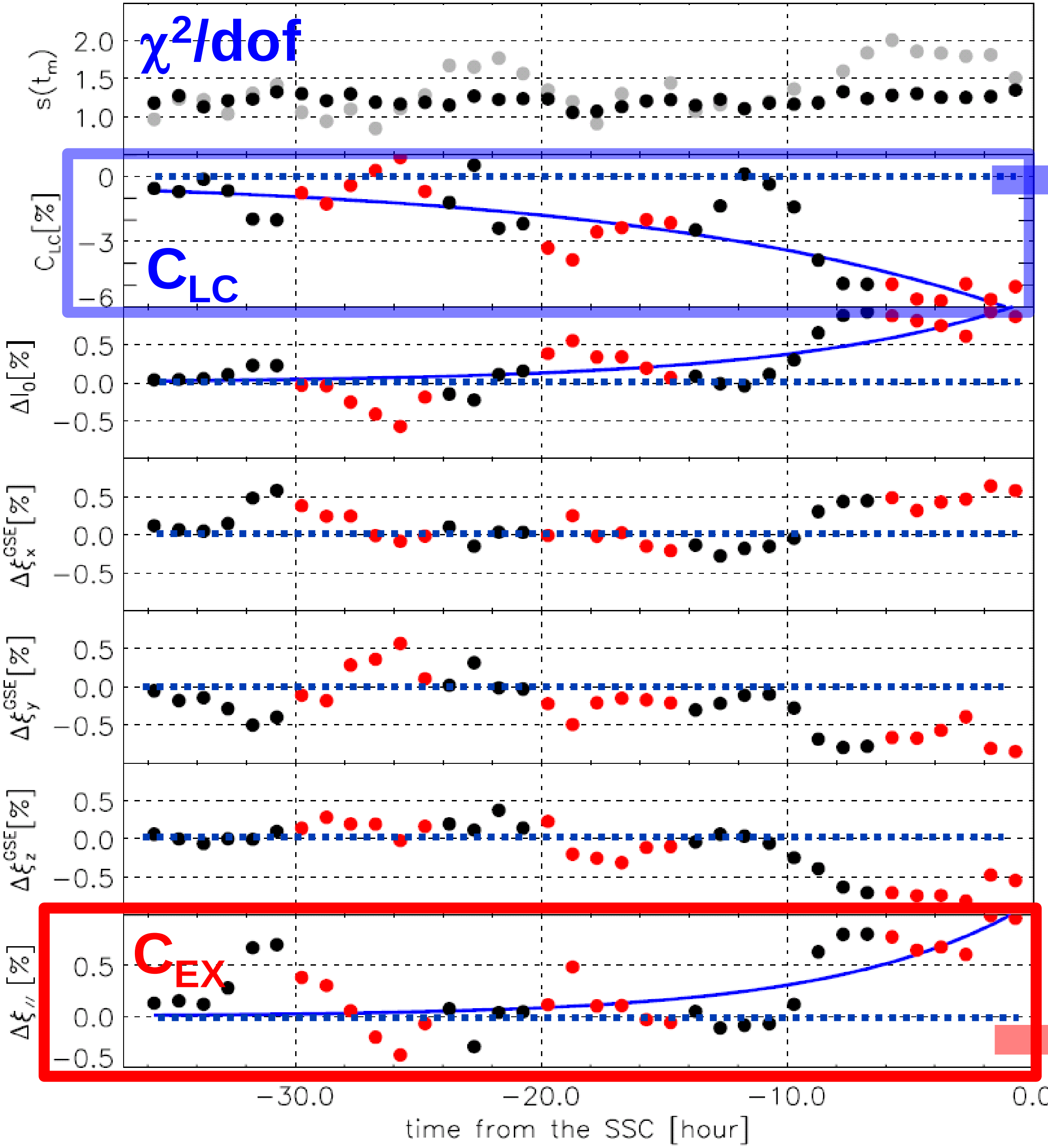


**×2 of FD size (-3 %)**

$$-6.5(\%)\exp\left(\frac{t}{15.6\ (\text{hr})}\right)$$

**×2 of typical $\lambda_{||}$**

$$\theta_0 = 35° \rightarrow \theta_{Bn} = 23°$$

($\theta_{Bn} = 56°$ **from R-H relation)**

$$\Delta I/I = \gamma \Delta E/E$$ **(Shock reflection)**

$$\sim 2\gamma V_{SW} \cos\theta_{Bn}/c = +1.0\ (\%)$$

**$V_{SW}$=1030 km/s, $\gamma$=2.7**

**$\theta_{Bn}$=56°**

$$+1.1(\%)\exp\left(\frac{t}{7.7\ (\text{hr})}\right)$$

# New detector in Mexico
## for filling a gap existing in GMDN

**Collaboration between Mexico & Japan**
**PI: Prof. Y. Matsubara of STEL, Nagoya Univ.**

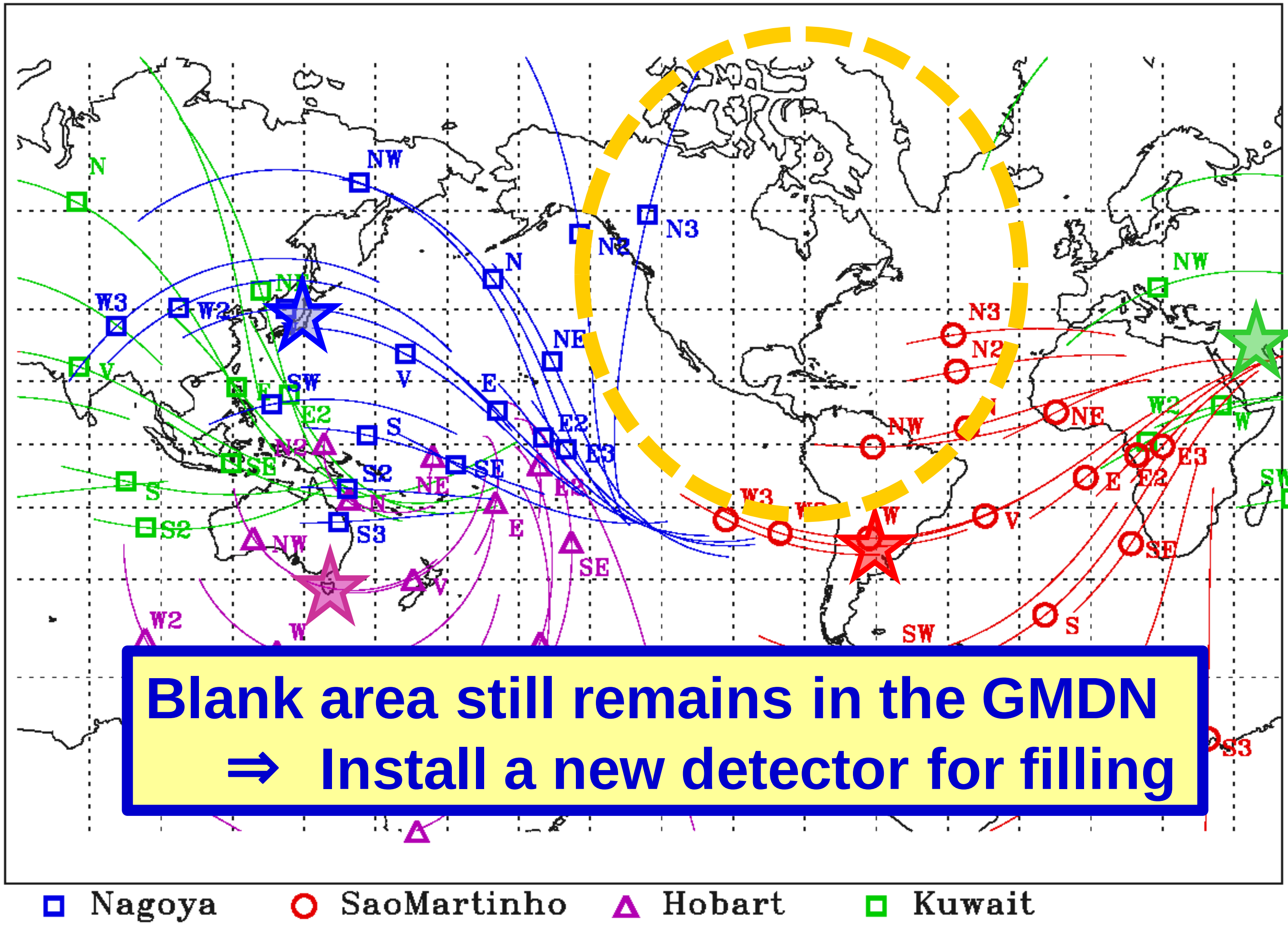


- ☆ indicates the location of the detector.
- ○□△ display the asymptotic viewing directions of median energy CRs corrected for the geomagnetic bending.
- Thin lines indicate the spread of viewing direction for the central 80 % of the energy response to primary CRs.

# SciCRT

## (SciBar for the Cosmic Ray Telescope )

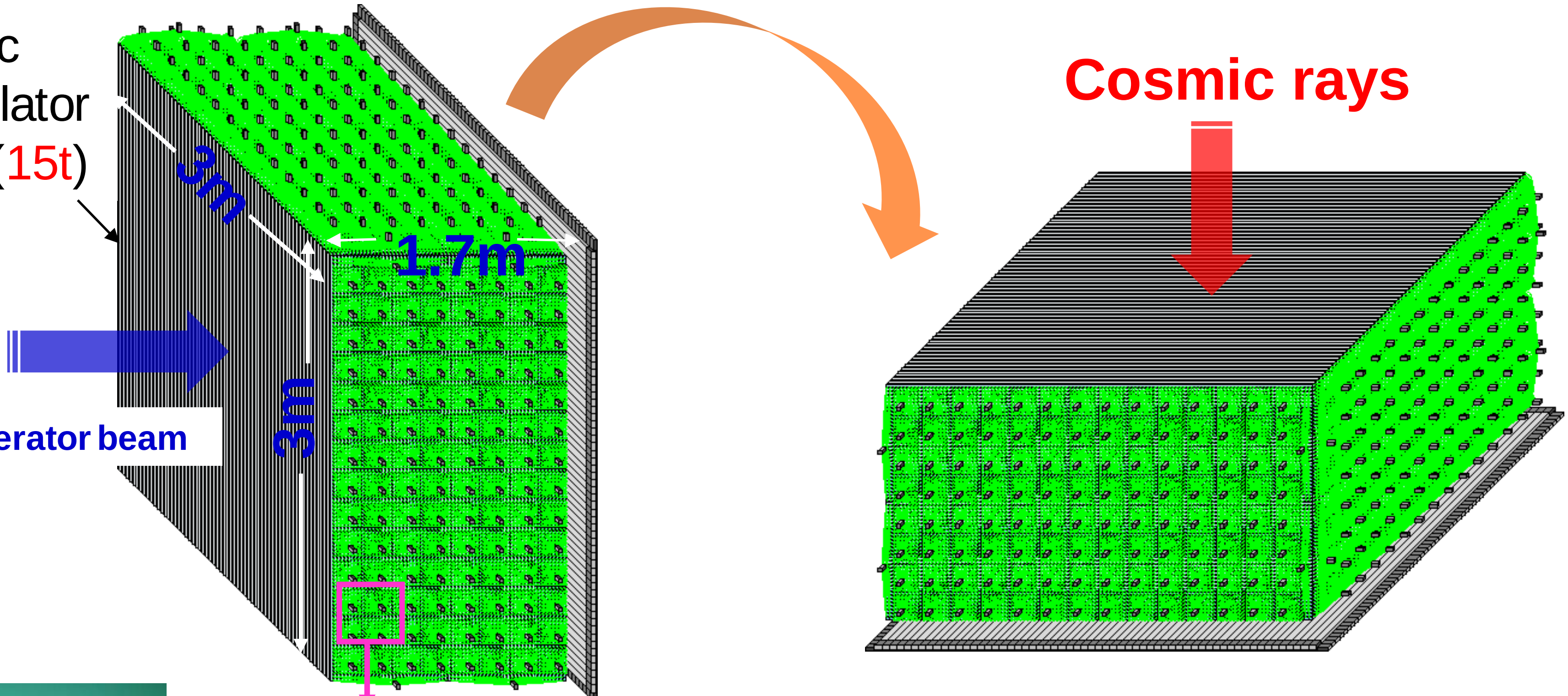


64cn Multi-Anode PMT
(Hamamatsu H8804)

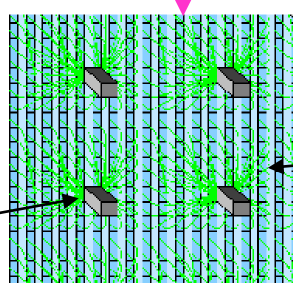

Wave-length shifting fiber

**Consists of 14,848 scinti.-bars (2.5x1.3x300 cm$^3$ each) in 128 horizontal layers viewed by 64ch MAPMTs.**

**Nagai+**
**Astroparticle Phys. 59 2014**

# § 3. - 1 Cosmic ray precursors

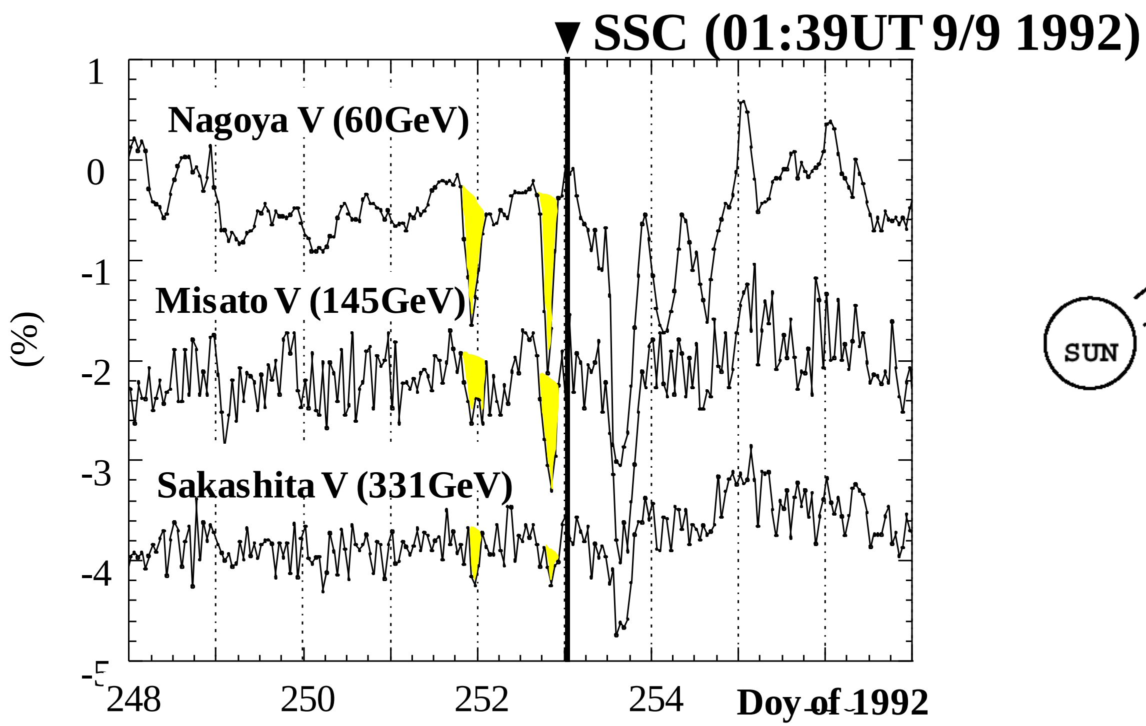


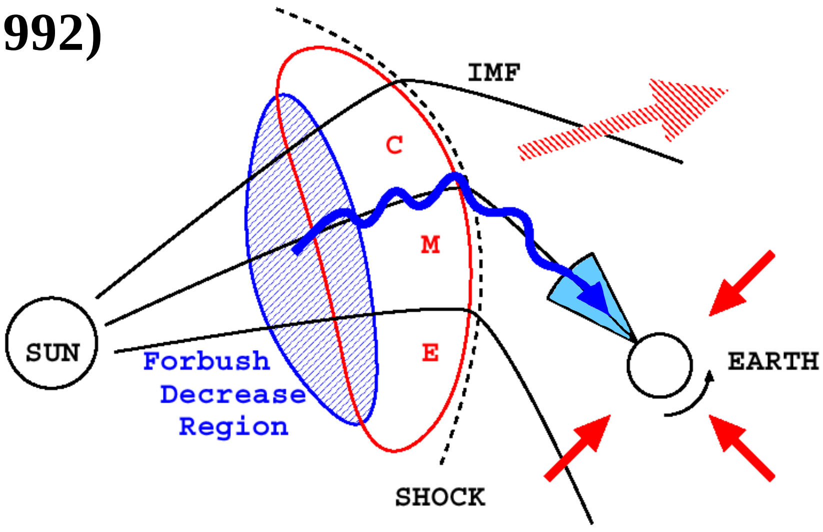


**"Loss-cone" precursor**
**Nagashima+, PSS 40, 1992**

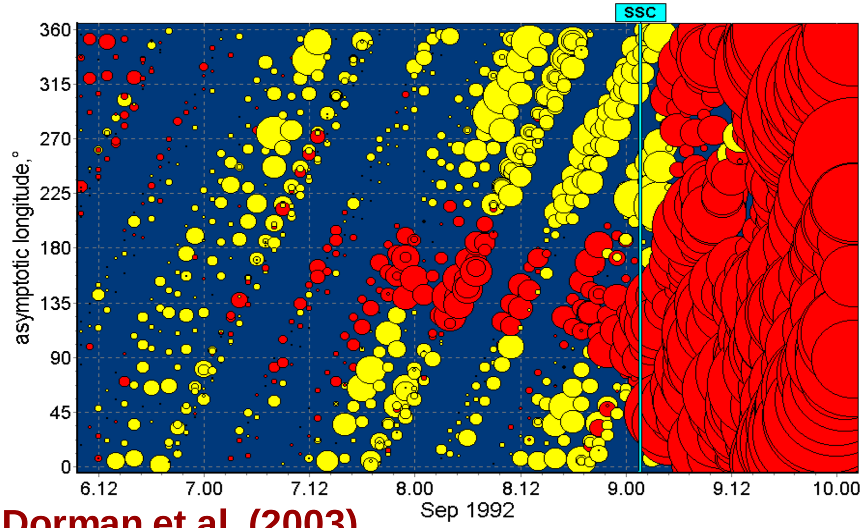


Dorman et al. (2003)

- **CRs from FD region travel to the upstream Earth with the speed of light overtaking the shock ahead.**
- **Prediction is possible even 24 h preceding the CME arrival.**
- **Focused in narrow p.a. region**
  **⇒ Need better angular resolution & better sky coverage**

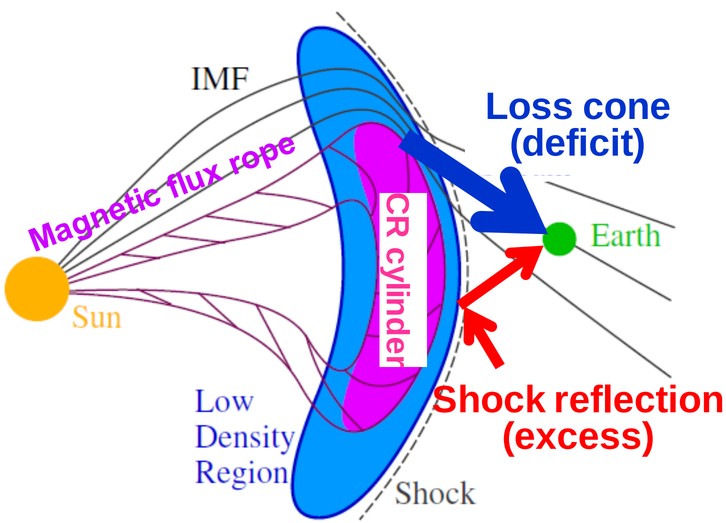


# With network coverage improved
# 133 (74%) of 181 storms in 2001-07 analyzed

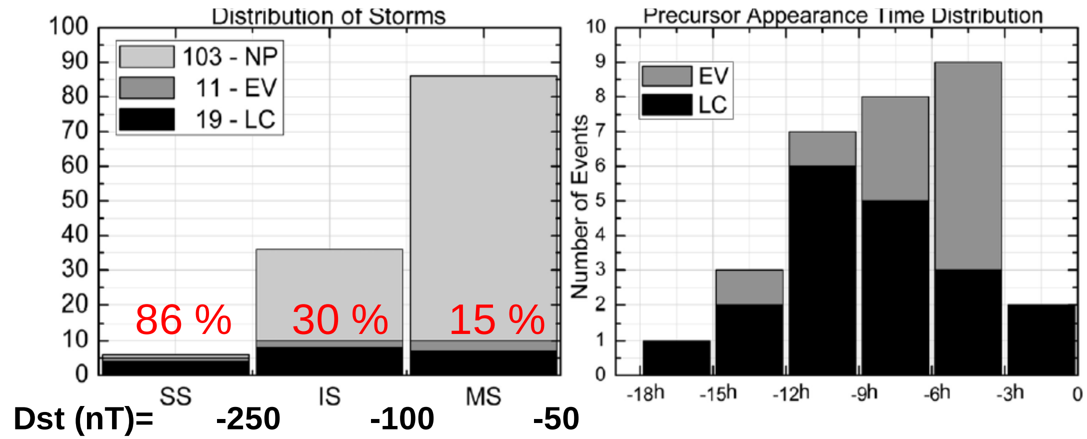


**Leerungnavarat+, ApJ 593, 2003**

**Rockenbach+, GRL 38, 2011**

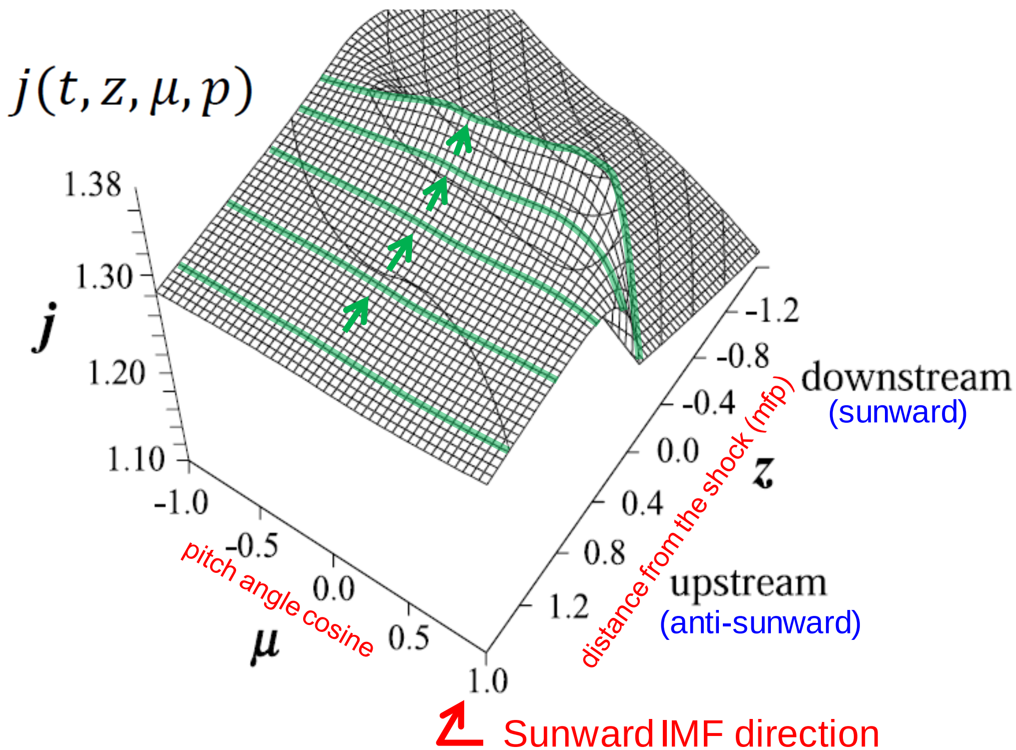


- **GMDN with better sky coverage is capable for detecting more precursors.**
- **The precursor is seen as the deficit intensity of CRs arriving from the sunward IMF.**

  **loss-cone (LC) precursor**
- **CRs reflected and accelerated by the approaching shock are also observed as an excess intensity.**

  **precursory excess**

# Numerical solutions

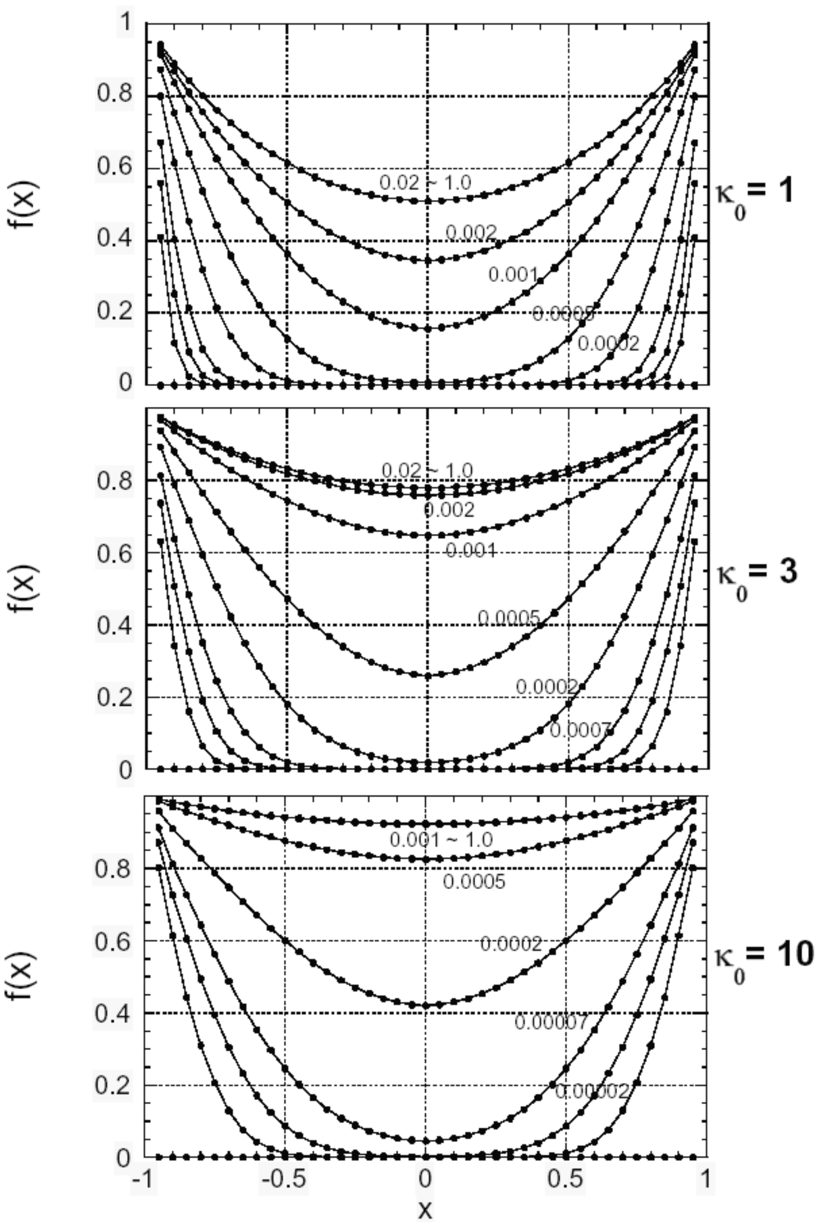


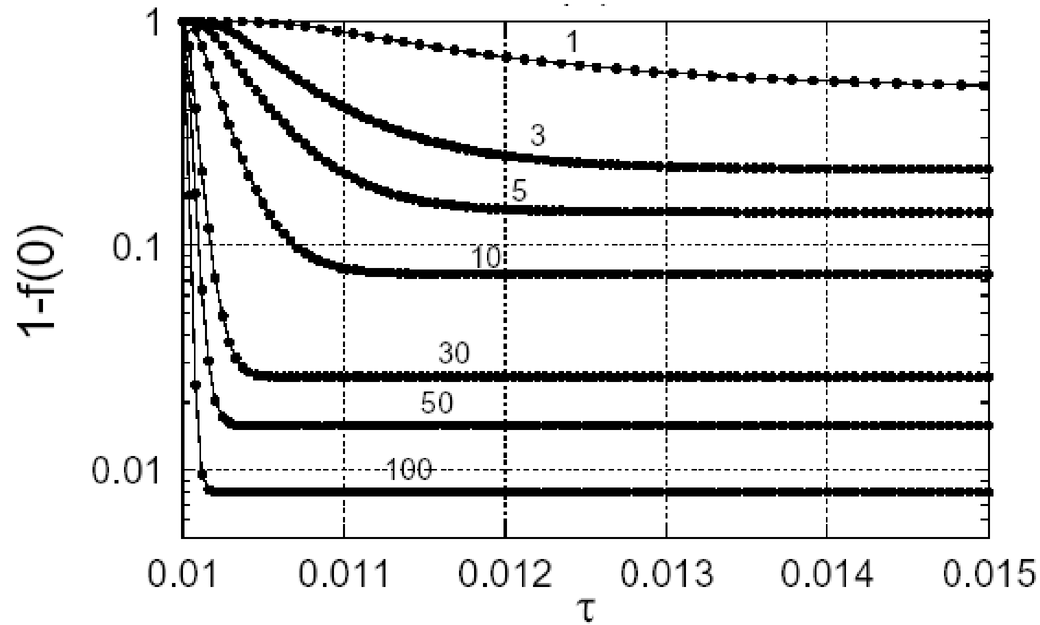


- $\kappa_0$ appropriate to the observed FD size is 10 ~ 50.
- f (x) rapidly becomes stationary, much earlier than the 1st contact with Earth at t=1.
- We use stationary f (x) for best-fitting.

# Stationary solution

$$\frac{\partial^2 f}{\partial x^2} + \frac{1}{x}\frac{\partial f}{\partial x} = \Gamma f \qquad : \Gamma = \frac{2(2+\gamma)}{3\kappa_0}$$

*f(x)* is given by a polynomial expression….

$$f(x) = \sum_{n=0}^{\infty} a_n x^n \qquad \begin{aligned} a_n &= \frac{\Gamma}{n^2} a_{n-2} && : n = 0, 2, 4\cdots \\ &= 0 && : n = 1, 3, 5\cdots \end{aligned}$$

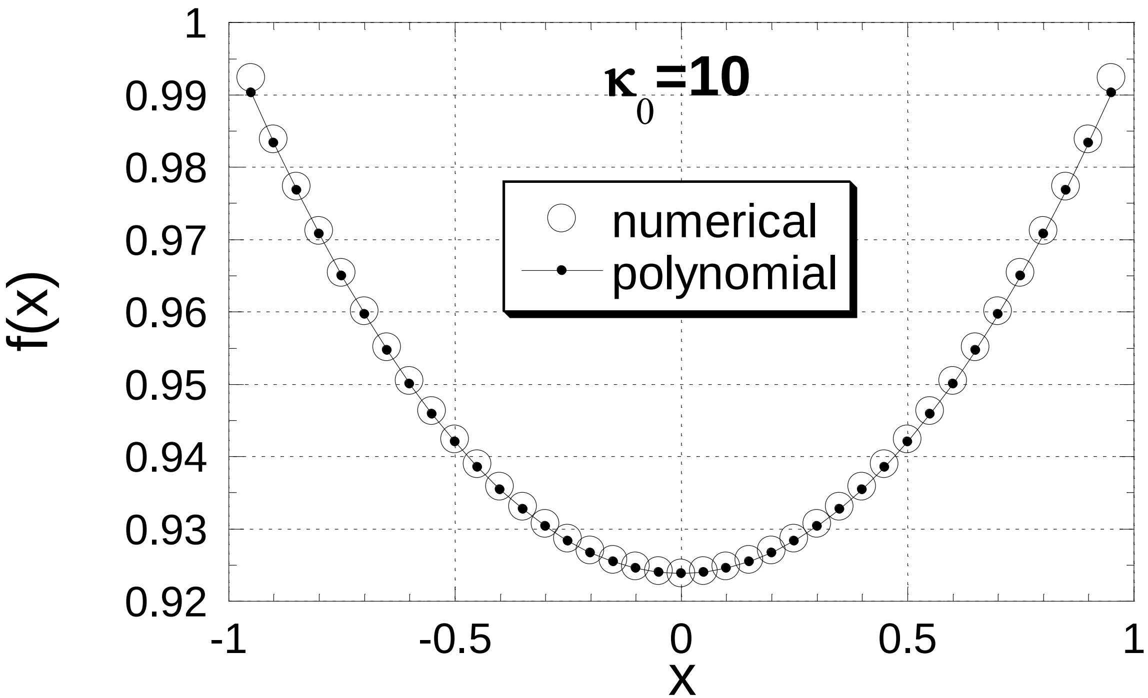


Use polynomial f(x)（n≦6）
for best-fitting to the data

# Best-fitting to the data

## (with stationary f(x) )

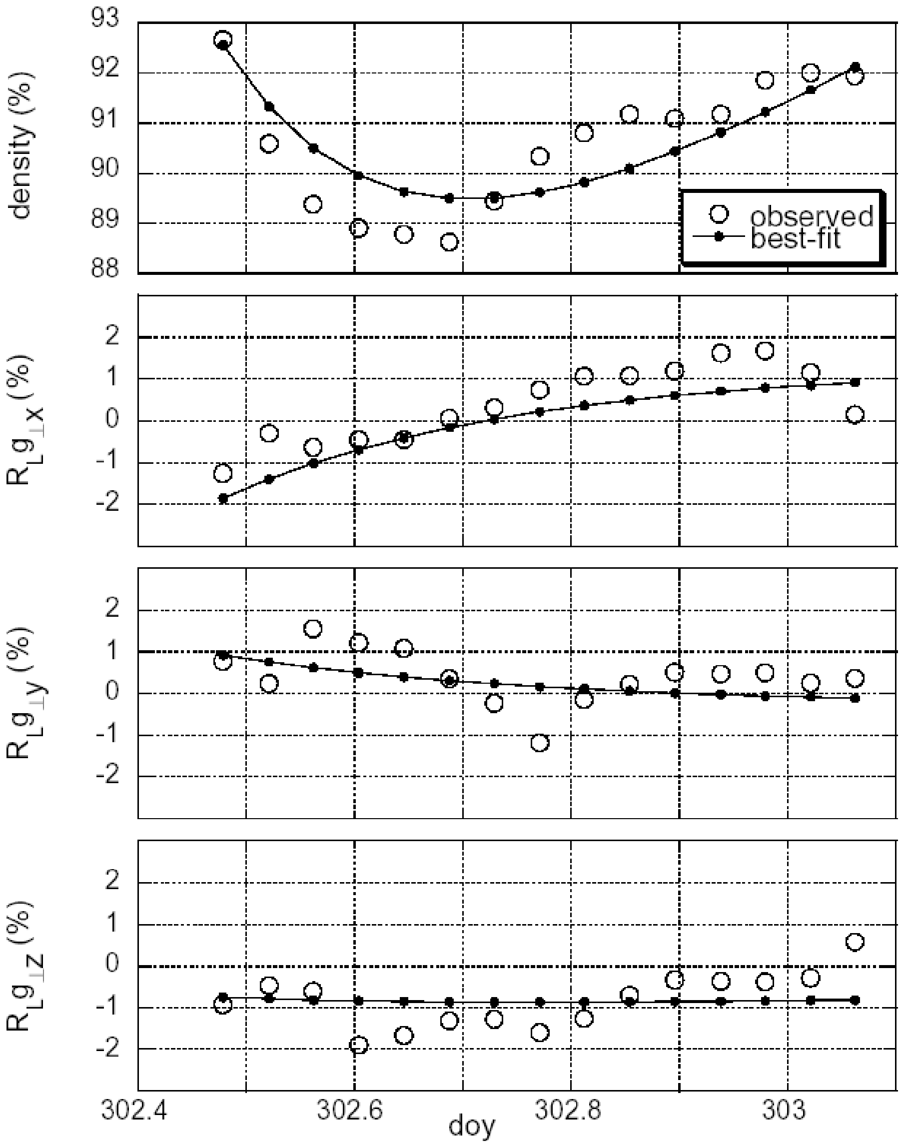


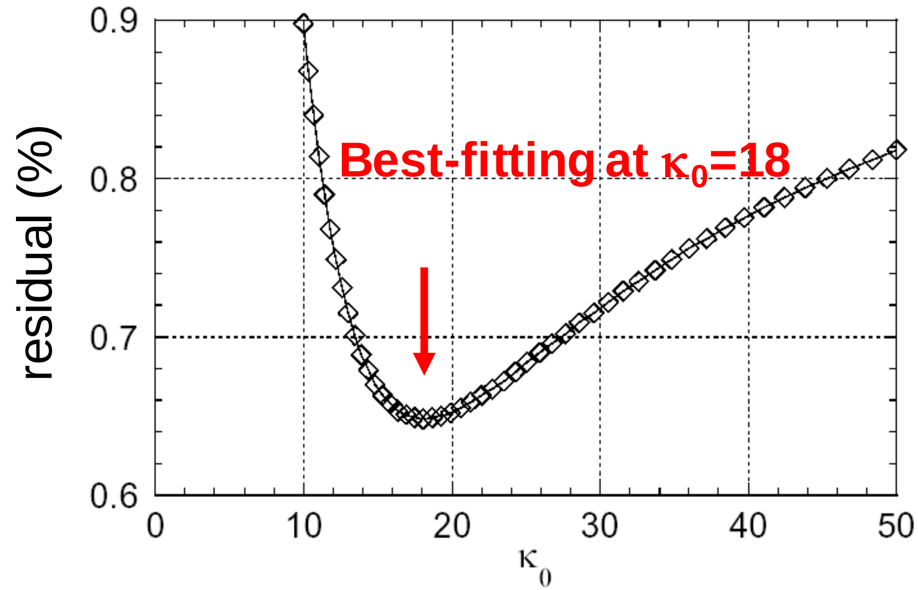


$\kappa_\perp = \kappa_0 v_0 R_0 = 1.6\times10^{21}$ (cm$^2$/s)

($v_0$=0.21 AU/day, $R_0$=0.17 AU)

$\kappa_{//} \sim 3.0\times10^{23}$ (cm$^2$/s) for muon

$\therefore \kappa_\perp / \kappa_{//} \sim 0.005$ for muon

(Munakata+, 2006)

# Galactic Cosmic Rays (GCRs)

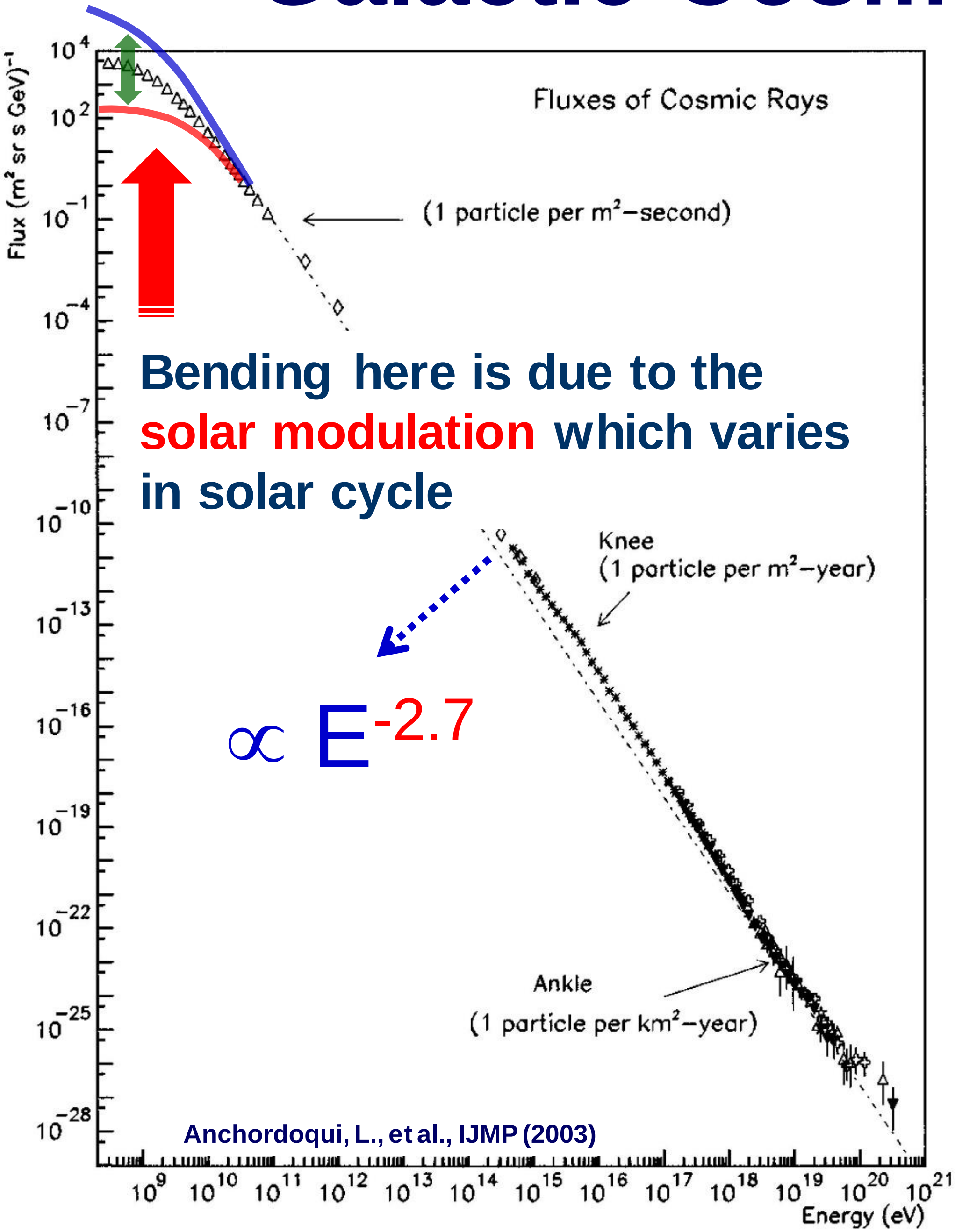


- ~85 % **protons**
- ~10 % **helium nuclei**
- a few % **heavier nuclei**
- ~1 % **electrons**

**Observables**

- Energy spectrum
- Elementary & isotopic compositions
- **Isotropic intensity** (**GCR density**)
- **Anisotropy** (**GCR streaming**)

# Solar activity cycle & GCR

(solar magnetic dipole reverses every 11 years)

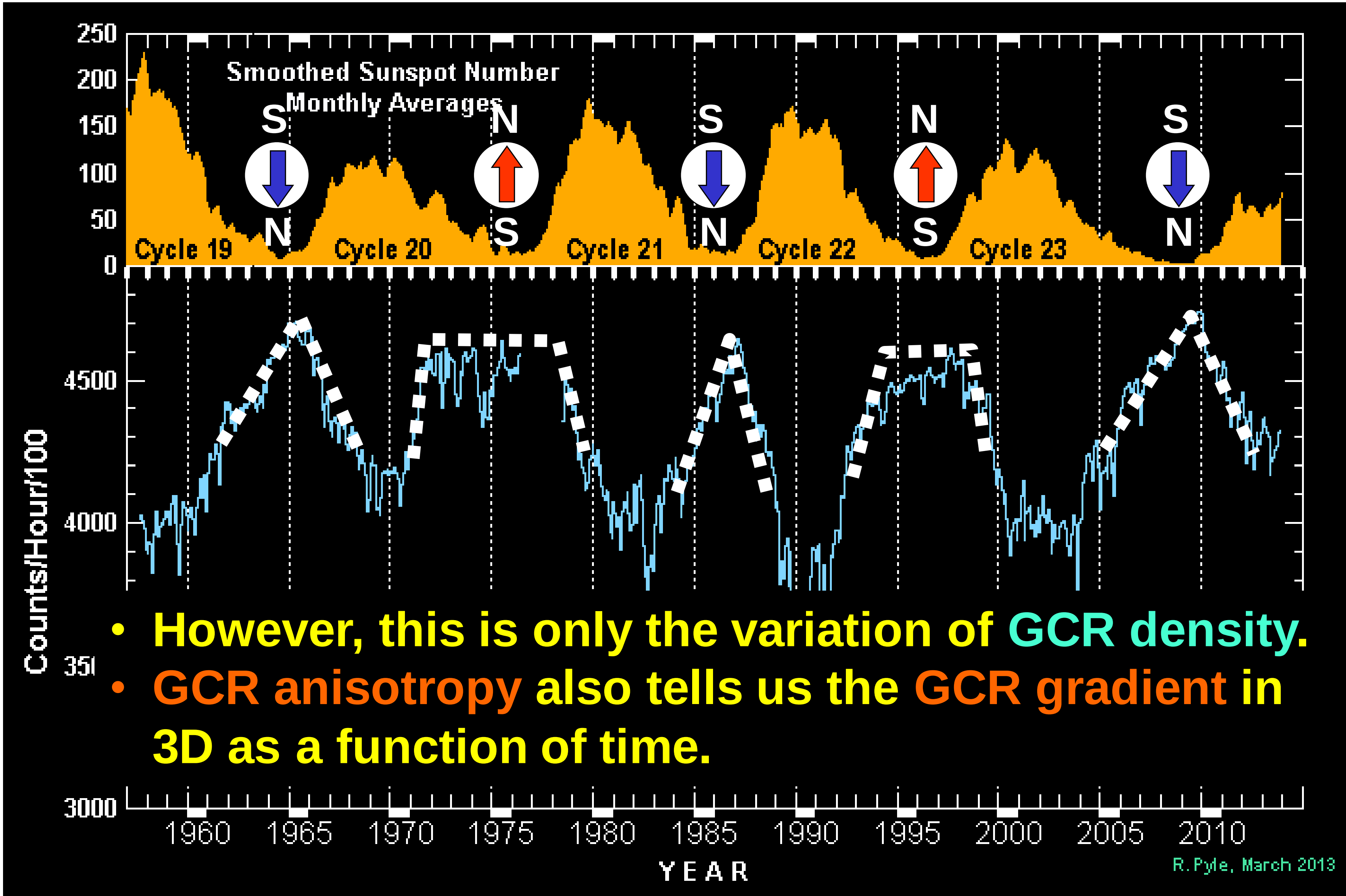


- However, this is only the variation of GCR density.
- GCR anisotropy also tells us the GCR gradient in 3D as a function of time.

# Cosmic ray observations with muon detector & neutron monitor

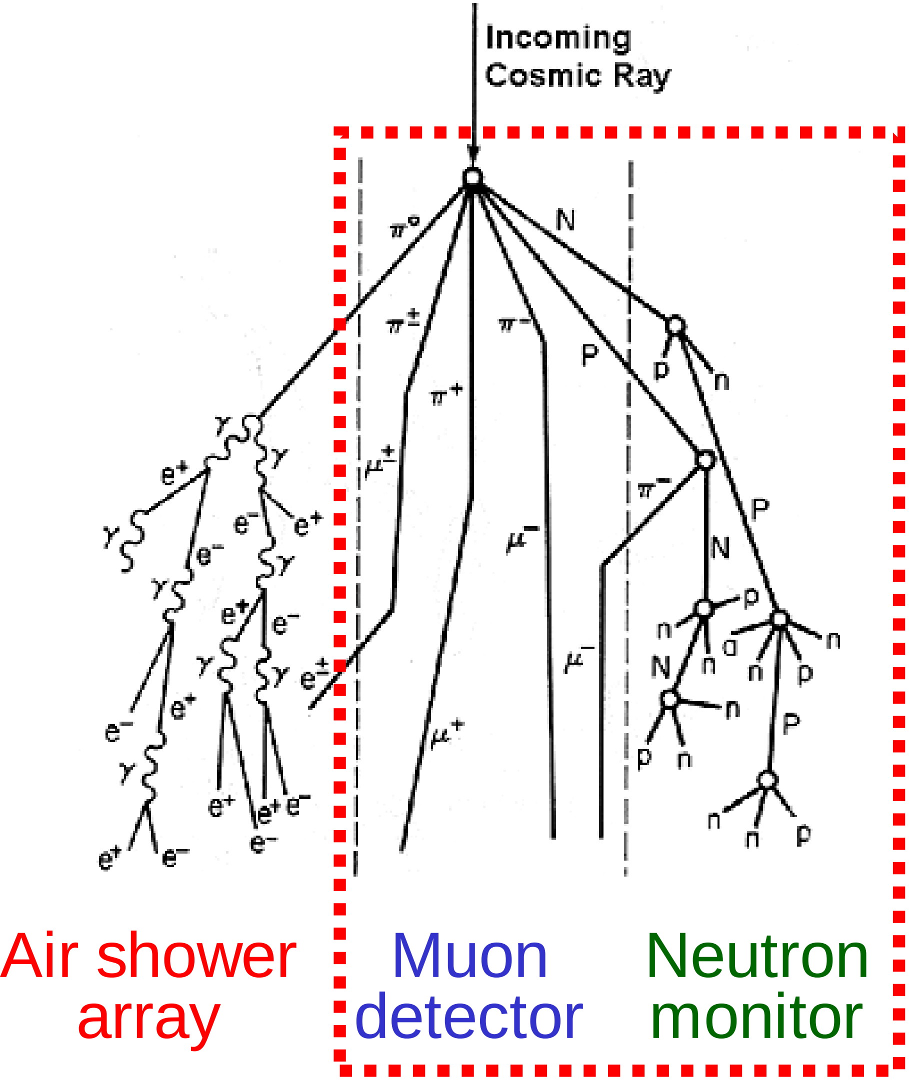


- Ground-based detectors measure byproducts of the interaction of primary cosmic rays (mostly protons) with Earth's atmosphere.
- Neutron monitor detects neutrons produced by **elastic scattering** from atmospheric nuclei.
- Muon detector measures muons produced by **inelastic (strong) interaction**.

$E_{1ry}$ (GeV) = **50~100**, **1~30** → observations of **inner heliosphere** & **space weather**

# Global Muon Detector Network (GMDN)

**Kaz. Munakata**[1], C. Kato[1], S. Yasue[1], J. W. Bieber[2], P. Evenson[2], T. Kuwabara[2], M. R. DaSilva[3], A. Dal Lago[3], N. J. Schuch[4], M. Tokumaru[5], M. L. Duldig[6], J. E. Humble[6], I. Sabbah[7,8], H. K. Al Jassar[9], M. M. Sharma[9]

**GMDN collaboration**

[1] **Shinshu University**, **JAPAN**
[2] Bartol Research Institute, **USA**
[3] INPE, **BRAZIL**
[4] CRS/INPE, **BRAZIL**
[5] STE Laboratory, **JAPAN**
[6] University of Tasmania, **AUSTRALIA**
[7] College of Health Science, **KUWAIT**
[8] Alexandria University, **EGYPT**
[9] Kuwait University, **KUWAIT**

**15** people from **9** institutes in **6** countries working with **4** muon detectors in operation at…

**Nagoya**, **Hobart**, **São Martinho**, **Kuwait**

**(36 m²)** **(16 m²)** **(32 m²)** **(9 m²)**

# Geomagnetic E-W effect

Looking equatorial plane from north pole…

B directs from south to north on the equatorial plane

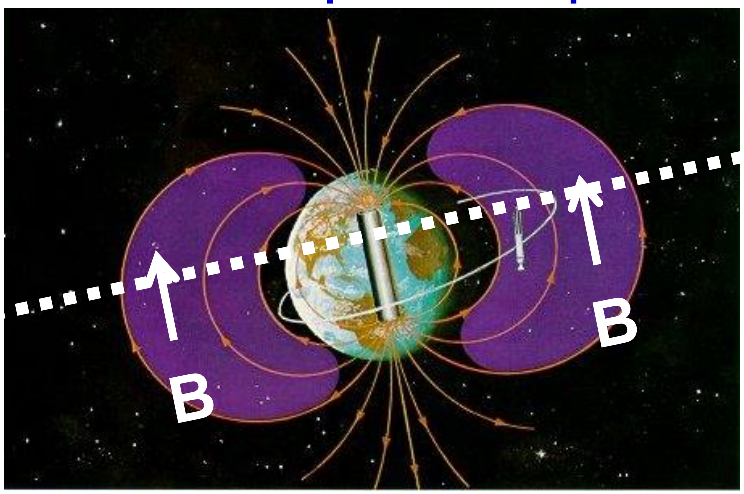


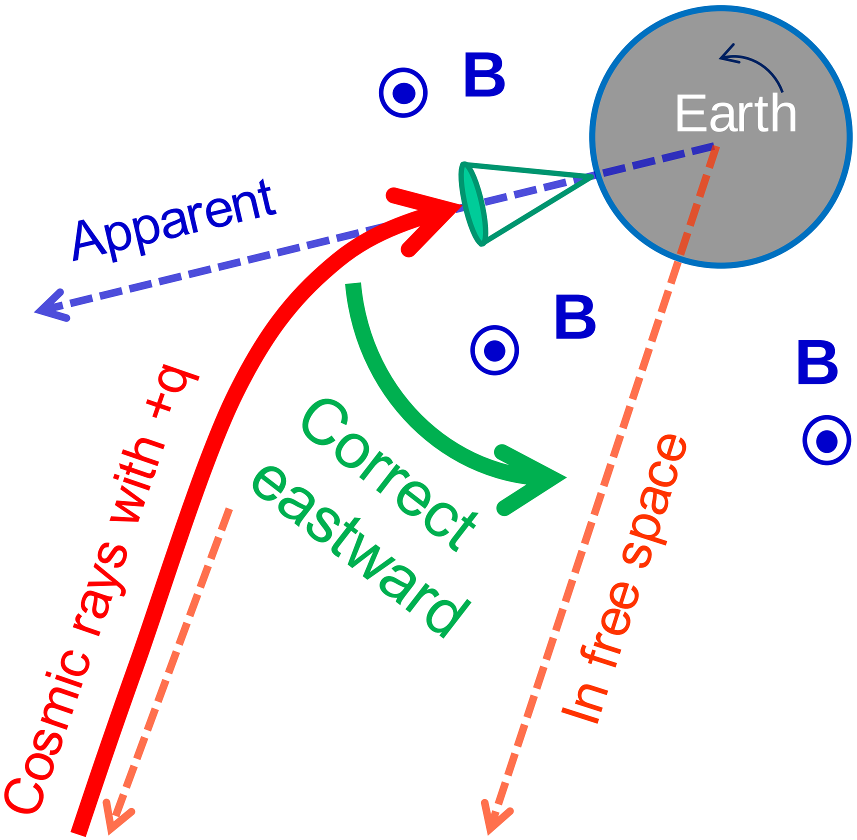

# Spread of viewing direction

(only for vertical channel of PS detector)

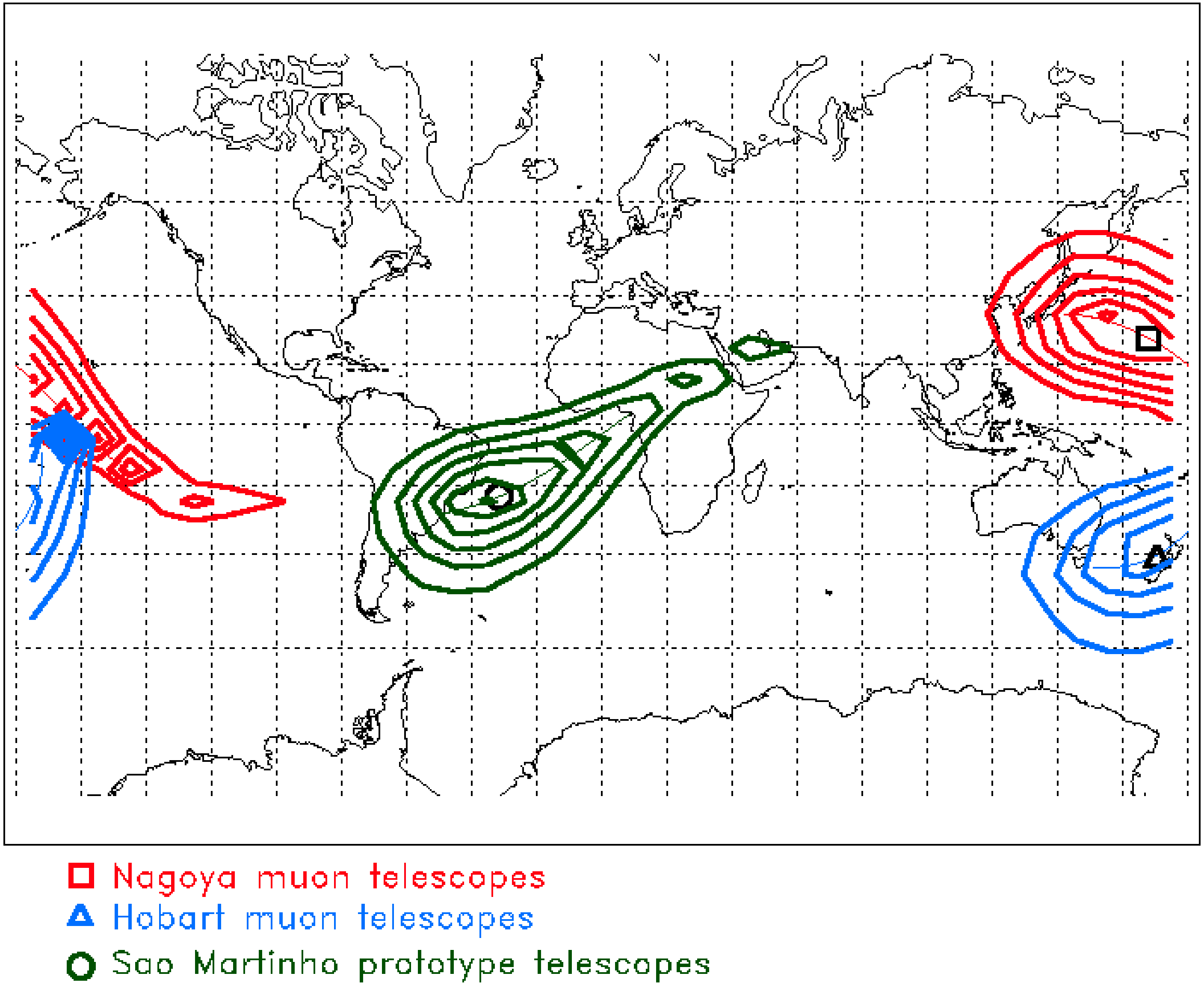

# Drift model (Jokipii et al., ApJ, 213, 1977)

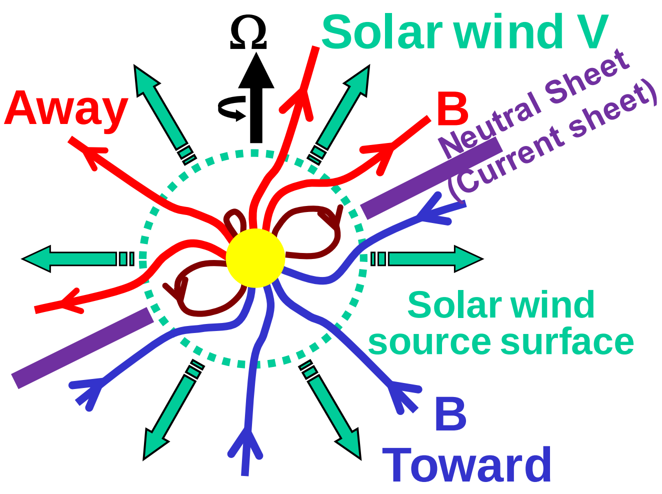


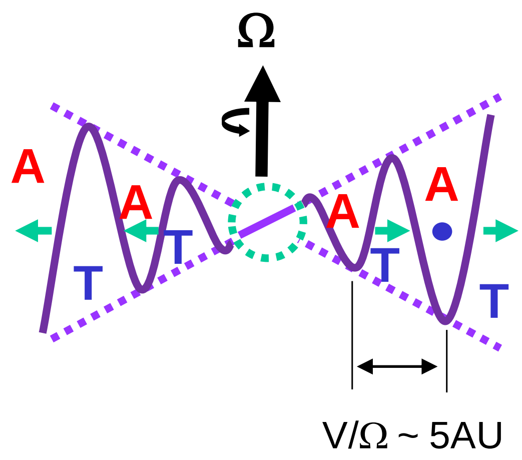



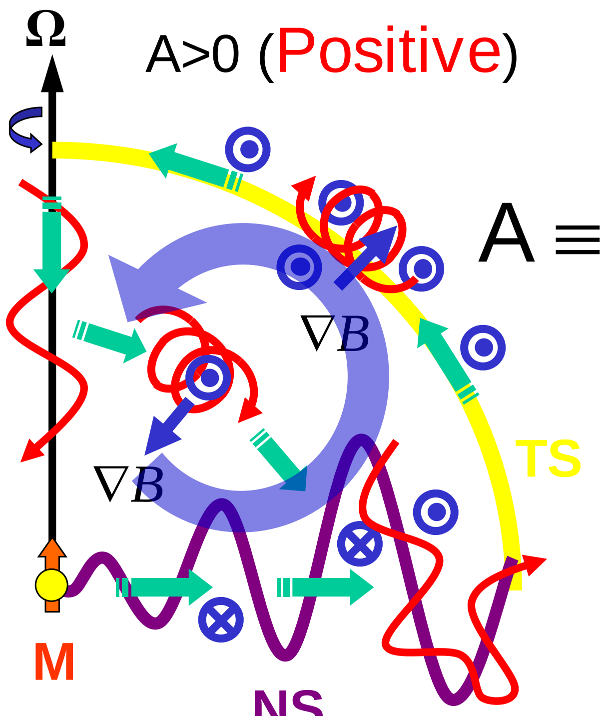


$$A \equiv \Omega \cdot M$$

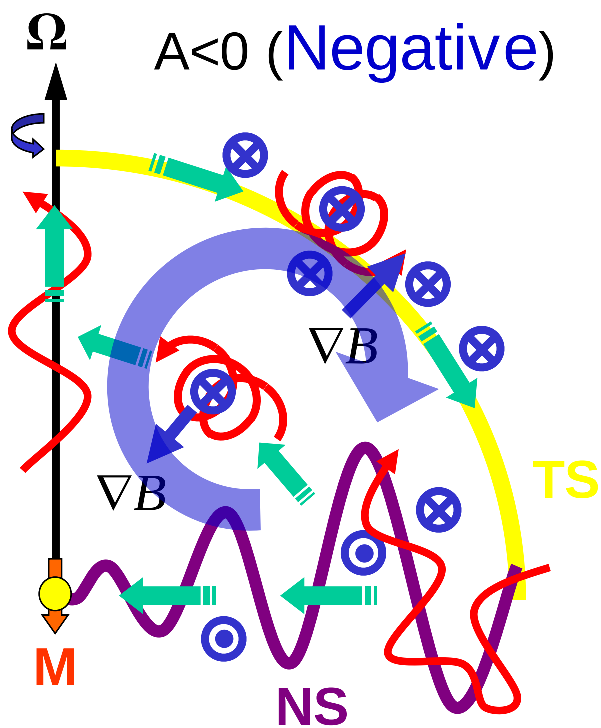

# Drift model predictions

(Kota & Jokipii, 265, 573, 1983)

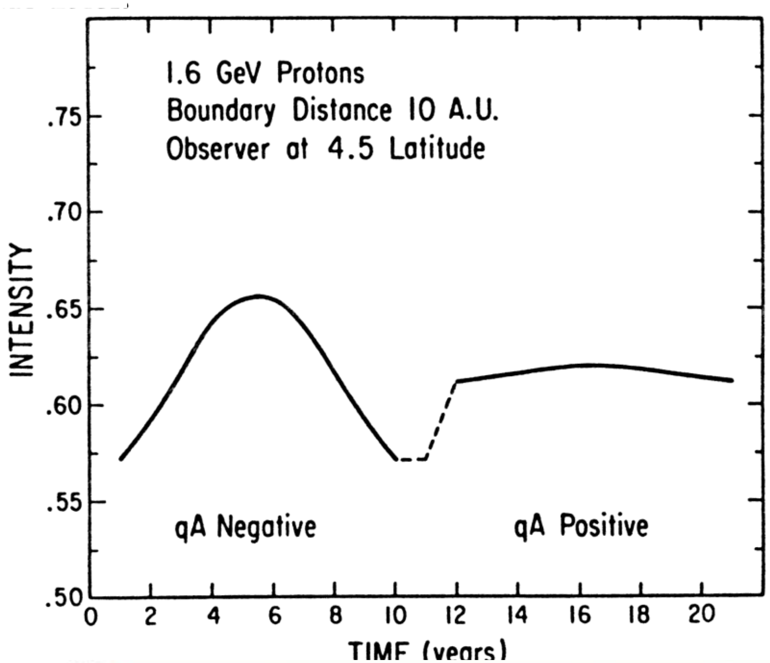


- Reproduces the solar cycle variation of GCR density from the variation of NS tilt-angle.
- Predicts local minimum (maximum) of GCR density on the NS for A>0 (A<0).

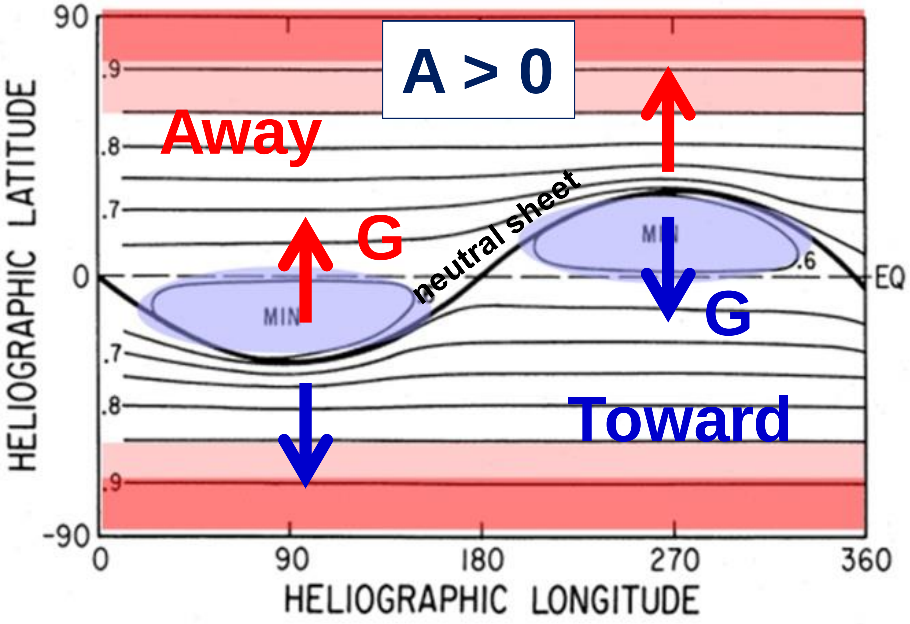


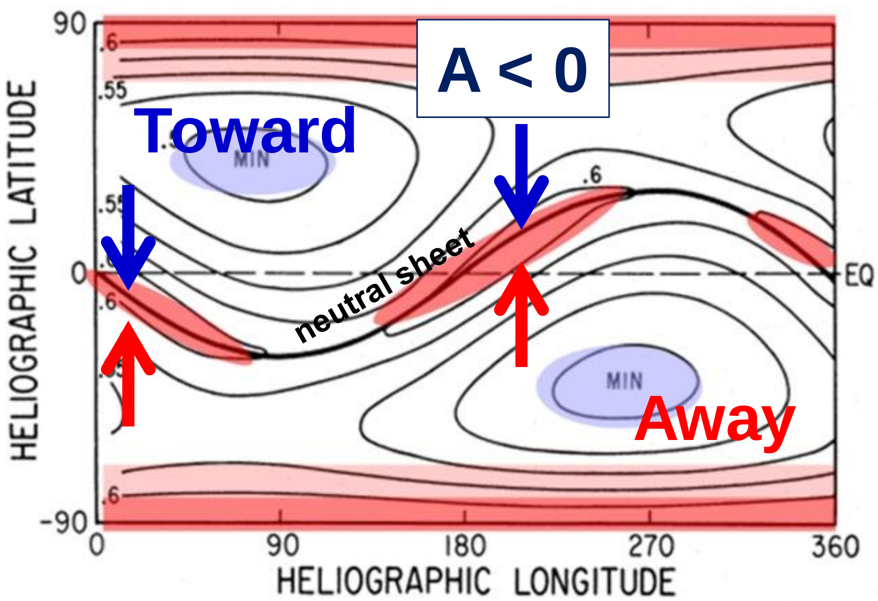

# Solar activity cycle & GCR

(solar magnetic dipole reverses every 11 years)

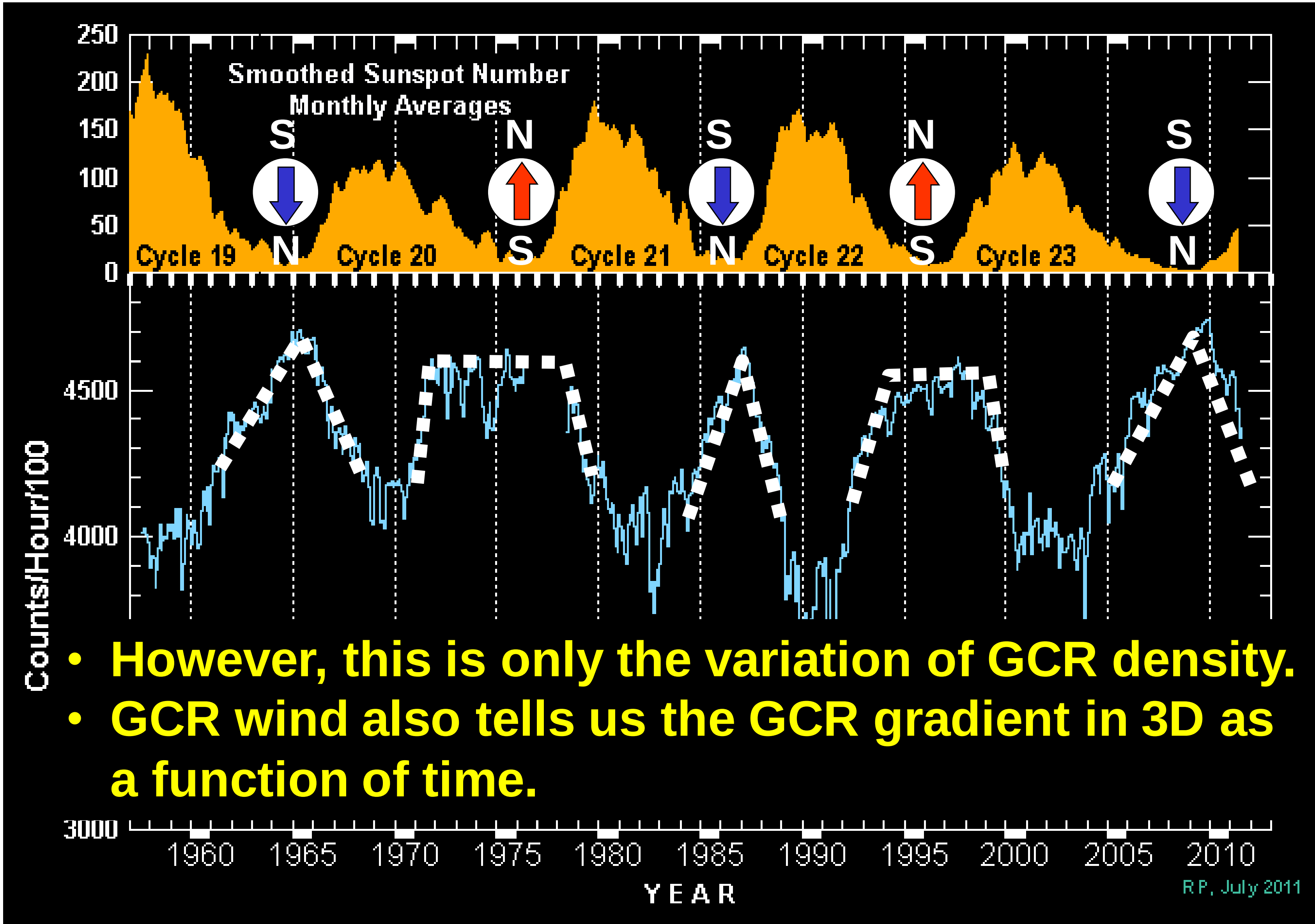


- However, this is only the variation of GCR density.
- GCR wind also tells us the GCR gradient in 3D as a function of time.

# Solar cycle variation of gradient (I)

## NS gradient

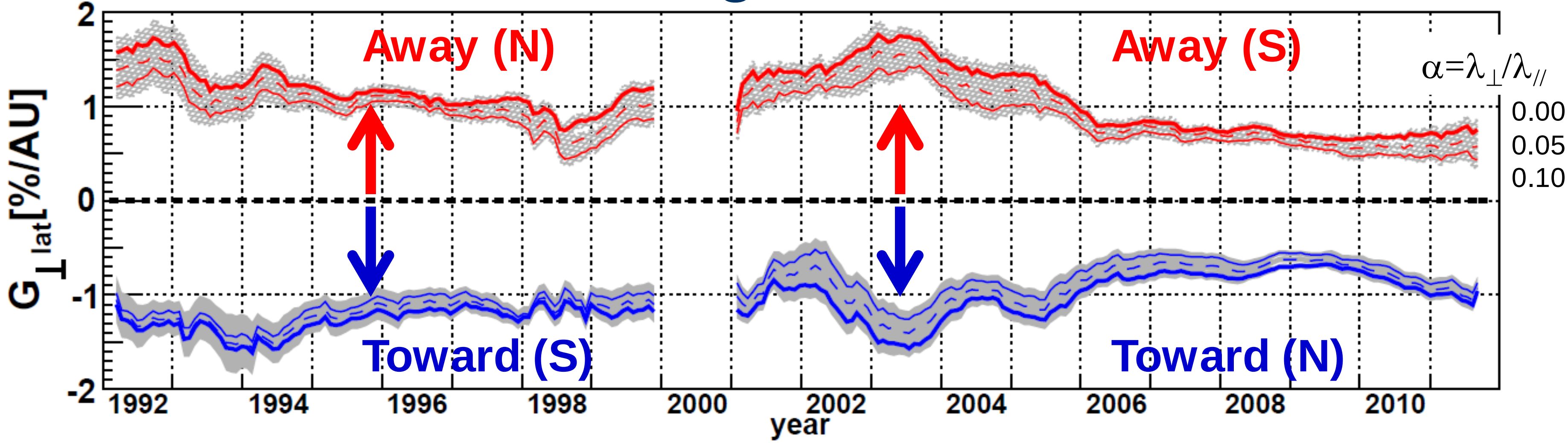


## Bi-directional gradient $(G_N - G_S)/2$

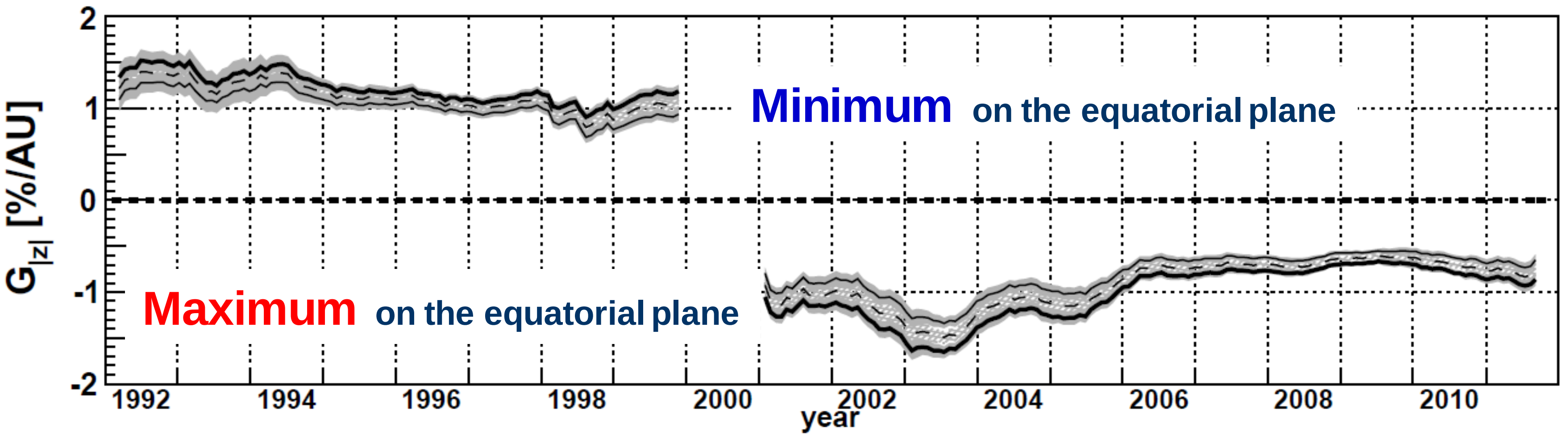

# Solar cycle variation of gradient (II)

## Radial gradient

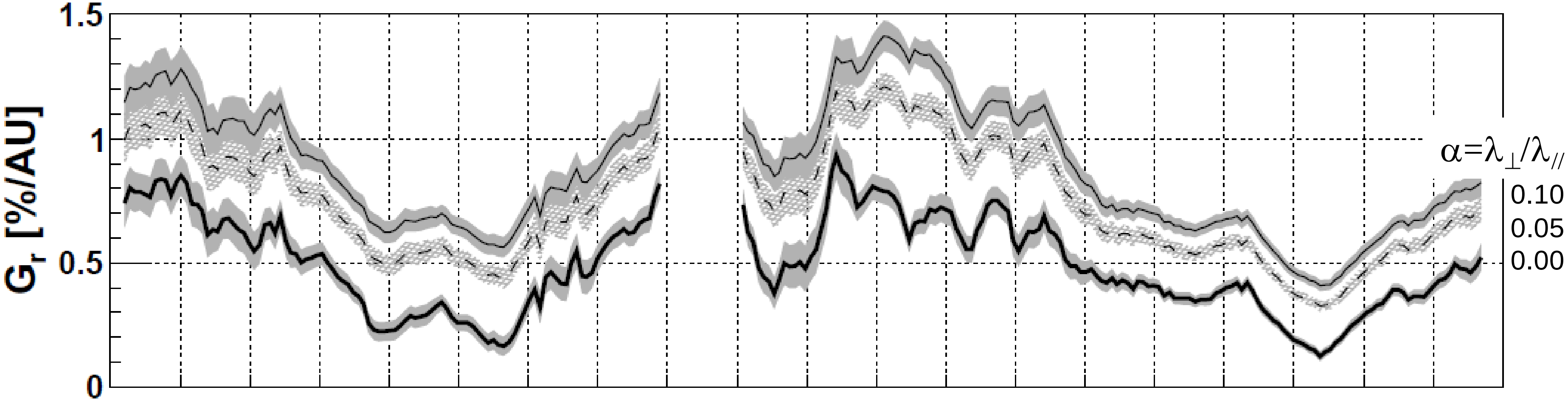


- **Observed radial gradient remains positive indicating the dominant convection effect by the solar wind.**
- **Observed radial gradient shows a clear 11y solar cycle variation.**
- **Shows no clear 22y variation predicted by drift model.**

# Drift effect on the GCR transport

$$\boldsymbol{\kappa} = \boldsymbol{\kappa}^{S} + \boldsymbol{\kappa}^{A} = \begin{bmatrix} \kappa_{\parallel} & 0 & 0 \\ 0 & \kappa_{\perp} & 0 \\ 0 & 0 & \kappa_{\perp} \end{bmatrix} + \begin{bmatrix} 0 & 0 & 0 \\ 0 & 0 & +\kappa_T \\ 0 & -\kappa_T & 0 \end{bmatrix}$$

$$\boldsymbol{\nabla} \cdot \left( \boldsymbol{\kappa}^{A} \frac{\partial U}{\partial \mathbf{r}} \right) = \frac{\partial \kappa_T}{\partial y}\frac{\partial U}{\partial z} - \frac{\partial \kappa_T}{\partial z}\frac{\partial U}{\partial y} \equiv -\boxed{\mathbf{v}_{\mathrm{D}}} \cdot \boldsymbol{\nabla} U$$

drift velocity

$$\mathbf{v}_{\mathrm{D}} = \left(0, \frac{\partial \kappa_T}{\partial z}, -\frac{\partial \kappa_T}{\partial y}\right) = \frac{pv}{3Ze}\left(\frac{1}{B^2}\underline{\boldsymbol{\nabla} \times \mathbf{B}} + \frac{1}{B^4}\underline{\mathbf{B} \times \boldsymbol{\nabla} B^2}\right) \quad \nabla \cdot \mathbf{v}_{\mathrm{D}} = 0$$

curvature drift　　gradient drift

$$\frac{\partial U}{\partial t} + \boldsymbol{\nabla} \cdot \left( \frac{2+\gamma}{3} U \mathbf{V}_{\mathrm{SW}} - \boldsymbol{\kappa}^{S} \cdot \boldsymbol{\nabla} U + \boxed{\mathbf{v}_{\mathrm{D}} U} \right) = -\frac{\partial}{\partial p}\left(\frac{1}{3} p \mathbf{V}_{\mathrm{SW}} \cdot \boldsymbol{\nabla} U\right)$$

drift streaming

**Reverses with B polarity ⇒ 22y variation, T/A dependence**

**Charge dependent modulation ⇒ 11/22y change of $e^+/e^-$, $\bar{p}/p$**

# Propagation eqs. of atmospheric muons

$N(E,y)$ : number of nucleons (p, n)

$$\frac{\mathrm{d}N(E,\ y)}{\mathrm{d}y} = -\frac{1}{\lambda_N(E)}N(E,y) + \int_E^{E_0} \frac{F_{NN}(E,E')}{\lambda_{NN}(E')\cdot E}N(E',y)\mathrm{d}E' \quad : \ y = x\ \sec\theta$$

N → N, X N → N

$\pi(E,y)$ : number of pions

$$\frac{\mathrm{d}\pi(E,\ y)}{\mathrm{d}y} = -\left(\frac{1}{\lambda_\pi(E)} + \frac{\varepsilon_\pi(y)}{E\cdot y}\right)\pi(E,y)$$

π → π, X π → μ decay (decrease of π)

$$+\int_E^{E_0} \frac{F_{N\pi}(E,E')}{\lambda_N(E')\cdot E}N(E',y)\mathrm{d}E' + \int_E^{E_0} \frac{F_{\pi\pi}(E,E')}{\lambda_\pi(E')\cdot E}\pi(E',y)\mathrm{d}E'$$

N → π π → π

$\mu(E,y)$ : number of muons

$$\frac{\mathrm{d}\mu(E,y)}{\mathrm{d}y} = \int_E^{E(m_\pi/m_\mu)^2} \frac{\varepsilon_\pi}{y}\cdot\pi(E',y)\frac{\mathrm{d}E'}{p'^2}\left\{1-\left(\frac{m_\mu}{m_\pi}\right)^2\right\}^{-1}$$

π → μ decay (increase of μ)

$$\frac{\mathrm{d}P_\mu(E,y)}{\mathrm{d}y} = -\frac{\varepsilon_\mu}{E\cdot y}\cdot P_\mu(E,y) \qquad E = E_f + \beta(y_f - y)$$

μ → e decay (decrease of μ) Ionization loss of μ

# Muon response fn. $R(p, x, \theta, p_{\mu c})$

$J(p)$ : Energy spectrum of primary GCRs

$Y(p, x, \theta, p_{\mu})$ : No. of μ with $p_{\mu}$ produced from a **primary GCR with p** (Yield fn.)

Momentum of 1ry GCR

$$R(p, x, \theta, p_{\mu c}) = \int_{p_{\mu c}}^{\infty} J(p) \cdot Y(p, x, \theta, p_{\mu}) dp_{\mu}$$

Parameters of muon detector

Momentum of muons

R [/m²/s/sr/GV] is given in a table by Murakami (1976)

$x$ : Atmospheric depths ×4 : 550, 720, 940, 1030 [g/cm²]

$\theta$ : Zenith angles ×5 : 0, 16, 32, 48, 64 [°]

$p_{\mu c}$ : Muon threshold energies ×26 :0.178 ~ 5620 [GeV]

# Energy responses of NM and GMDN to primary GCRs

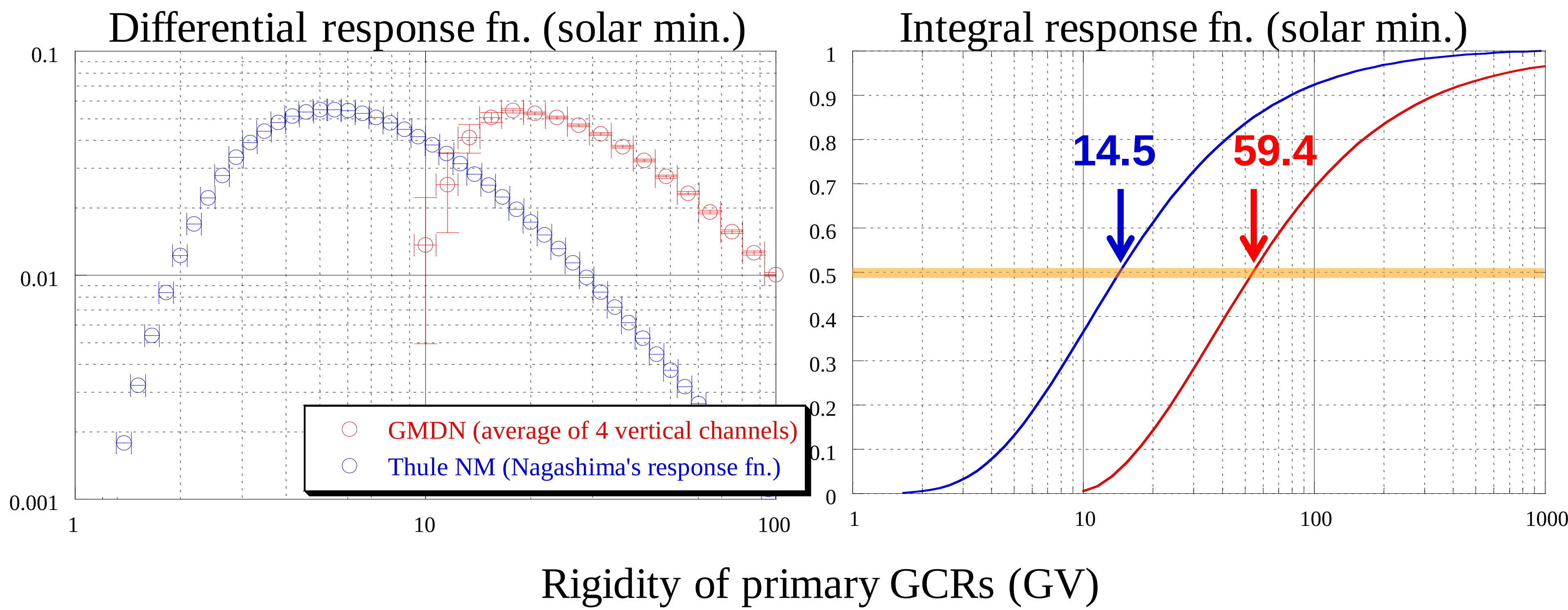

# Muon count rate

$$I(x) = \sum_k \Delta(S\Omega)_k \int_{p_c(\theta_k,\phi_k)}^{\infty} R(p, x, \theta_k, p_{\mu c}(\theta_k, \phi_k))\, dp$$

$\theta_k, \phi_k$ : zenith and azimuth angles $p_c(\theta_k, \phi_k)$: geomagnetic cut-off rigidity

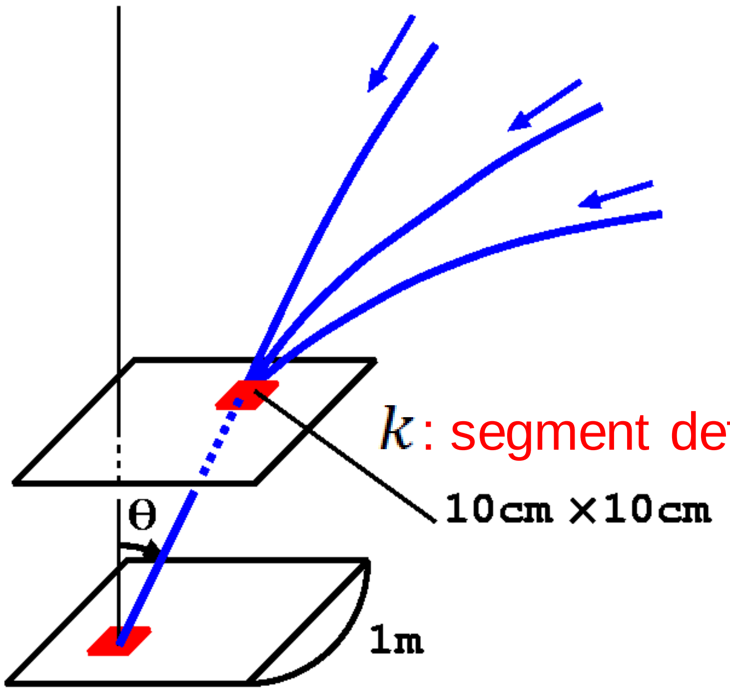


$k$ : segment detector

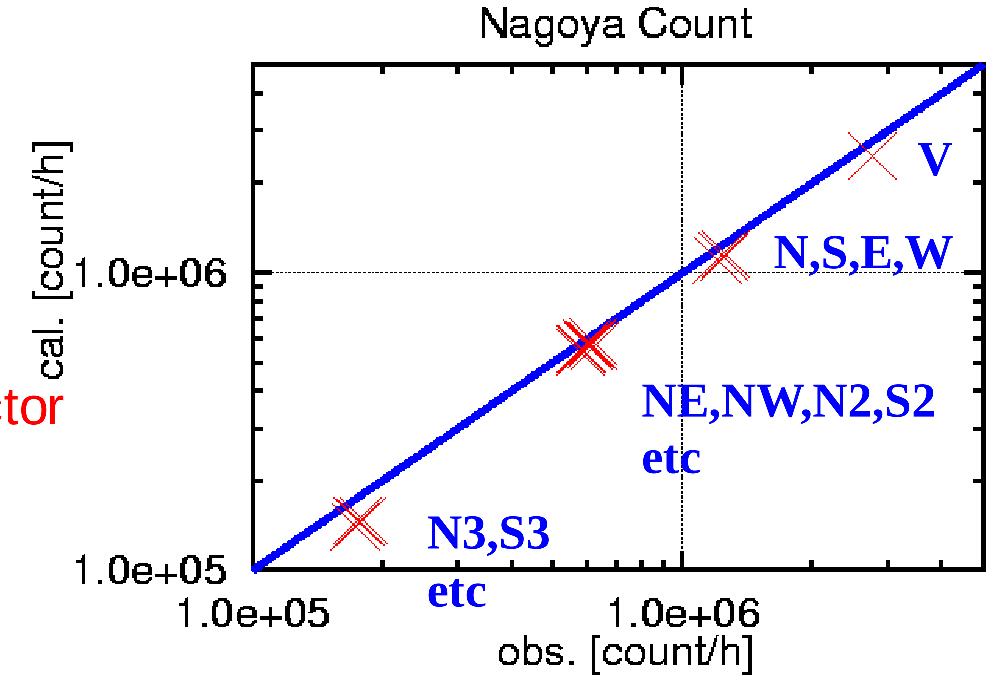

# Response function: $R(p, x, \theta, p_{\mu c})$ [/m$^2$/s/sr/GV]

$J(p)$ : GCR rigidity spectrum

$Y(p, x, \theta, p_\mu)$ : No. of muons with $p_\mu$ produced by a GCR with p（Yield function）

GCR

$$R(p, x, \theta, p_{\mu c}) = \int_{p_{\mu c}}^{\infty} J(p) \cdot Y(p, x, \theta, p_\mu) dp_\mu$$

Muon detector

$x$（atmospheric depth）: 550, 720, 940, 1030 [g/cm$^2$]

$\theta$（zenith angle）: 0, 16, 32, 48, 64 [°]

$p_{\mu c}$（muon threshold rigidity）: 26 values in 0.178 ~ 5620 [GV]

$$
\begin{aligned}
D(t) &= \textstyle\sum_{n=0}^{\infty}\sum_{m=0}^{n}(A_n^m \cos m\omega t + B_n^m \sin m\omega t) \\
&= A_0^0 c_0^0 + A_1^0 c_1^0 + (c_1^1 x_1^1 + s_1^1 y_1^1)\cos\omega t + (-s_1^1 x_1^1 + c_1^1 y_1^1)\sin\omega t \\
&= A_0^0 c_0^0 + x_1^1(c_1^1 \cos\omega t - s_1^1 \sin\omega t) + y_1^1(s_1^1 \cos\omega t + c_1^1 \sin\omega t) + A_1^0 c_1^0
\end{aligned}
$$

$$
\begin{aligned}
F(\chi) &= \textstyle\sum_{n=0}^{\infty}\sum_{m=0}^{n}\eta_n P_n^m(\cos\theta_R) P_n^m\left(\cos\theta_J\right)\cos m\left(\alpha_J - \alpha_R\right) \\
&= \textstyle\sum_{n=0}^{\infty}\sum_{m=0}^{n}\eta_n P_n^m(\cos\theta_R) P_n^m\left(\cos\theta_J\right)\cos m\omega(t - t_R) \\
&= \textstyle\sum_{n=0}^{\infty}\sum_{m=0}^{n}(x_n^m \cos m\omega t + y_n^m \sin m\omega t)
\end{aligned}
$$

$$
\begin{pmatrix} A_n^m \\ B_n^m \end{pmatrix} = \begin{pmatrix} c_n^m & s_n^m \\ -s_n^m & c_n^m \end{pmatrix} \begin{pmatrix} x_n^m \\ y_n^m \end{pmatrix}
$$

$$
c_{n\,i(k,l)}^{m} = \frac{1}{I_{i(k,l)}^{cal}} (S\Omega)_{k,l} \int_{P_c}^{\infty} R(p, x, \theta_{k,l}, p_{\mu c}(\theta_{k,l}, \phi_{k,l})) P_n^m\left(\cos\theta_{k,l}^{or}(p)\right) \cos m\left(\psi_{k,l}^{or}(p) - \psi_i^{st}\right) dp
$$

$$
s_{n\,i(k,l)}^{m} = \frac{1}{I_{i(k,l)}^{cal}} (S\Omega)_{k,l} \int_{P_c}^{\infty} R(p, x, \theta_{k,l}, p_{\mu c}(\theta_{k,l}, \phi_{k,l})) P_n^m\left(\cos\theta_{k,l}^{or}(p)\right) \sin m\left(\psi_{k,l}^{or}(p) - \psi_i^{st}\right) dp
$$

# possible Canadian muon detectors

## Parameters set for calculations

| | Ottawa | Vancouver |
|---|---|---|
| Latitude | 45.4N | 45.2N |
| Longitude | 75.7W | 123.0W |
| Altitude | 70m | 60m |

## Obtained detector response (5m × 5m PRC detector)

| | Ottawa | Vancouver |
|---|---|---|
| Cut-off rigidity | 1.7GV | 2.6GV |
| Median rigidity | 52.4GV | 52.5GV |
| Hourly trigger rate | 6,315,000 | 6,304,000 |

Notes: Using Nagashima's muon response function + IGRF-11 geomagnetic field model (2010). Cut-off and median rigidities are the values at vertical direction

# current GMDN

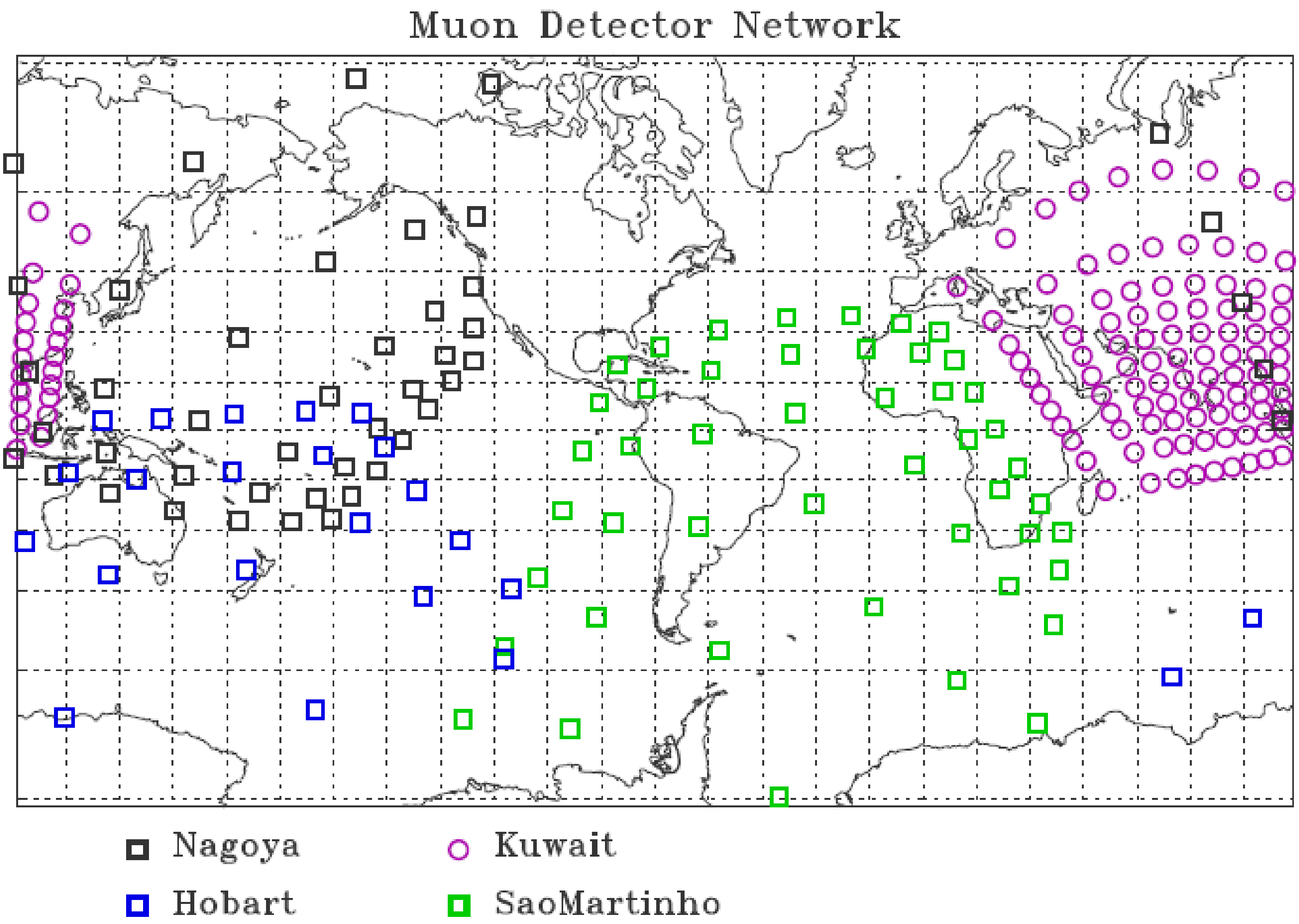

# current GMDN + Ottawa

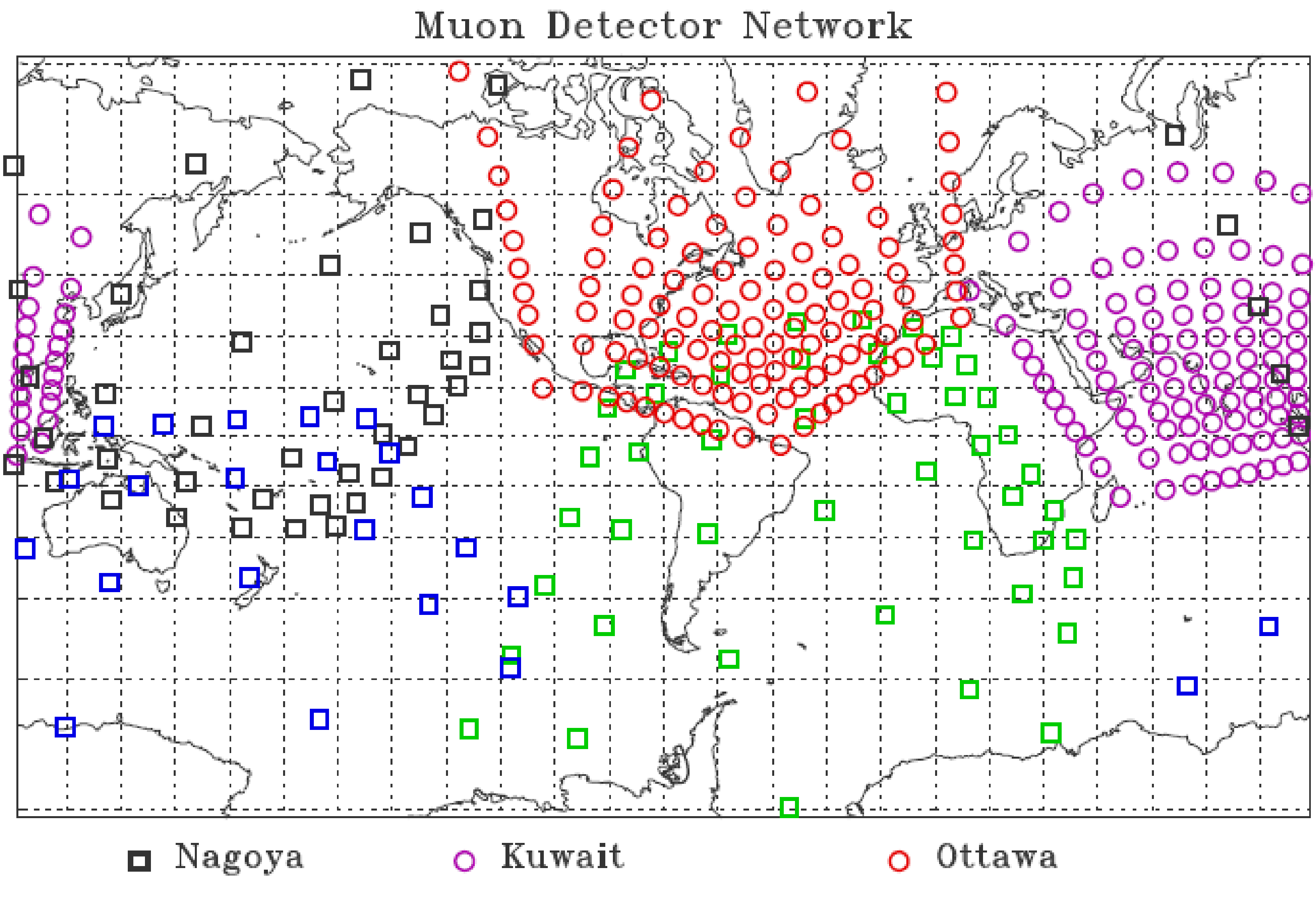

# current GMDN + Vancouver

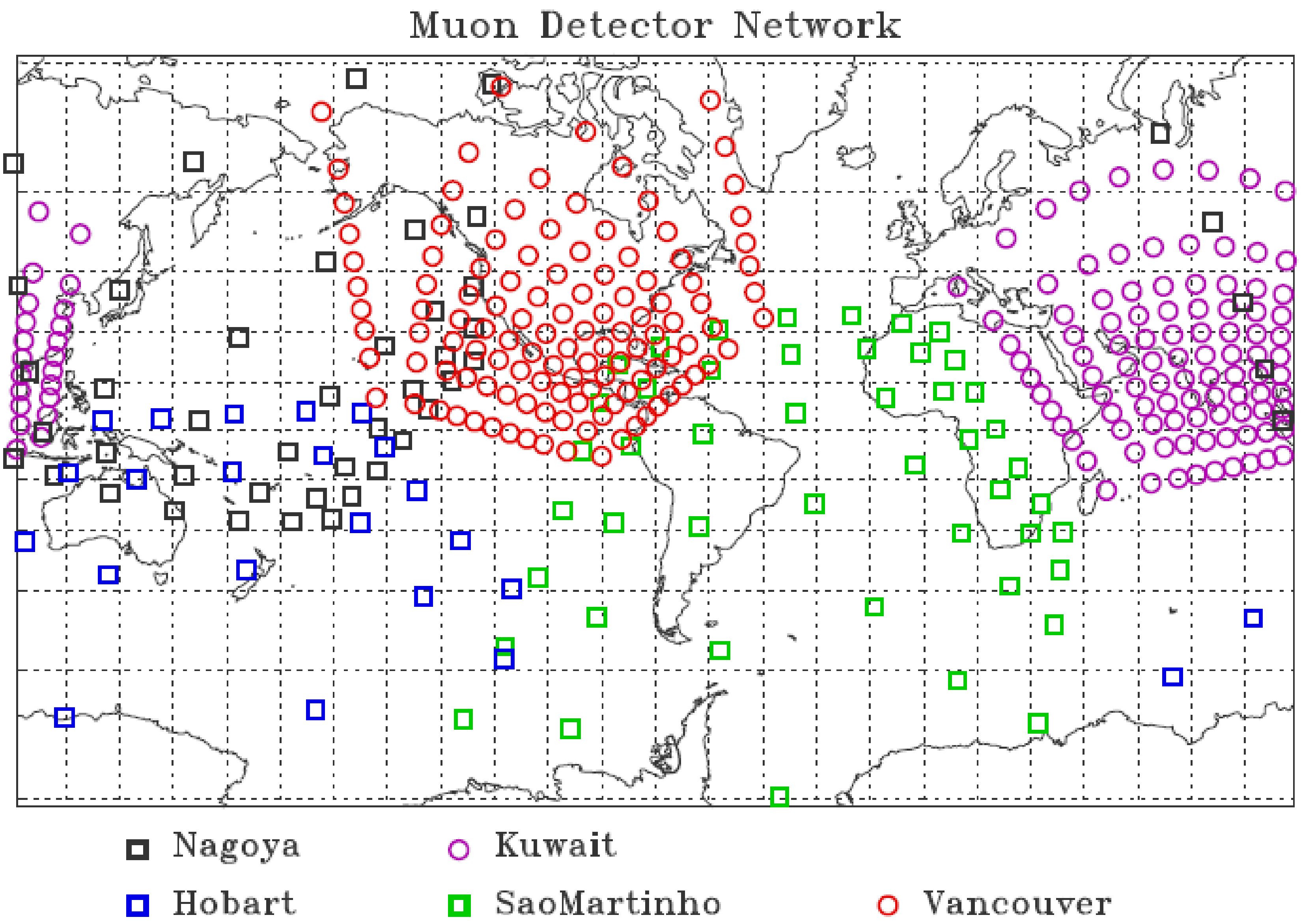

# Cost of 5x5m$^2$ detector with PRCs

| item | Spec. | producer | Cost (USD/¥100) |
|---|---|---|---|
| Proportional counter tube | 5 m long, 0.1 m $\phi$ x200 | CI industry Co. | 90,000 |
| Amplifier board | 50 boards | CI industry Co. | 1,750 |
| Cables (EHT + signal) | 50 pairs | CI industry Co. | 15,000 |
| EHT distributor | | CI industry Co. | 6,500 |
| Steel frame | | CI industry Co. | 14,500 |
| Lead brick | 0.2x0.1x0.5 m$^3$ x1250 | Mitsui Metal Co. | 40,000 |
| FPGA recorder unit | | Shinshu | 6,000 |
| Barometer | Digi-quartz | Paroscientific Co. | 7,000 |
| PC , GPS, DC_PS… etc. | | | 3,000 |
| total | | | **183,800** |

# Cost of 5x5m$^2$ detector with PSs

| item | Spec. | producer | Cost (USD/¥100) |
|---|---|---|---|
| Plastic scintillator | 0.5x0.5x0.1(0.05) m$^3$ x200 | CI industry Co. | 200,000 |
| Photomultiplier tube | 5” (R877) x50 | Hamamatsu photonics | 75,000 |
| Amplifier board | 50 pairs of pre & main | CI industry Co. | 1,750 |
| Cables (EHT + signal) | 50 pairs | CI industry Co. | 15,000 |
| EHT distributor | | CI industry Co. | 6,500 |
| Steel frame | | CI industry Co. | 14,500 |
| Lead brick | 0.2x0.1x0.5 m$^3$ x1250 | Mitsui Metal Co. | 40,000 |
| FPGA recorder unit | | Shinshu | 6,000 |
| Barometer | Digi-quartz | Paroscientific Co. | 7,000 |
| PC , GPS, DC_PS… etc. | | | 3,000 |
| total | | | **368,800** |

# Cost of each component

| item | Spec. | producer | Cost (USD/¥100) |
|---|---|---|---|
| Plastic scintillator | 0.5x0.5x0.1(0.05) $m^3$ | CI industry Co. | 1,000 |
| Photomultiplier tube | 5” (R877) | Hamamatsu photonics | 1,500 |
| Proportional counter tube | 5 m long, 0.1 m $\phi$ | CI industry Co. | 450 |
| Amplifier board | pre & main pair | CI industry Co. | 35 |
| Cables (EHT + signal) | | | 300 |
| EHT distributor | | CI industry Co. | 6,500 |
| Steel frame | | CI industry Co. | 14,500 |
| Lead brick | 0.2x0.1x0.5 $m^3$ | Mitsui Metal Co. | 32 |
| FPGA recorder unit | | Shinshu | 6,000 |
| Barometer | Digi-quartz | Paroscientific Co. | 7,000 |
| PC , GPS, DC_PS… etc. | | | 3,000 |

# Drift model (Jokipii et al., ApJ, 213, 1977)

$$qA \equiv q\mathbf{\Omega}\cdot\mathbf{M}$$

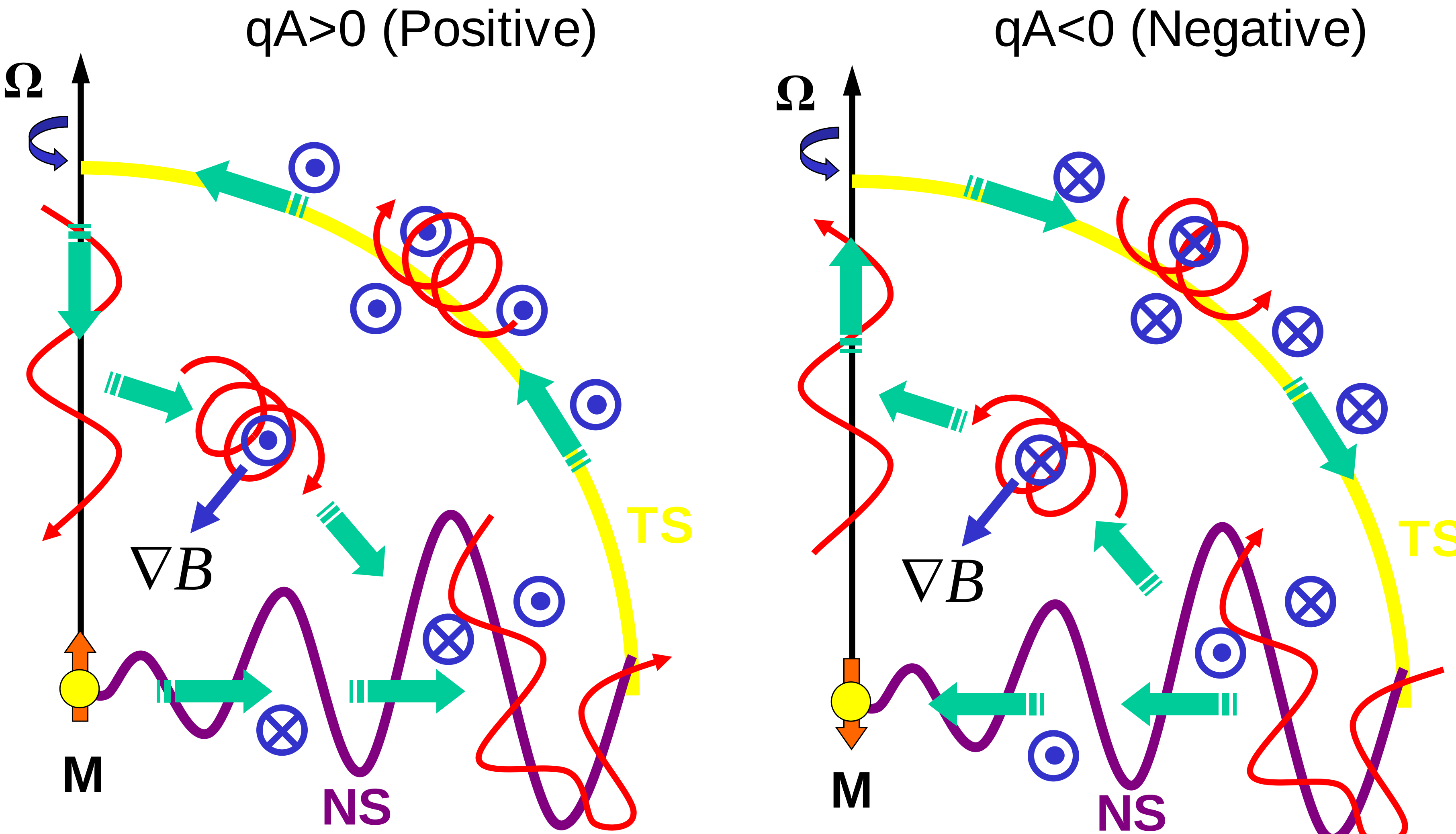

## We first correct the observed $\xi^{GSE}$, as ....

$$\xi^{GSE} + (2+\gamma)(\mathbf{V}_{SW} - \mathbf{v}_E) \equiv \xi_{//} + \xi_{\perp}$$

anisotropy

density gradient

$$\boldsymbol{\xi}_\perp(t) = R_L(t)(\alpha_\perp \mathbf{G}_\perp(t) - \mathbf{b}(t) \times \mathbf{G}_\perp(t)),$$

$$\alpha_\perp = \lambda_\perp(t)/R_L(t) = 3\kappa_\perp(t)/R_L(t)/c,$$

**b**(t): unit vector along the IMF

$$\mathbf{G}_\perp(t) = \begin{pmatrix} \alpha_\perp & b_z(t) & -b_y(t) \\ -b_z(t) & \alpha_\perp & b_x(t) \\ b_y(t) & -b_x(t) & \alpha_\perp \end{pmatrix}^{-1} \boldsymbol{\xi}_\perp(t)/R_L(t).$$

density gradient

anisotropy

**We haven't looked at $\xi_{//}$ yet...**

# São Martinho muon detector
## enlarged in December 2005

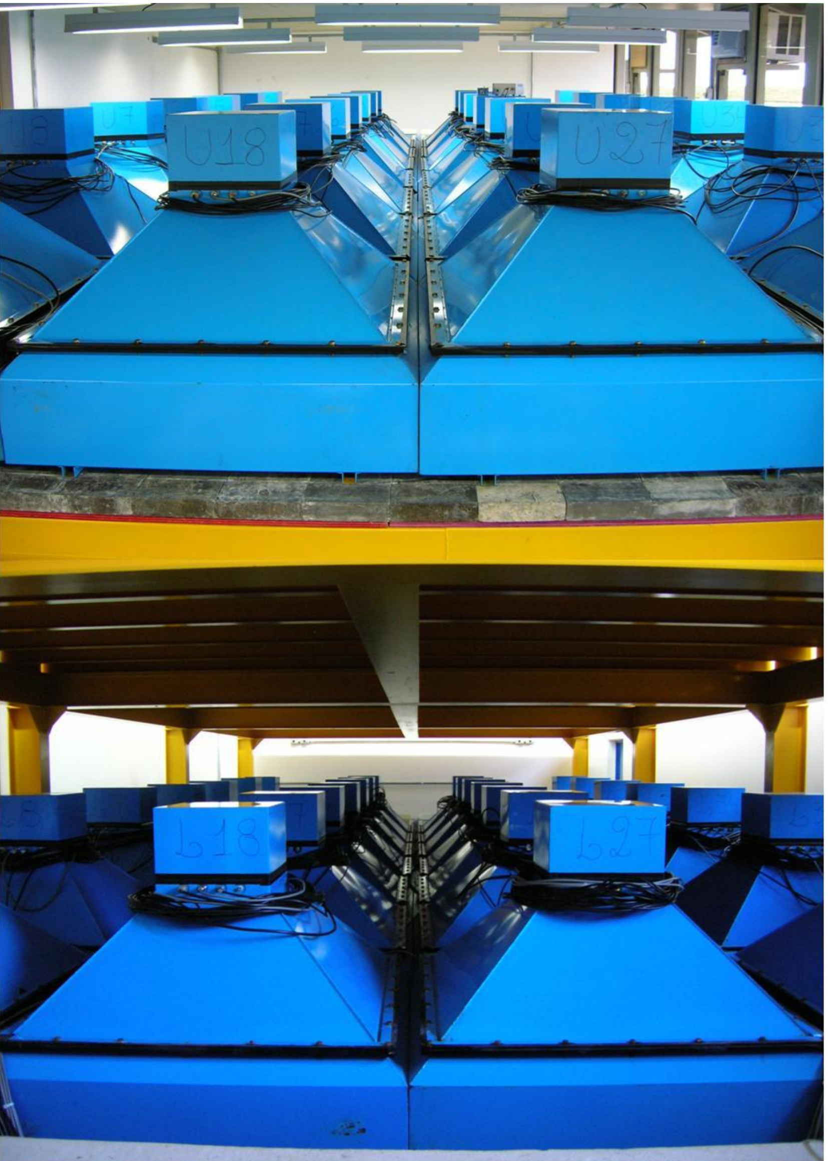


Two old (useless?) guys in between
**excellent young people!**

# Muon detector in Kuwait-City

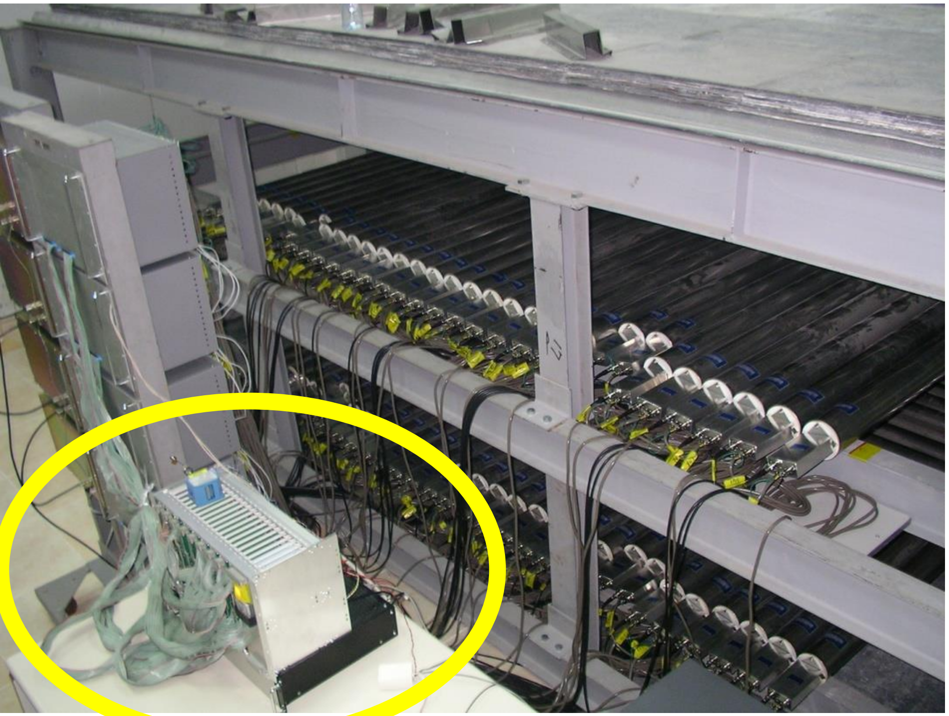

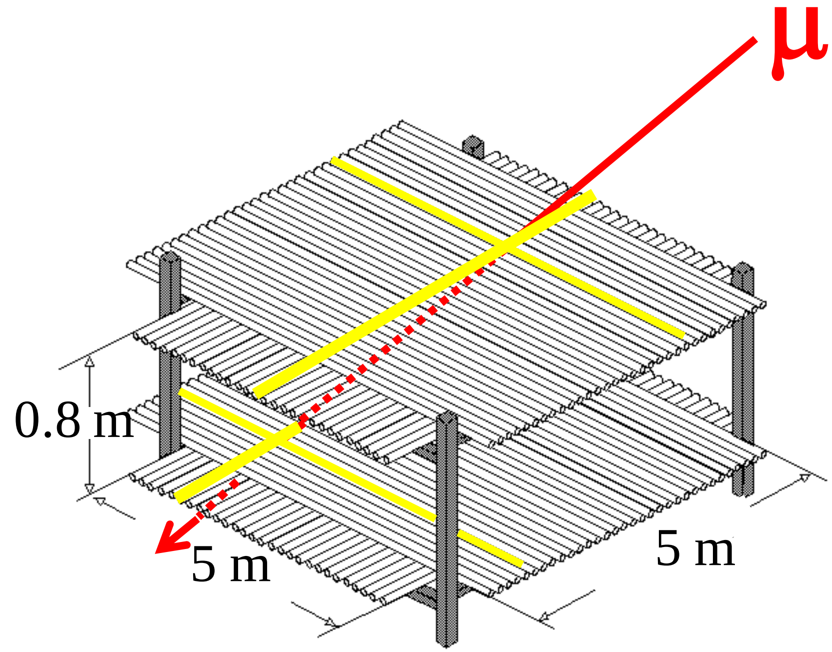


**FPGA（Xlinx XC2S200）**

- Fast identification of incident direction
- Count rate in 529 (23×23) directions can be stored in 5 FPGAs
- Flexible system can be realized
- Low power consumption

# New data recording system

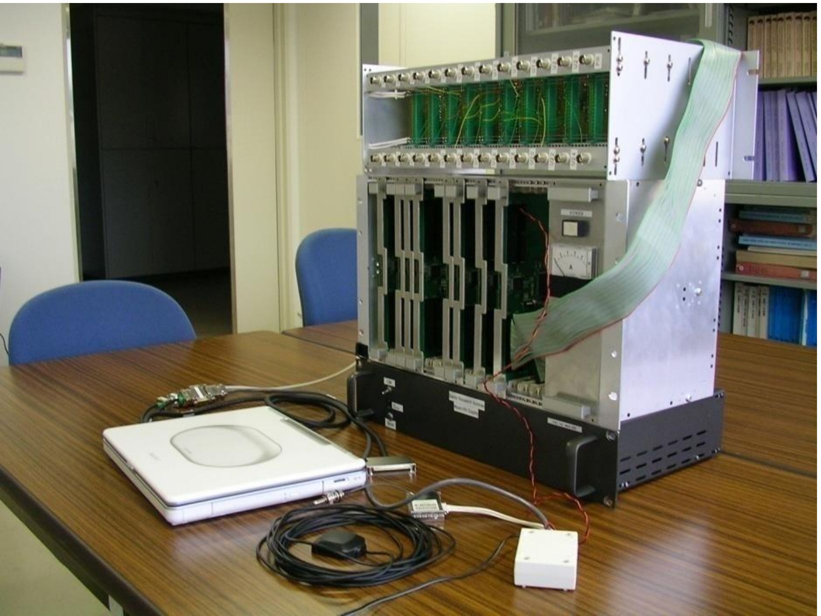

## FPGA（Xlinx XC2S200）

- Fast identification of incident direction
- Count rate in 441 (21×21) directions can be stored in 3 FPGAs
- Flexible system can be realized
- Low power consumption

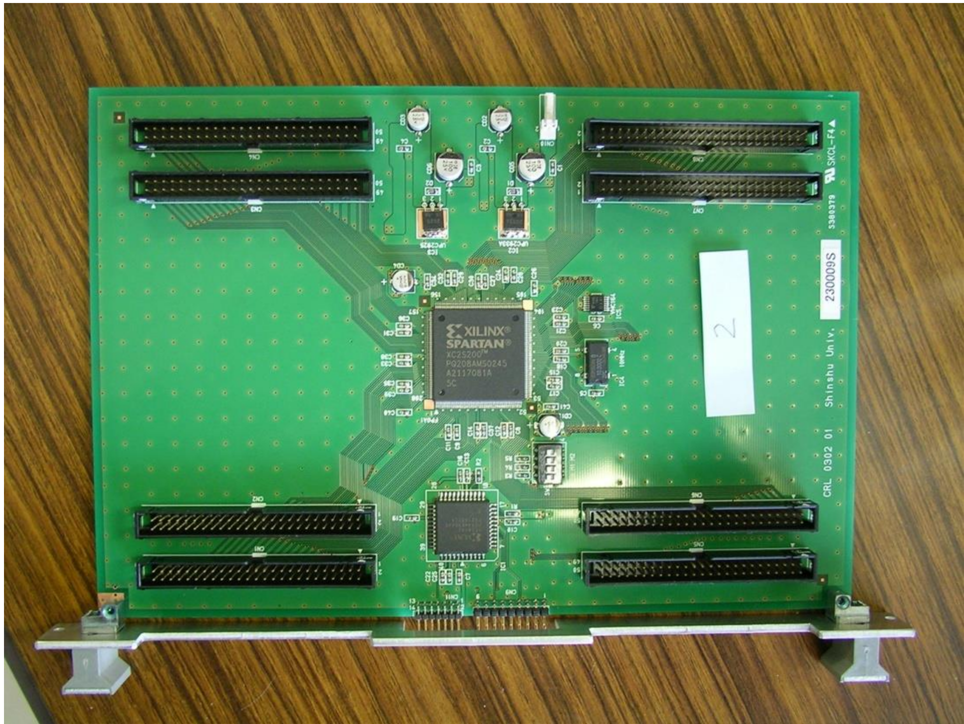

# A Loss-cone precursor observed with muon hodoscope on Oct. 28, 2003

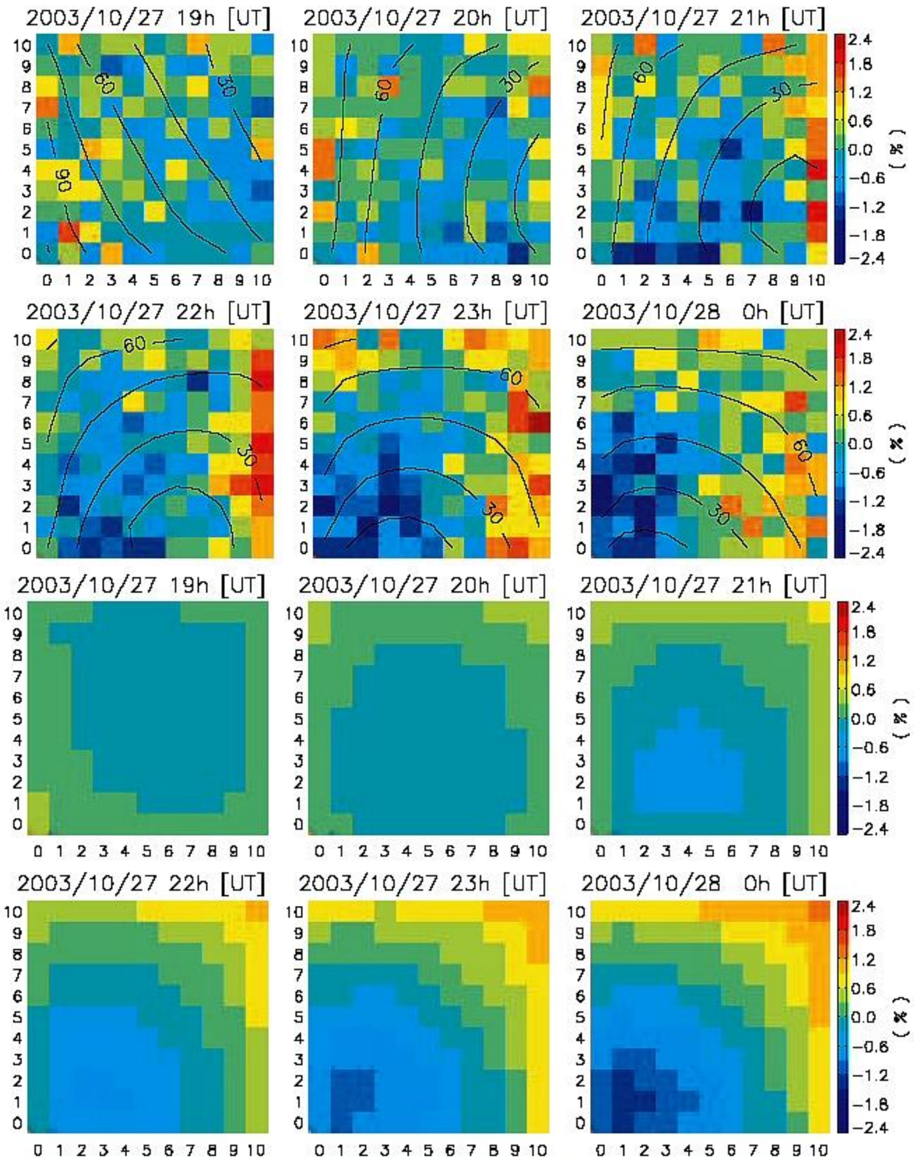


- Mt Norikura field of view over a 6-hr period prior to storm sudden commencement.

  TOP: Observations

  BOTTOM: Model

- Blue indicates lower intensity; Red indicates higher intensity

- See Munakata et al., *Geophys. Res. Lett.*, 32, L03S04-1, 2005.

$$f(\theta, P, \tau) = C_0\left(\frac{P}{30}\right)^{-1} \exp\left(\frac{\tau}{T_0(P/30)^\gamma}\right) \exp\left(-\frac{\theta^2}{2\theta_0^2}\right)$$

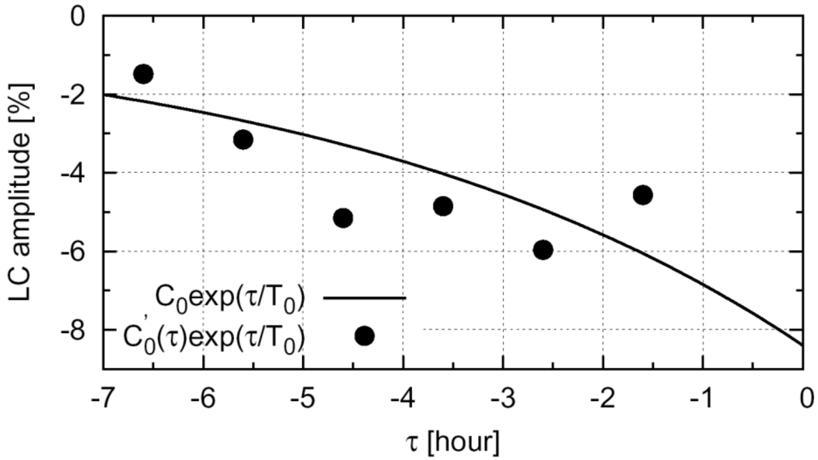


**Figure 5.** The best-fit LC amplitude at 30 GV as a function of time ($\tau$) measured from the SSC (solid curve). Also plotted are amplitudes derived from the best-fitting on an hourly basis (see text).

| $C_0$[%] | $T_0$[hour] | $\theta_0$[°] | $\theta_{HW}$[°] | $\gamma$ | S |
|---|---|---|---|---|---|
| -8.397 | 4.9 | 55 | 49.1 | 0.15 | 1.147 |

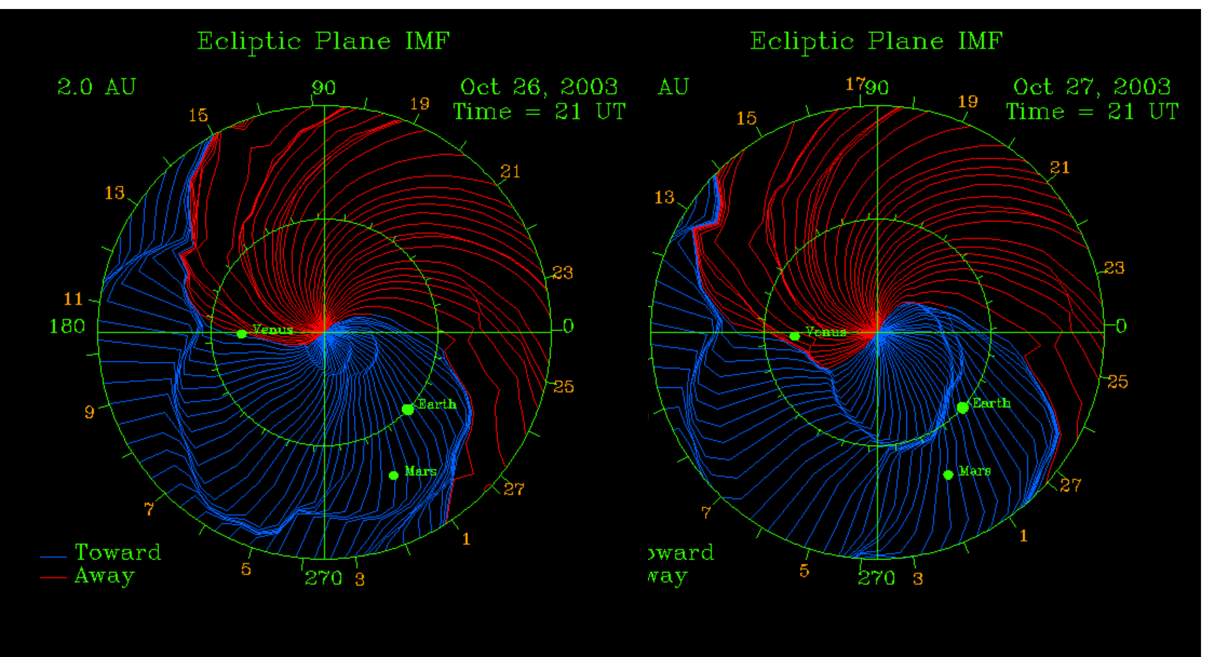


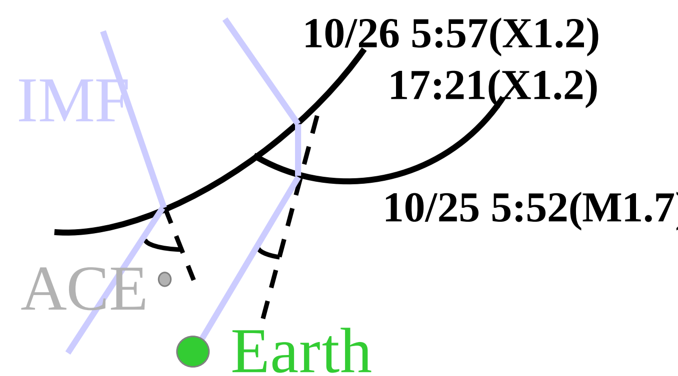

# Loss-cone precursor with a hodoscopes

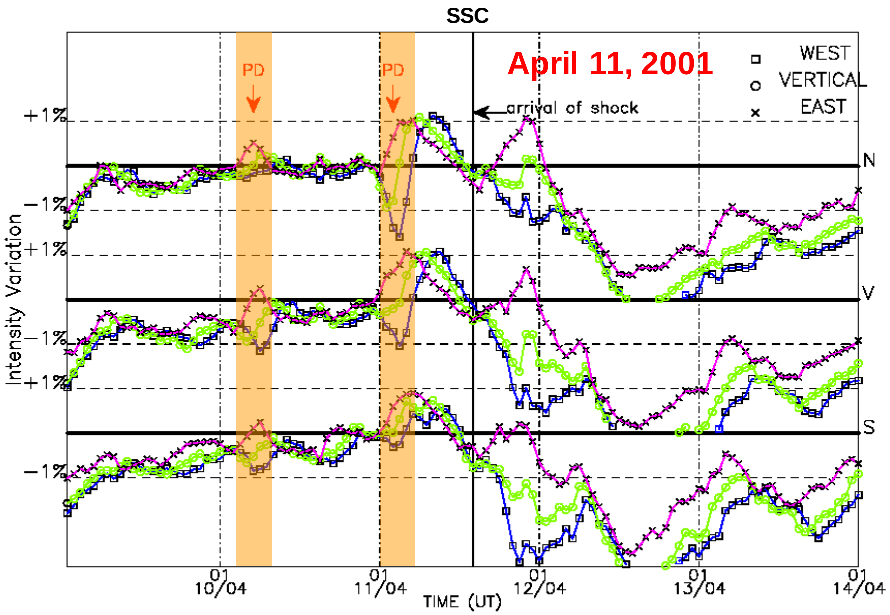


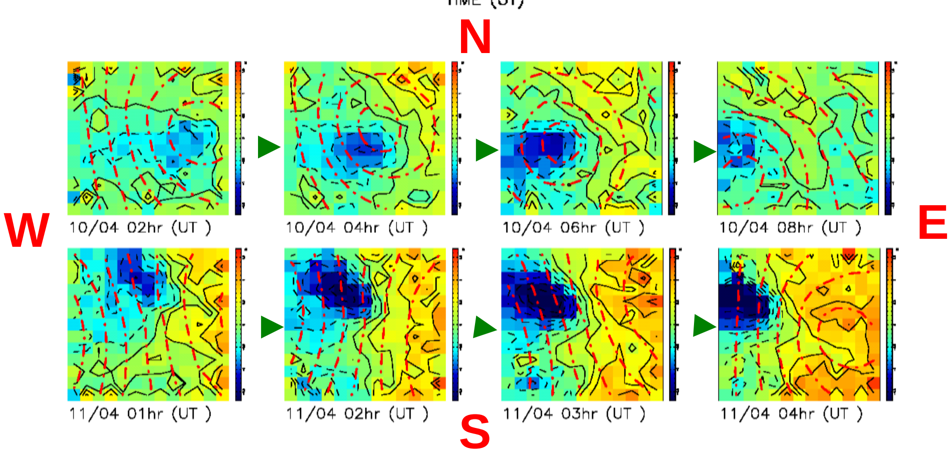


**SH2.2-6 Nonaka et al.**

- 560$m^2$ array of PC recording $1.8\times10^8$ muons/h with ~10° angular resolution (GRAPES3).
- Clearly detected the loss-cone precursor twice, ~24h preceding to a CME-event on April 11, 2001.
- Significant deviation of loss-cone center from sunward IMF is observed half a day preceding the SSC.

**SH2.2-5 Fujimoto et al.**

- 25$m^2$ PC array observed the same precursor.
- Loss-cone is 15° wide

**SH2.2-1-P-214 Petrukhin et al.**

- 9$m^2$ GMC array with ~7° angular resolution.
- "Tomography" of fluctuation in CME

**SH2.2-7 Szabelski et al.**

- 0.65$m^2$ GM array in operation in Poland.

**SH1.5-1-P-197 Yasue et al.**

- New recording system developed for muon telescope using FPGA & VHDL.

# Omni-directional measurement with Neutron Monitors (NM64)

Two main types:

- Proportional counter filled with $BF_3$ (NM64):
  $n + {}^{10}B \rightarrow \alpha + {}^{7}Li$
- Proportional counter filled with ${}^{3}He$:
  $n + {}^{3}He \rightarrow p + {}^{3}H$

Neutron Monitor in Doi Inthanon, Thailand

- Shipped from Japan in December 2001
- Construction completed in March 2007

# Princess Sirindhorn NM in Thailand

**World highest GM cut-off rigidity**

**⇒ Better response to high energy CRs**

**⇒ in between GMDN and SSE**

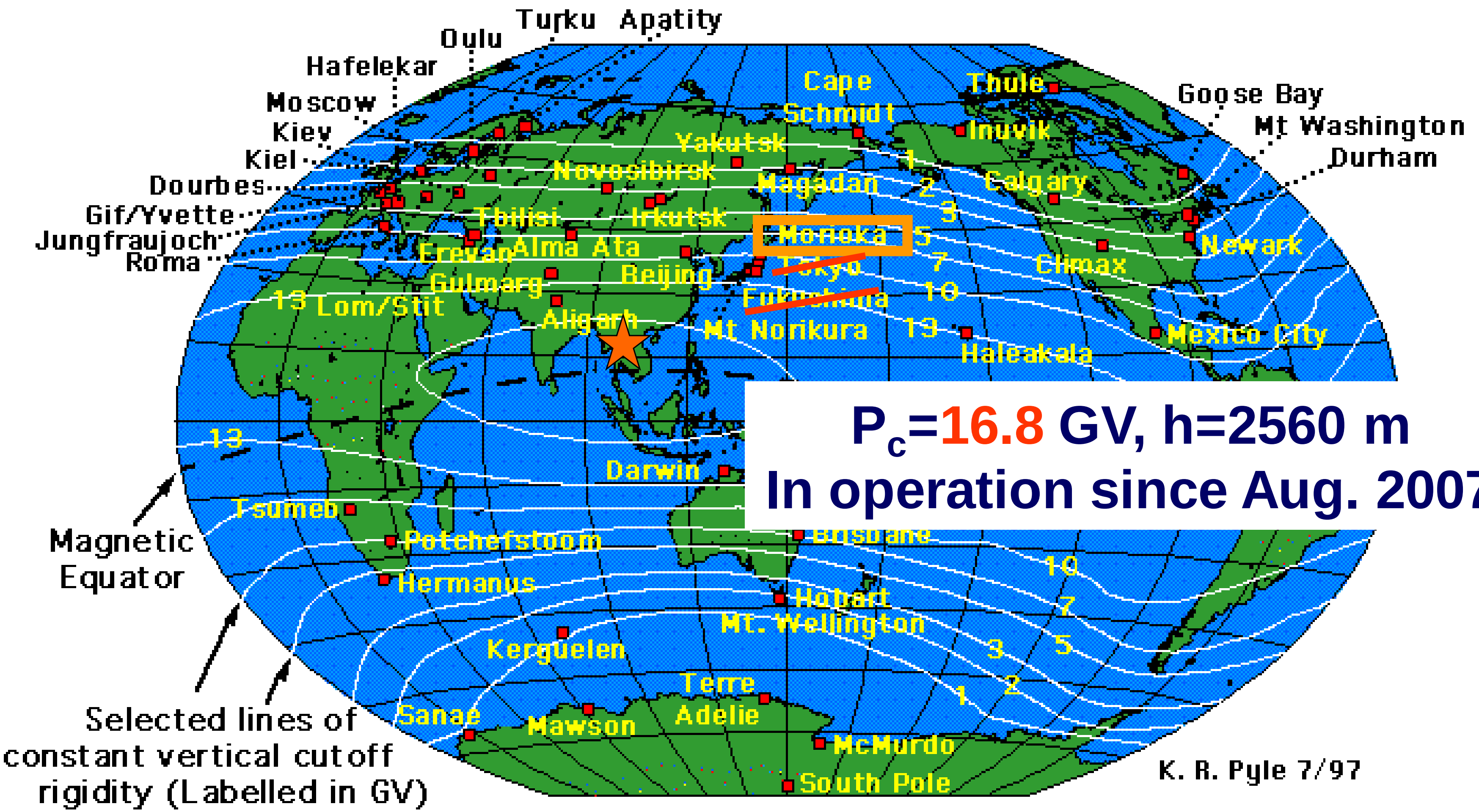


**$P_c$=16.8 GV, h=2560 m**

**In operation since Aug. 2007**

# PSNM opening ceremony

## (January 21, 2008 )


# Differential response functions

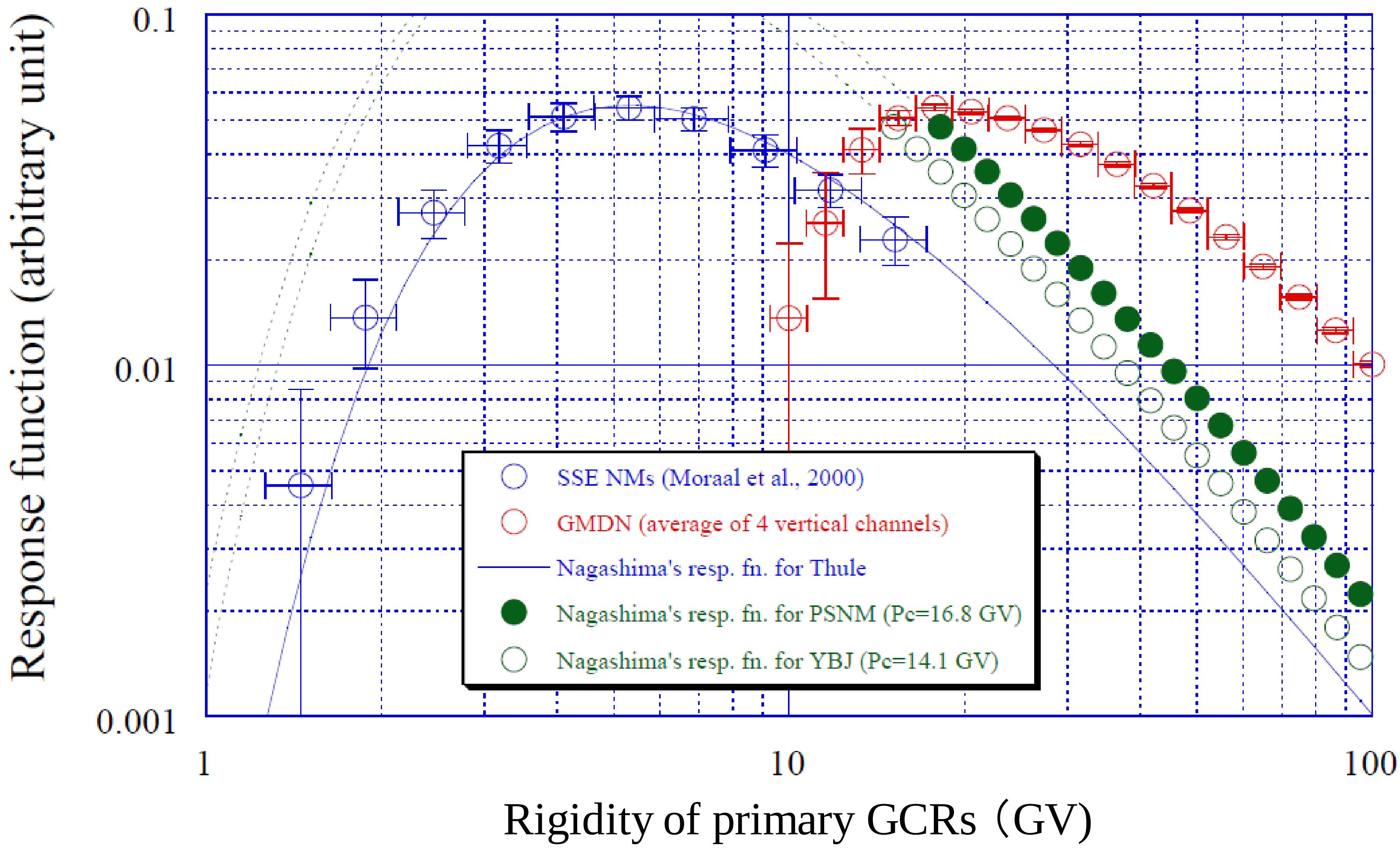

# Integrated response functions (solar min.)

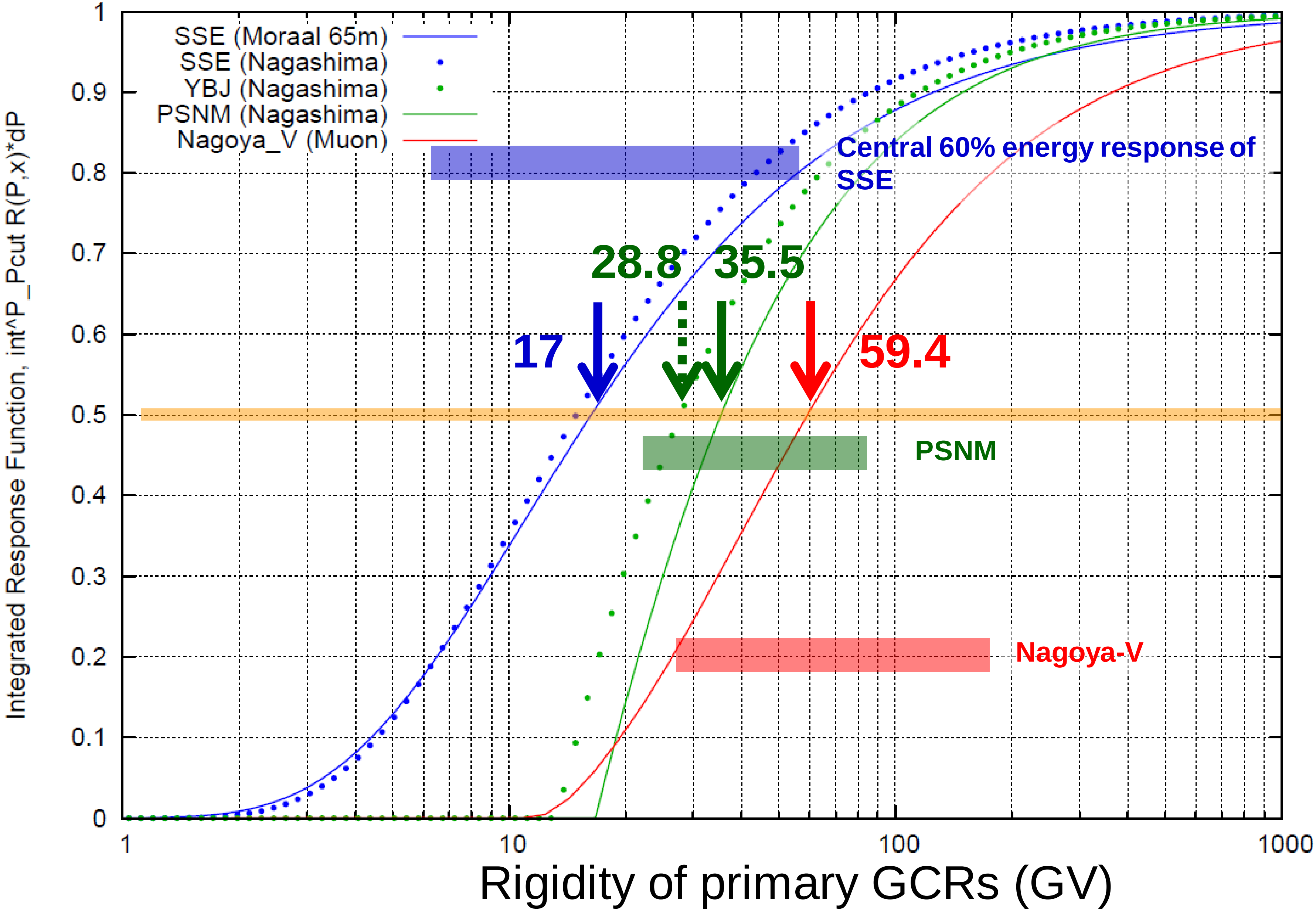

# Characteristics of NM & muon detector

| Station name | Type & location | $P_c$ (GV) | $P_m$ (GV) |
|---|---|---|---|
| Tixie Bay (**TB**) As a representative of SSE | 18 **NM64**s in Russia (71.6N, 128.9E: 0m) | 0.53 | **17** (SSE) |
| Tibet NM (**YBJ**) | 28 **NM64**s at Yangbajing, Tibet, China (30.11N, 90.53E: 4300m) | 13.7 | **28.8** |
| Princess Sirindhorn NM (**PSNM**) | 18 **NM64**s at Doi Inthanon, Thailand (18.59N, 98.49E: 2560m) | 16.8 | **35.5** |
| Nagoya (**Nagoya**) As a representative of GMDN | Multi-directional **muon detector** 36 $m^2$ PS at Nagoya, Japan (35.1N, 137.0E: 77 m) | 11.5 | **59.4** (GMDN) |

# *SPACESHIP EARTH* VIEWING DIRECTIONS

- **Optimized for solar cosmic rays**
- **9 stations view equatorial plane at 40-degree intervals**
- **Thule and McMurdo provide crucial 3-dimensional perspective**

**Circles denote station geographical locations. Average viewing directions (squares) and range (lines) are separated from station geographical locations because particles are deflected by Earth's magnetic field.**

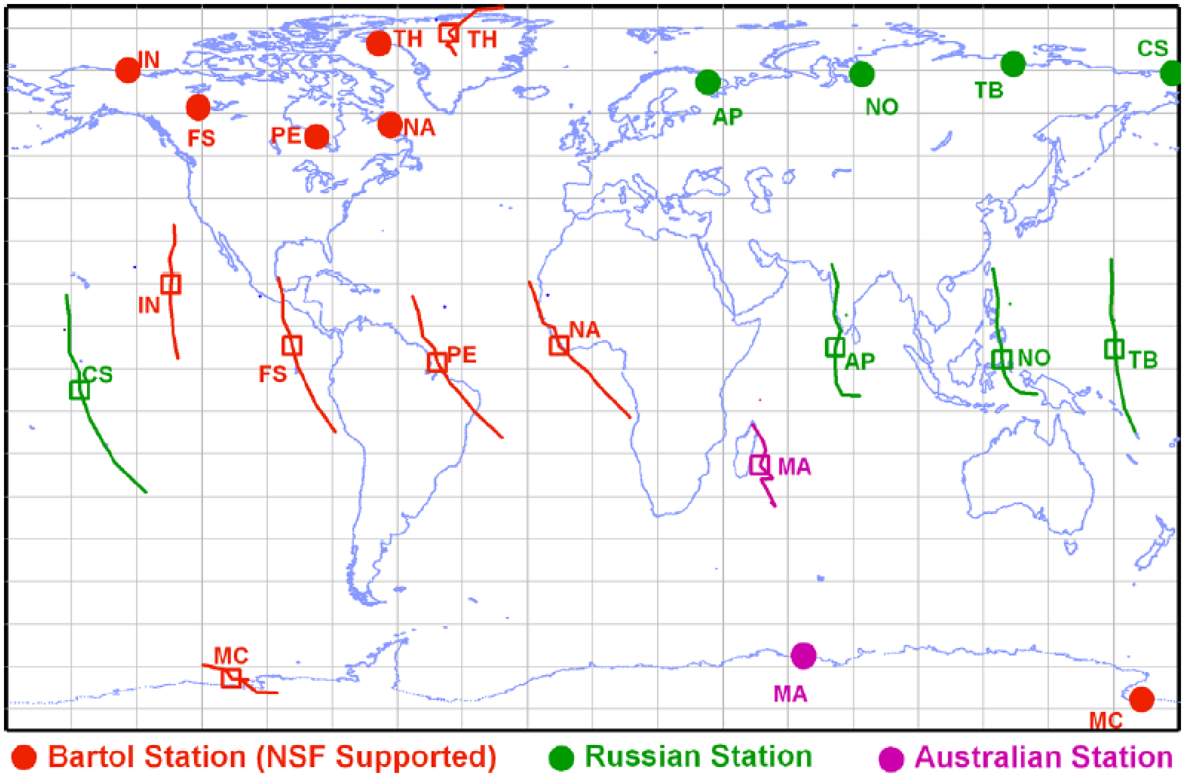


**STATION CODES**
**IN: Inuvik, Canada**
**FS: Fort Smith, Canada**
**PE: Peawanuck, Canada**
**NA: Nain, Canada**
**MA: Mawson, Antarctica**
**AP: Apatity, Russia**
**NO: Norilsk, Russia**
**TB: Tixie Bay, Russia**
**CS: Cape Schmidt, Russia**
**TH: Thule, Greenland**
**MC: McMurdo, Antarctica**

# Ground Level Enhancement (GLE)
## on January 20, 2005

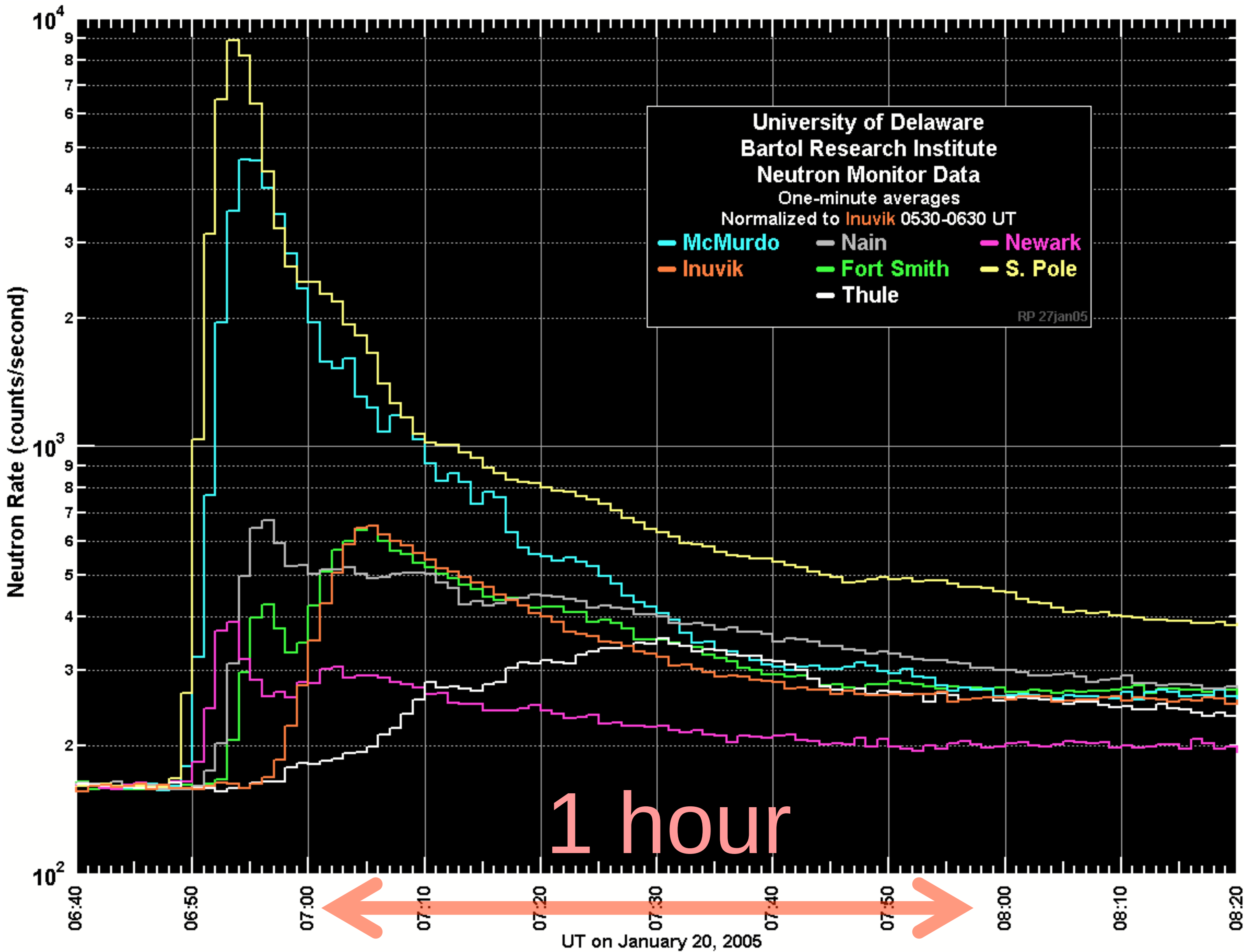

# Spaceship Earth
# (11 NMs network by Bartol Res. Inst.)

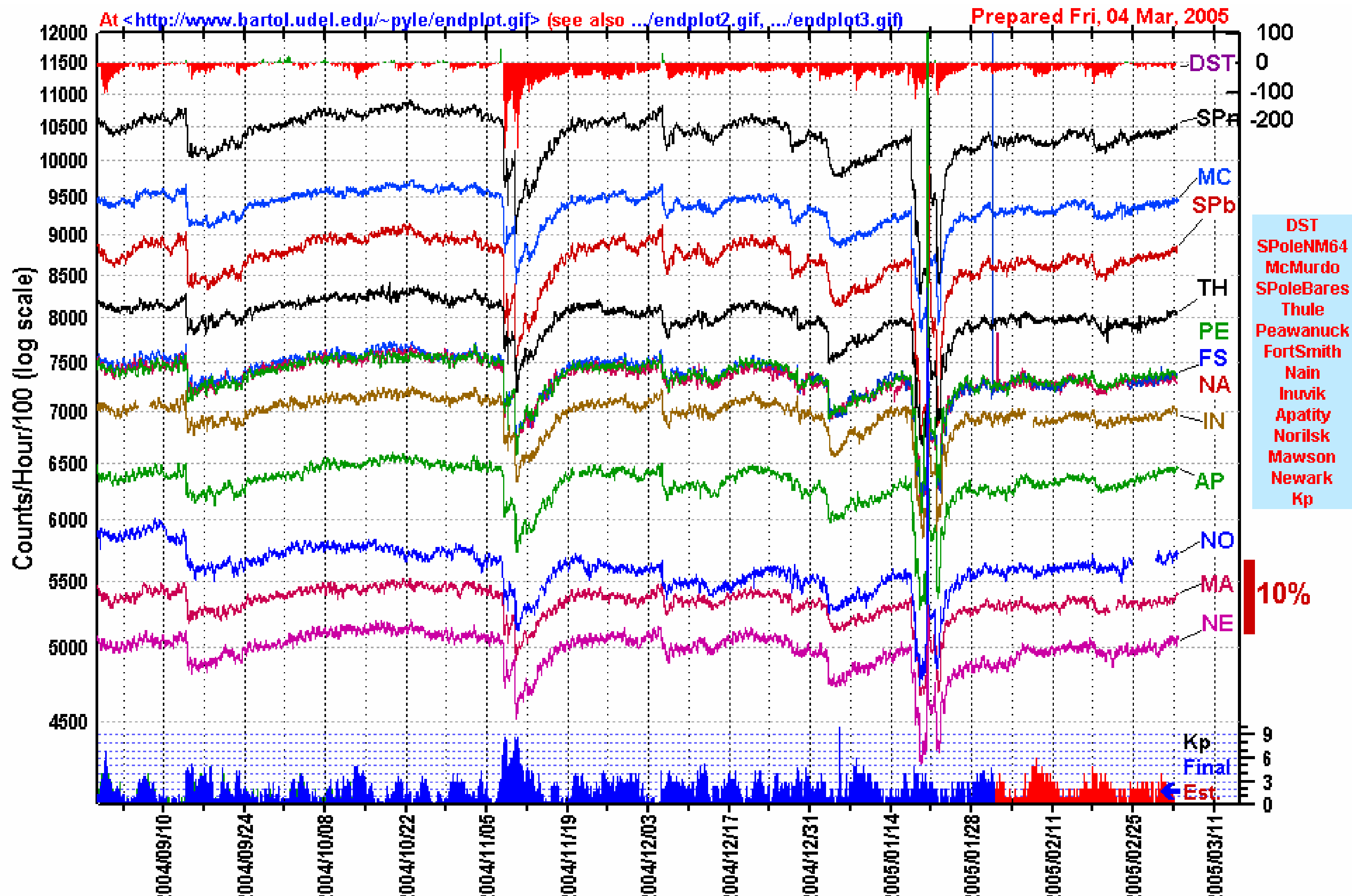

# Fitness to the vertical data

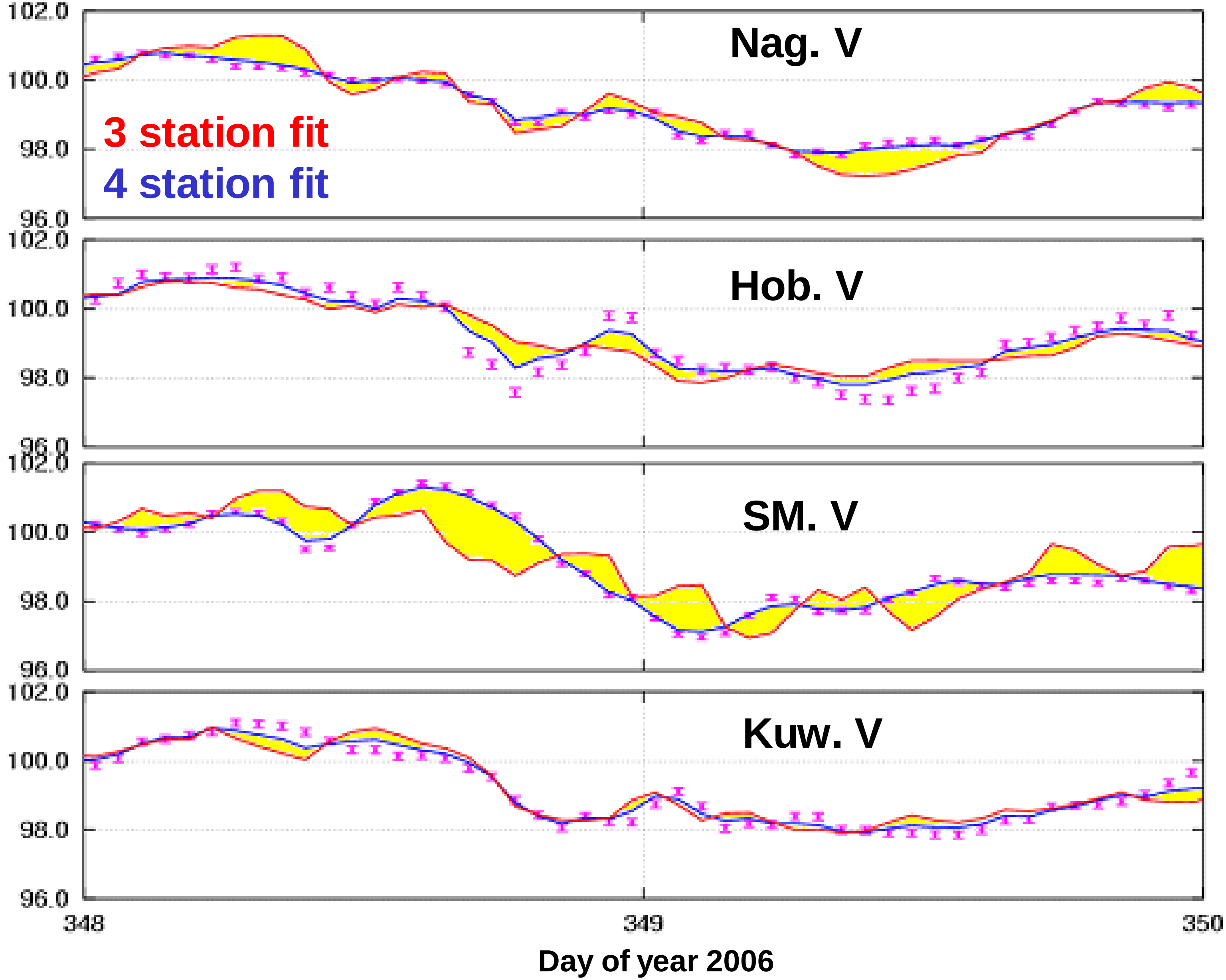

# What does GMDN tell us?

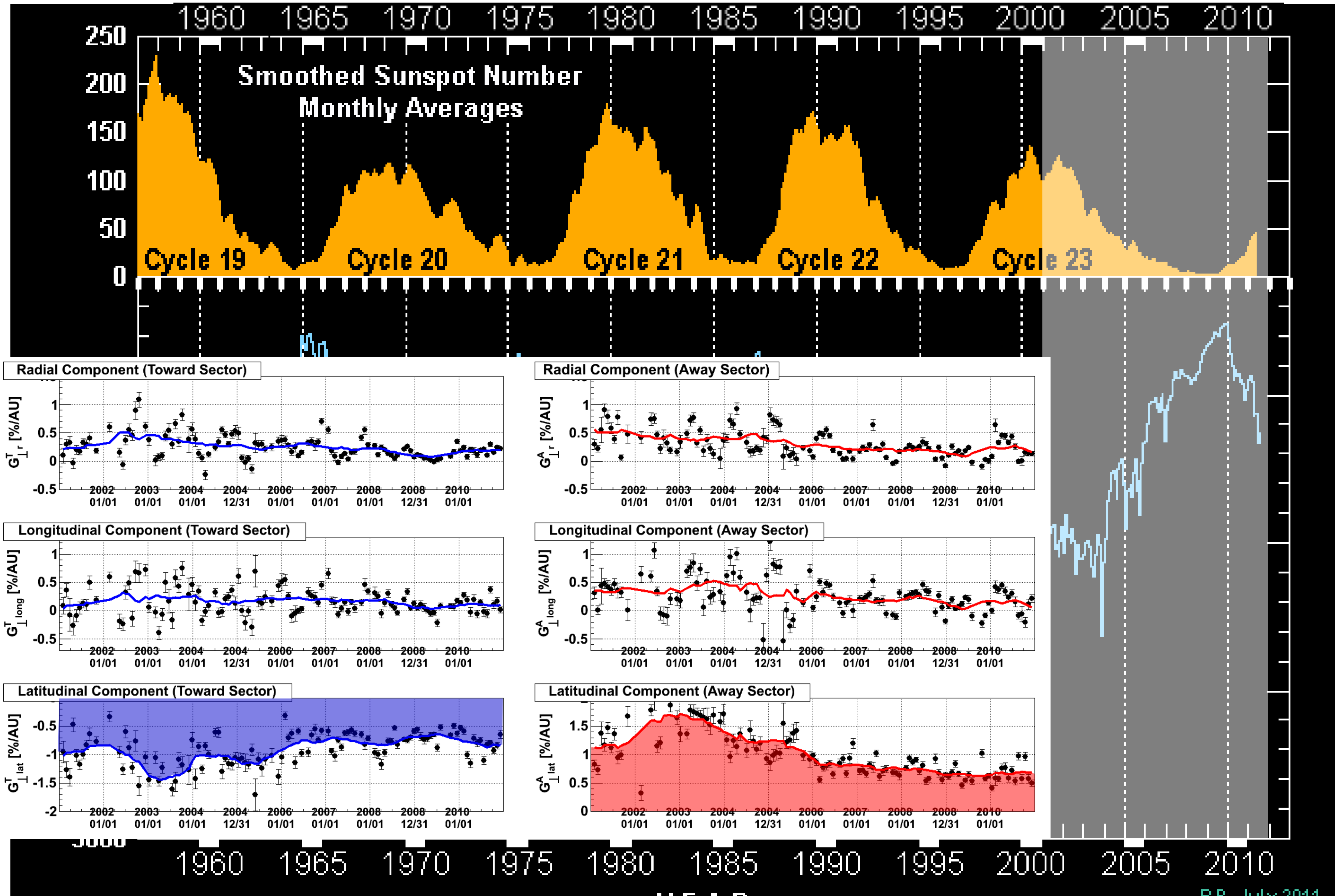


http://neutronm.bartol.udel.edu/

# Possible expansion of GMDN

## We plan to install a new detector in Mexico to fill the gap.

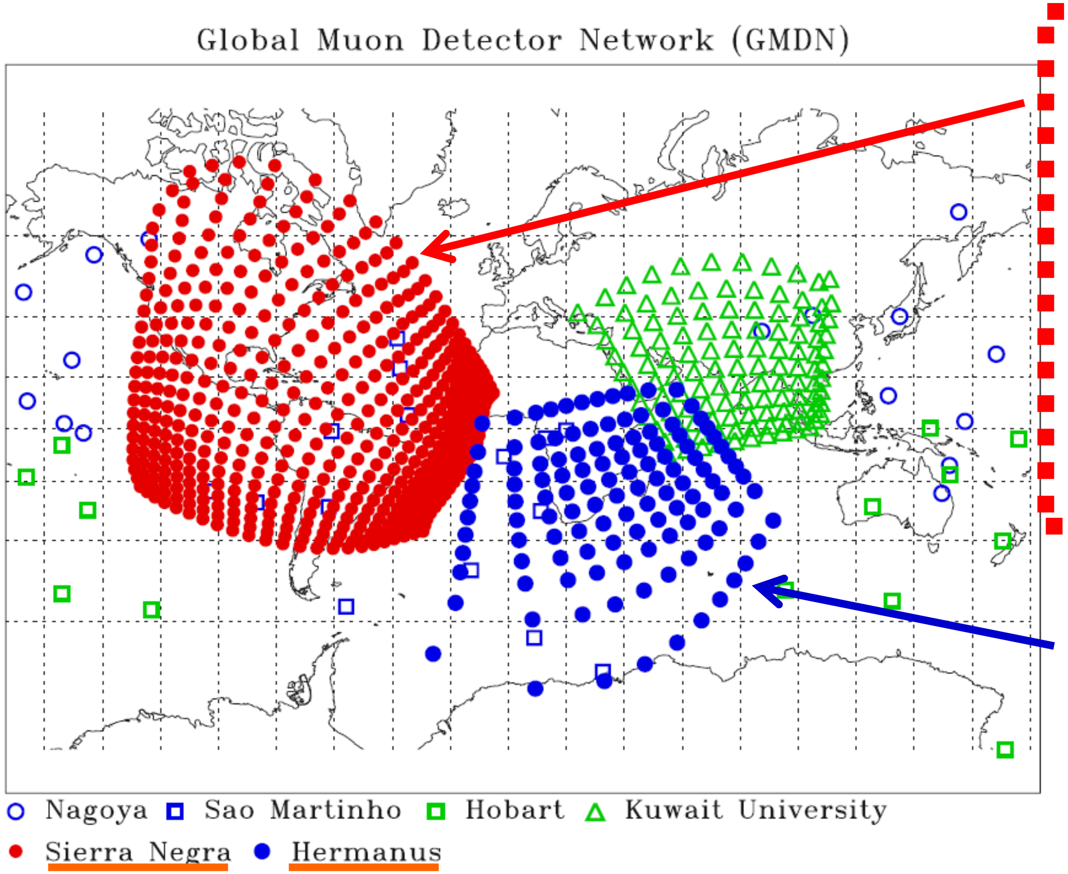


### Mt. Sierra Negra (Mexico)

- 4600 m a.s.l..
- 15k SciBars viewed by ~200 multi-anode PMTs.
- Primarily for the solar neutron detection, but can be used for muon measurement as well.

### Hermanus (South Africa)

- 200 PRC tubes in four horizontal layers will form a 25 $m^2$ muon detector.

# Preliminary results with mini-SciCR

**We trigger the muon measurement by 4-fold coincidence between the top & bottom x-y layers.**

## Observed 2D-maps of hourly count rate

$\log_{10}(I_{obs.})$ $(I_{obs.} - I_{cal.})/I_{cal.}$ $(I_{obs.} - I_{cal.})/\sigma I_{obs.}$

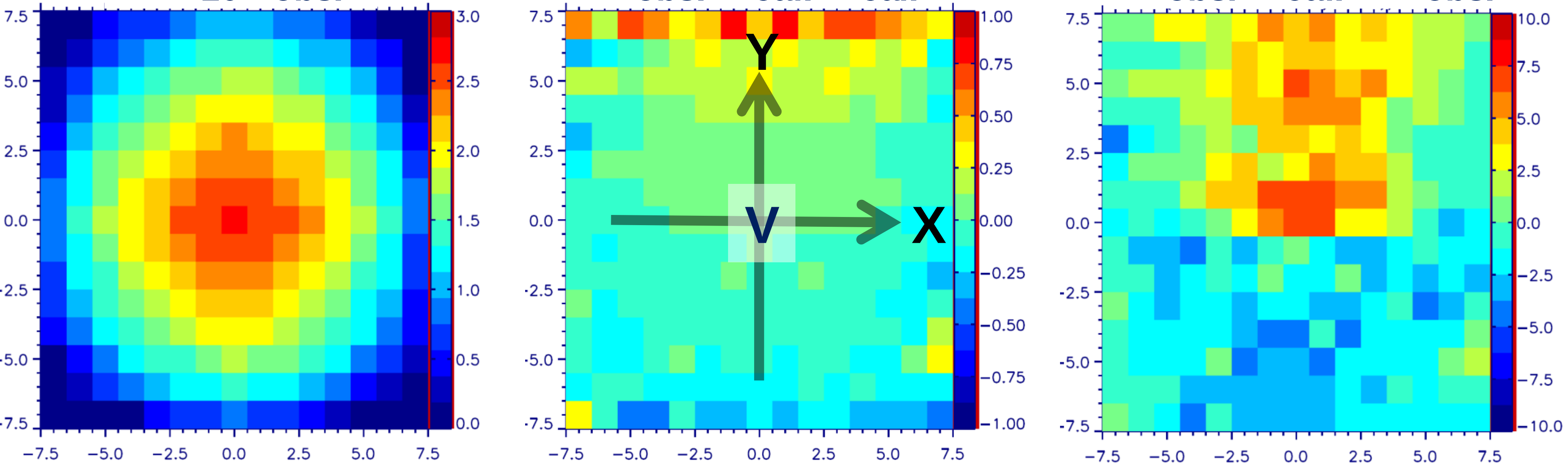


**Vertical count rate: 473 cph**

**(363 cph for SciCR with much higher angular resolution)**

**Geomagnetic cut-off rigidity (vertical incident): 7.9 GV**

**Median primary rigidity: 34 GV**

# Zenith angle distribution

$I_{muon} \propto \cos^{\sim 2}\theta$

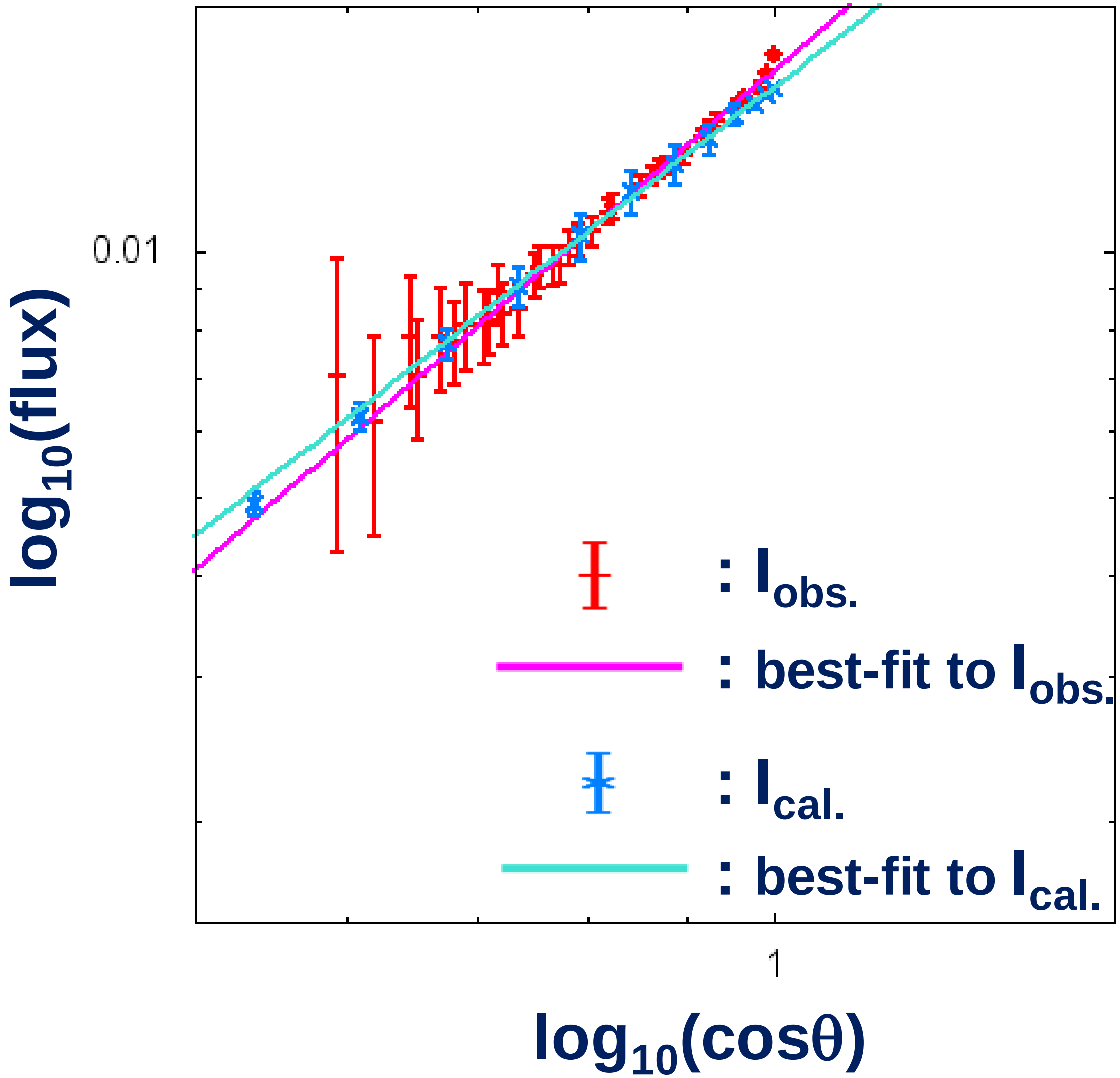

# Atmospheric pressure (barometer) effect

**(results from ~1 month measurement without lead layer)**

**Daily variations of $I_{obs.}$ & P**

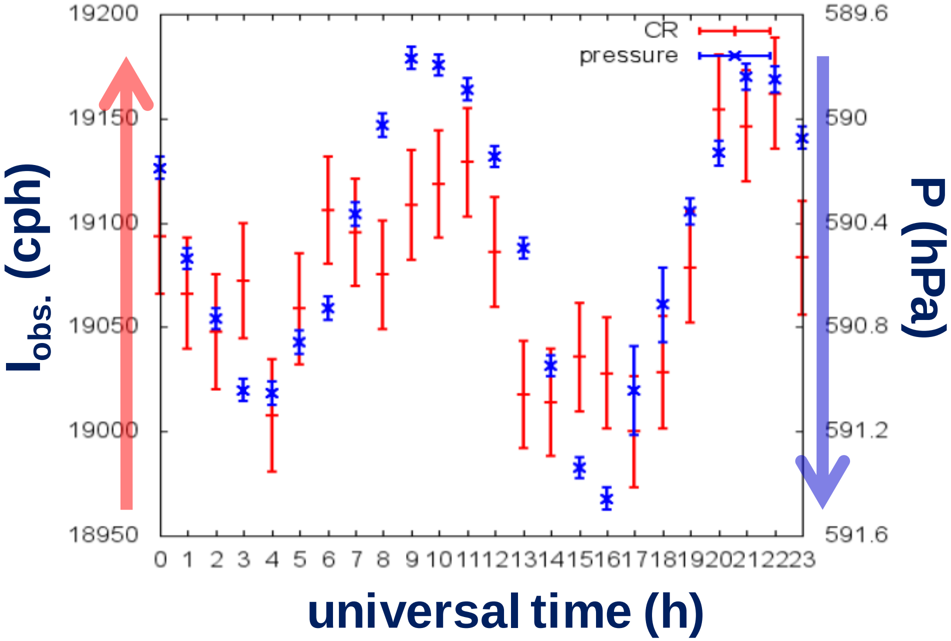


**Correlation between $I_{obs.}$ & P**

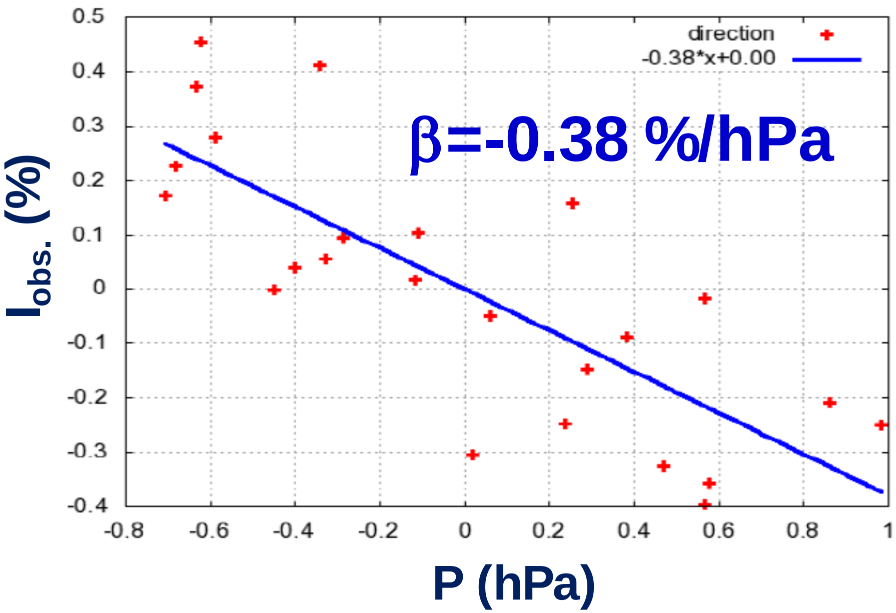


**β is larger than the typical ~-0.1 %/hPa for muons probably due to ~30 % contamination of AS particles.**

# Scintillator & WLS Fiber

## Scintillator

- Size : 1.3 × 2.5 × 300 $cm^3$
- Peak of emission spectrum : 420 nm
- $TiO_2$ reflector (white) : 0.25 mm thick

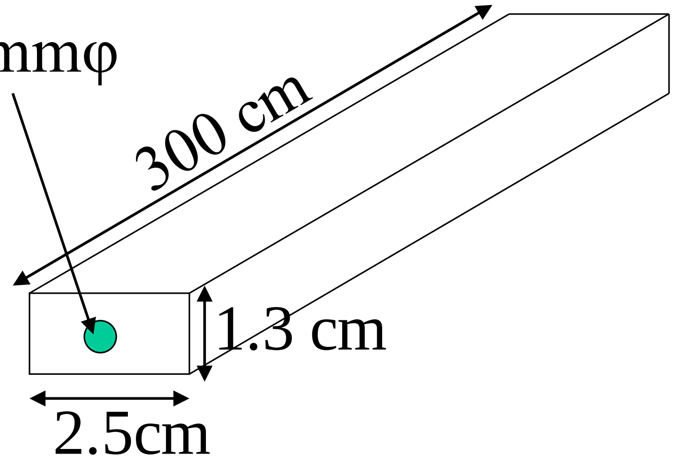


## Wave-length Shifting Fiber

- Kuraray
  - Y11(200)MS 1.5mmφ
  - Multi-clad
- Attenuation length ~3.6m
- Absorption peak ~430nm
- Emission peak ~476nm

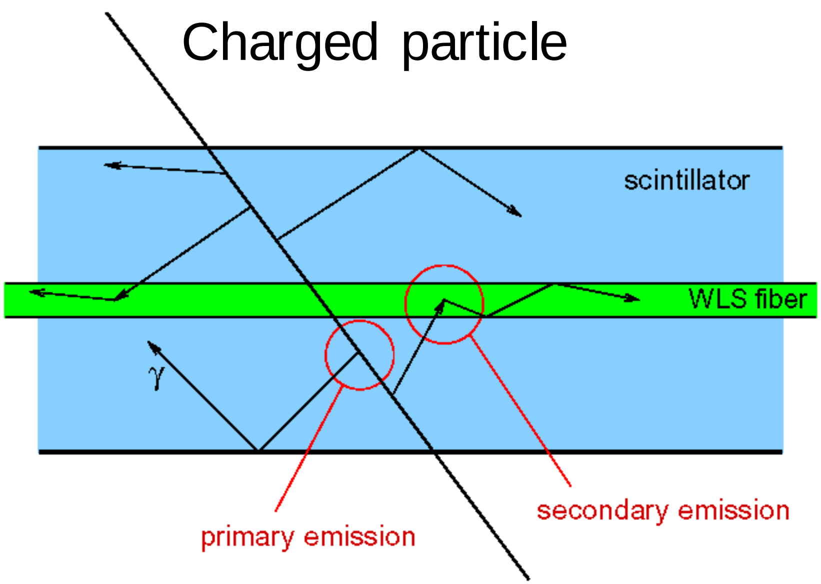

# SciCRT検出器(SciBar for the Cosmic Ray Telescope)

## スーパーブロック×８
## (シンチレータ16層ごとに鉄枠で支持)

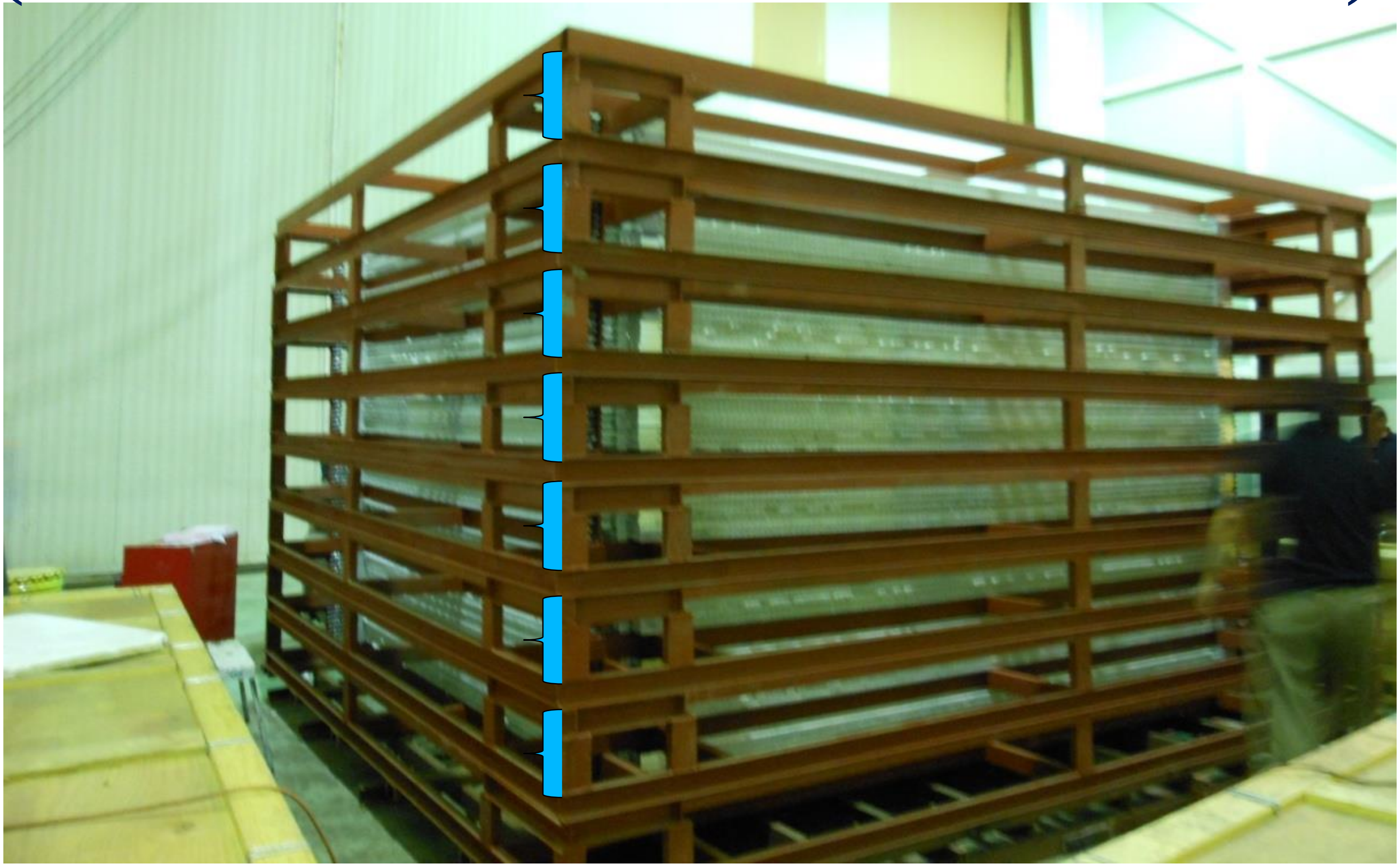

# ミューオン測定のトリガー条件

**最上下4層（各層のOR）の4 fold coincidence**

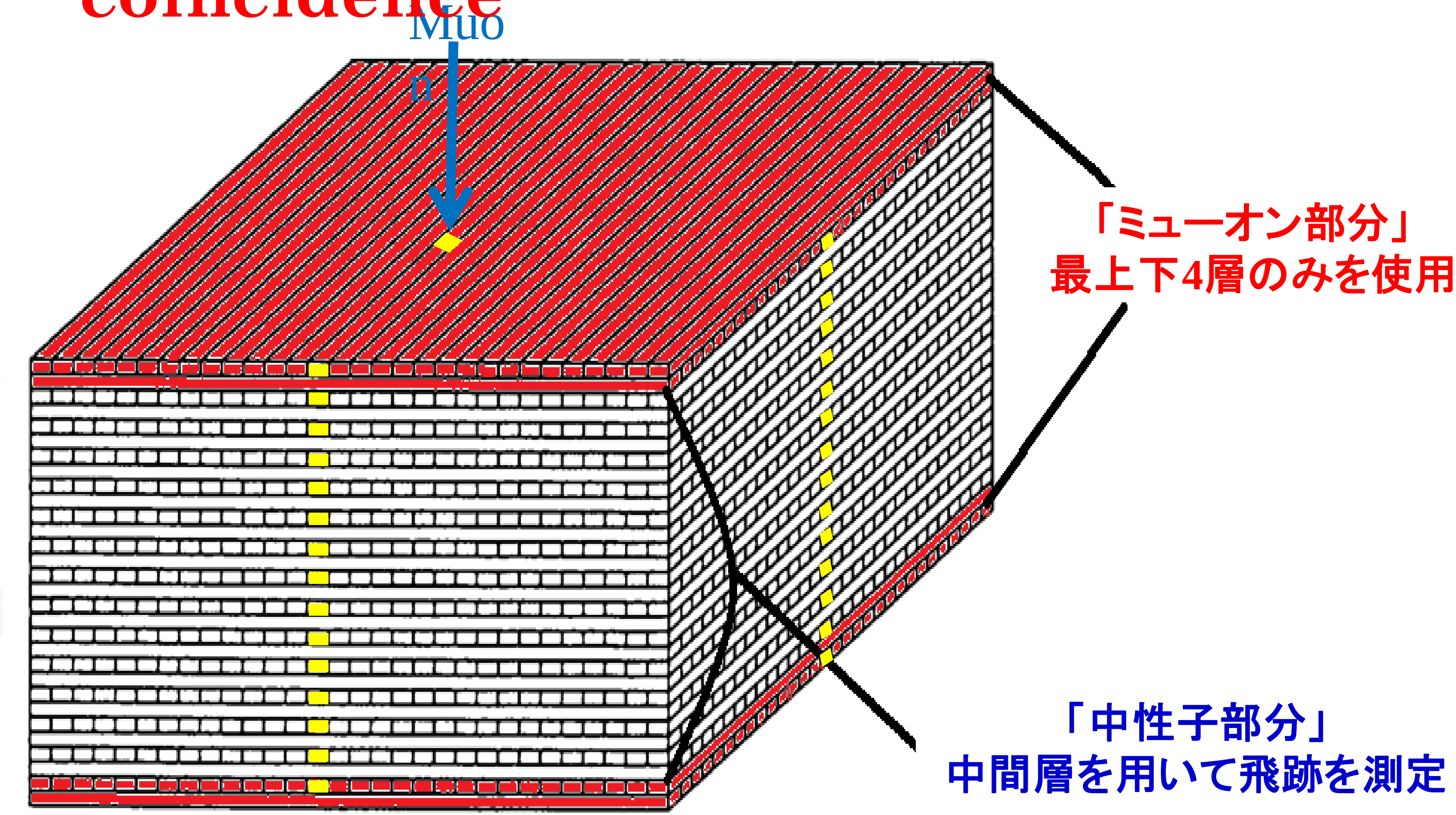

# 4 fold coin.によるmuon選択（1/4）

イベント例

1層で複数Hitしているイベントが多数あるため、
**最大エネルギー損失を記録したシンチバーを選択**

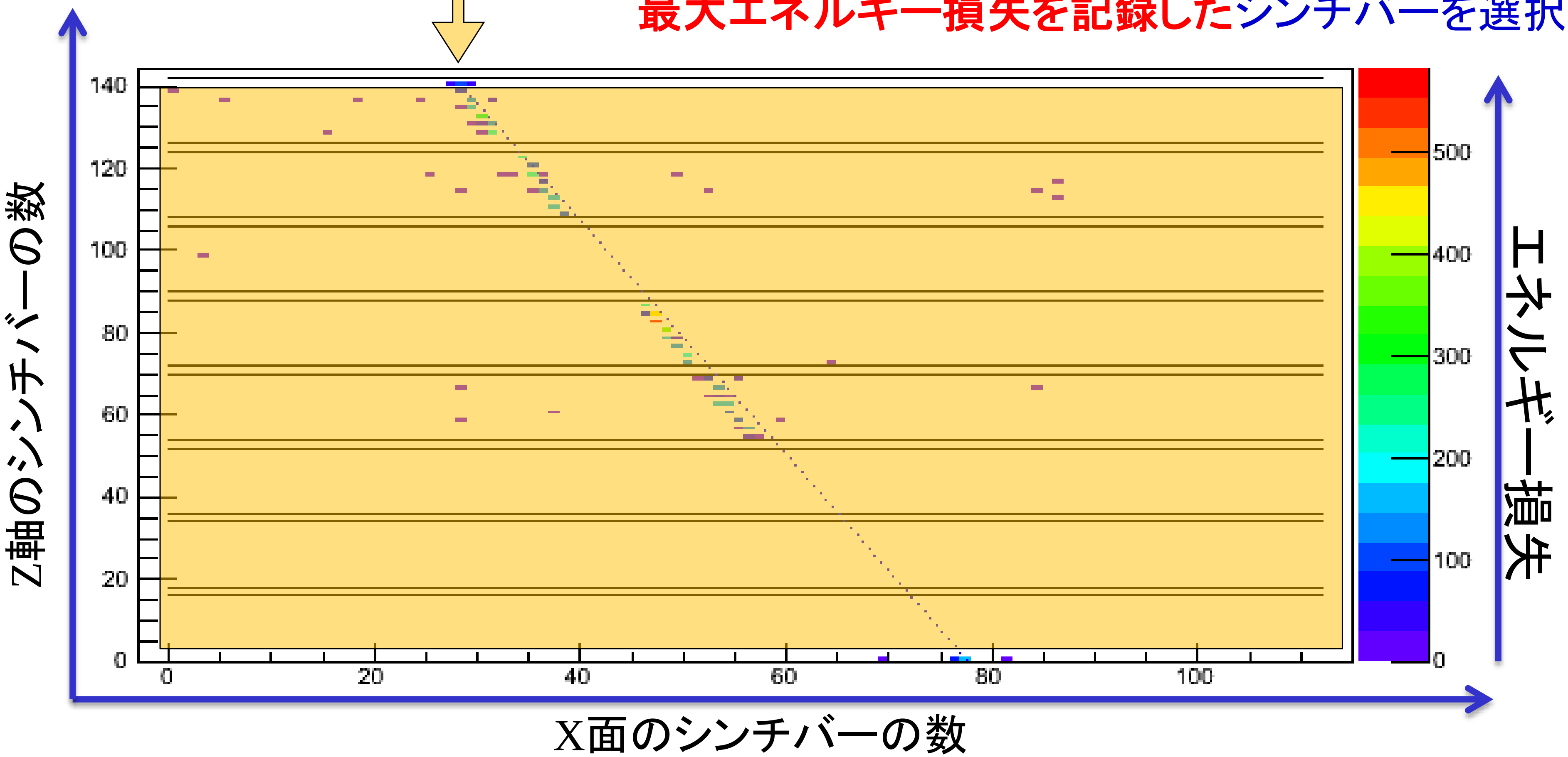


**4 fold coin.イベントで、中性子部分のトラックを調べ、**
**シングル・トラック・イベントをmuonとみなす。**

# 4 fold coin.によるmuon選択（2/4）

中性子部分のデータでトラックが見えているか判断するための指標を選び、トラック・イベントの方向を決定する。

1層でエネルギー損失が最大だったシンチバー

$$x_i^{cal} = az_i + b$$

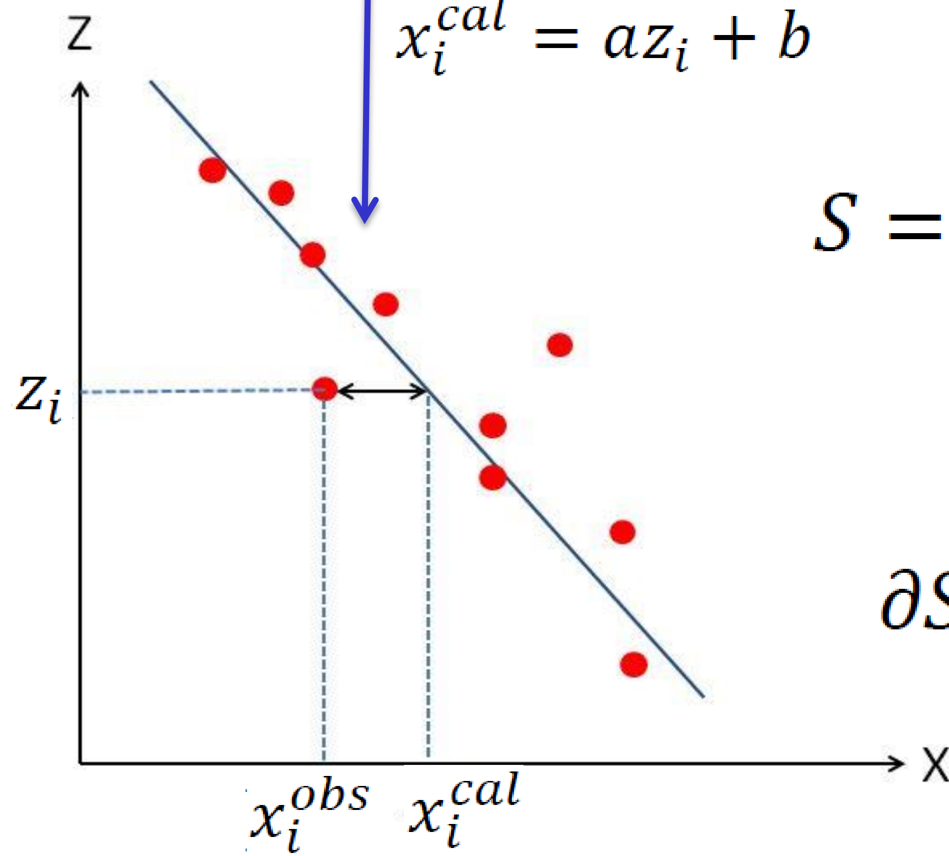


$$S = \frac{1}{n}\sum_{i=1}^{n}(x_i^{obs} - x_i^{cal})^2$$

Sを最小にするaとbを

$$\partial S/\partial a = \partial S/\partial b = 0$$

# 4 fold coin.によるmuon選択(3/4)

Sのヒストグラム

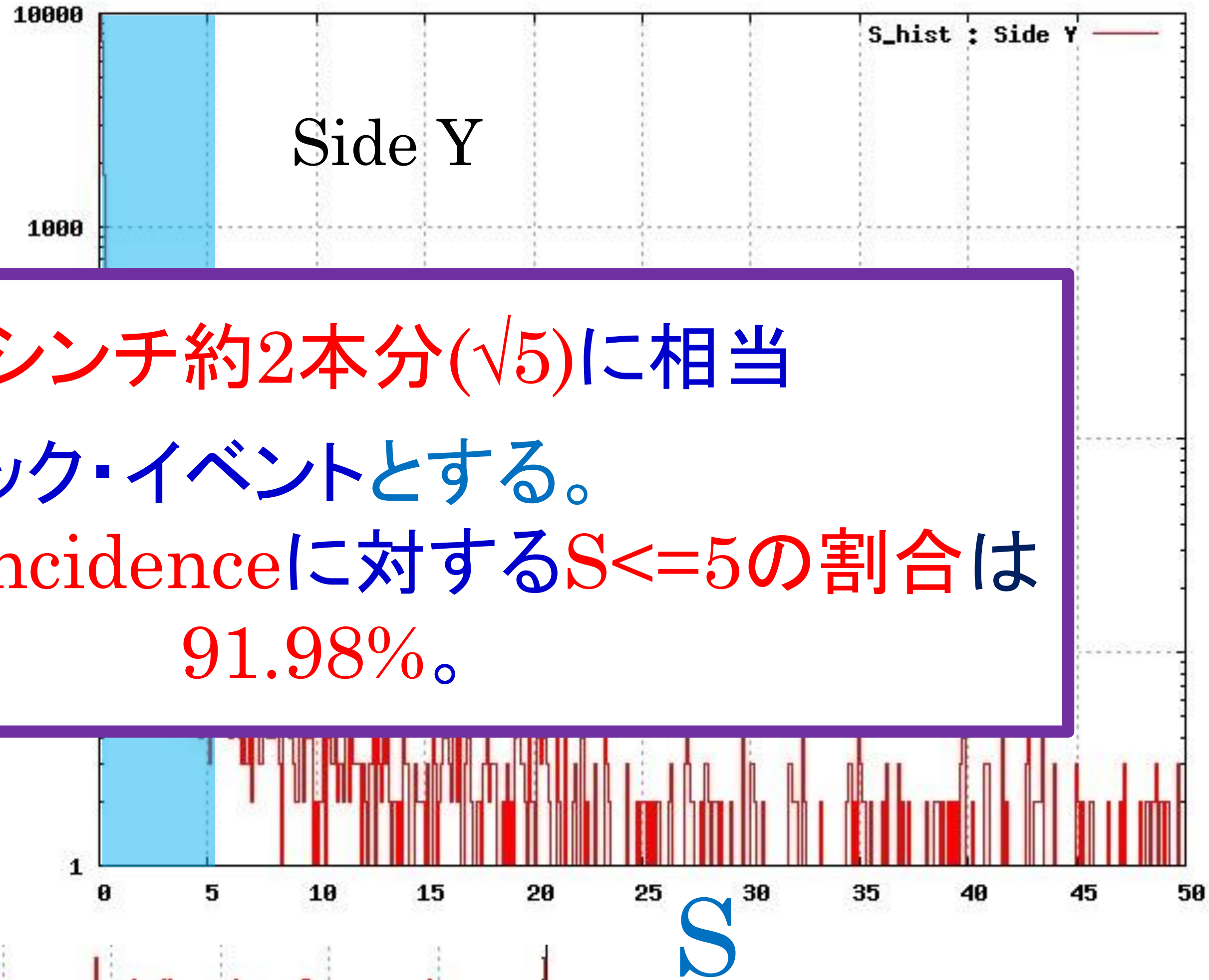


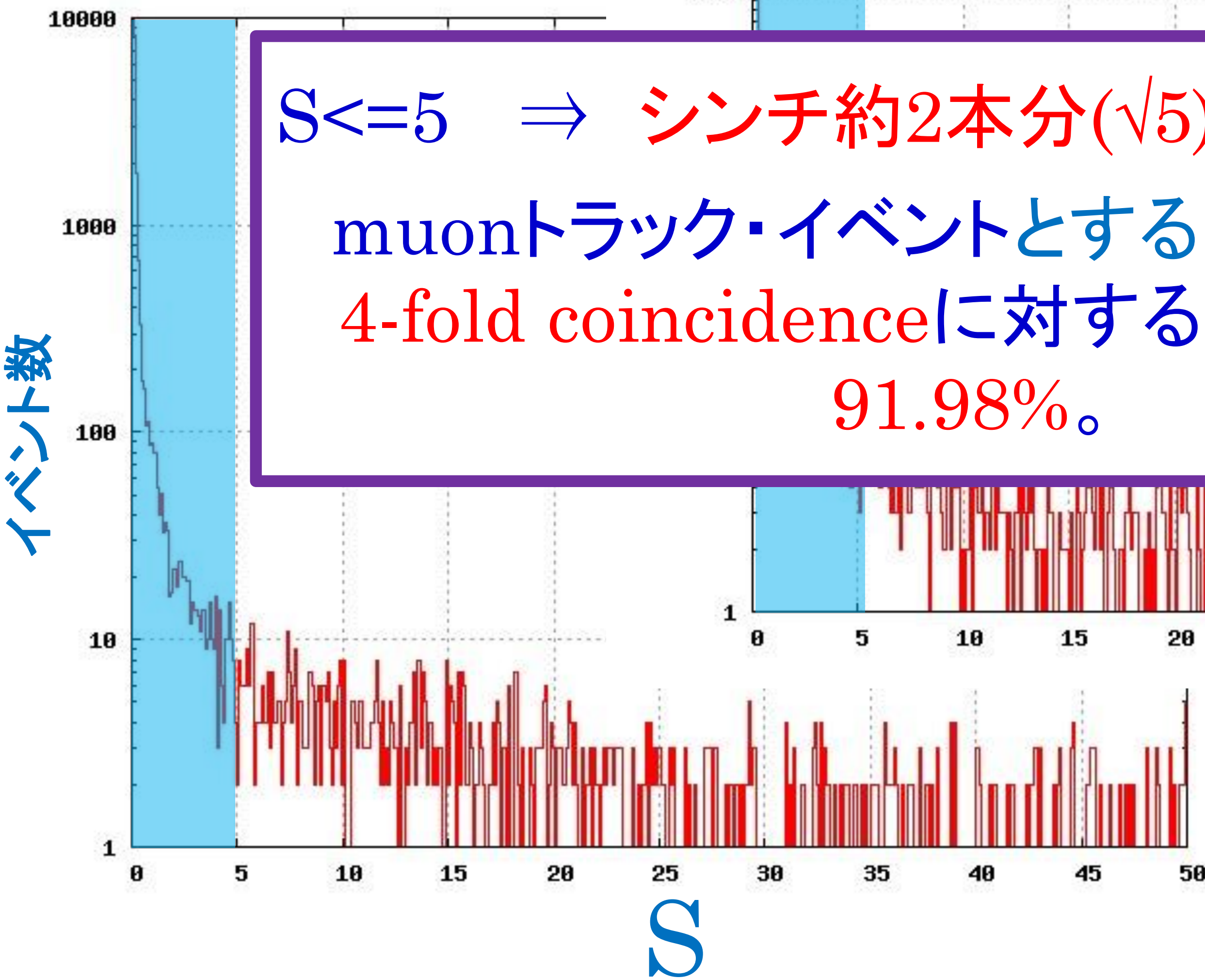


S<=5 ⇒ シンチ約2本分(√5)に相当

muonトラック・イベントとする。

4-fold coincidenceに対するS<=5の割合は

91.98%。

# 4 fold coin.によるmuon選択（4/4）

S<=5 のイベント例　⇒　muonトラック・イベント

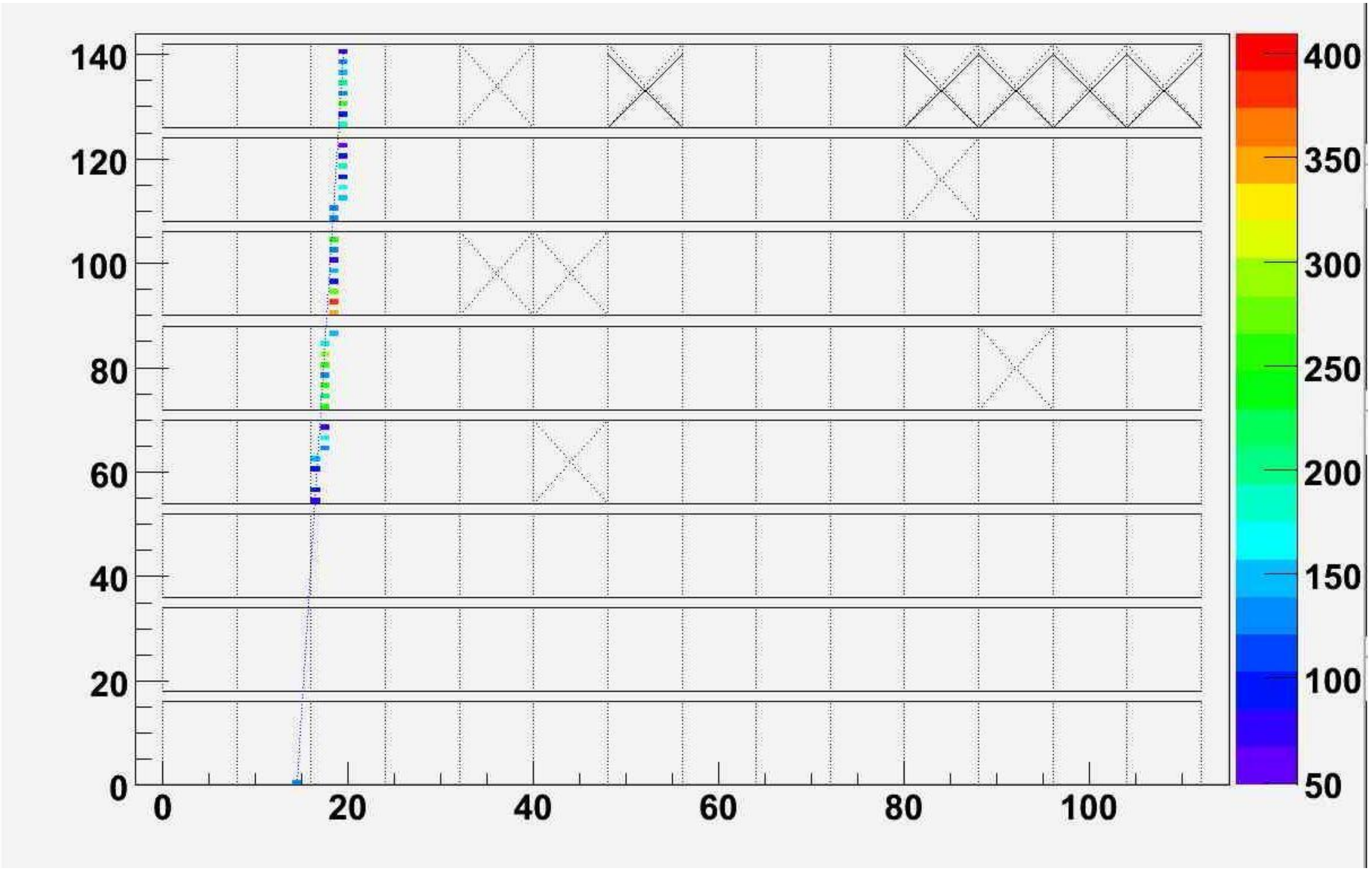


次にS<=5のイベントの中で・・・

中性子部分によるトラックと最上下4層（muon部分）のみで決定したトラックを比較する。

# 4 fold coin.による入射方向決定（1/2）

中性子部分のトラックを、最上下4層のヒット・パタンから求めたトラックと比較する。

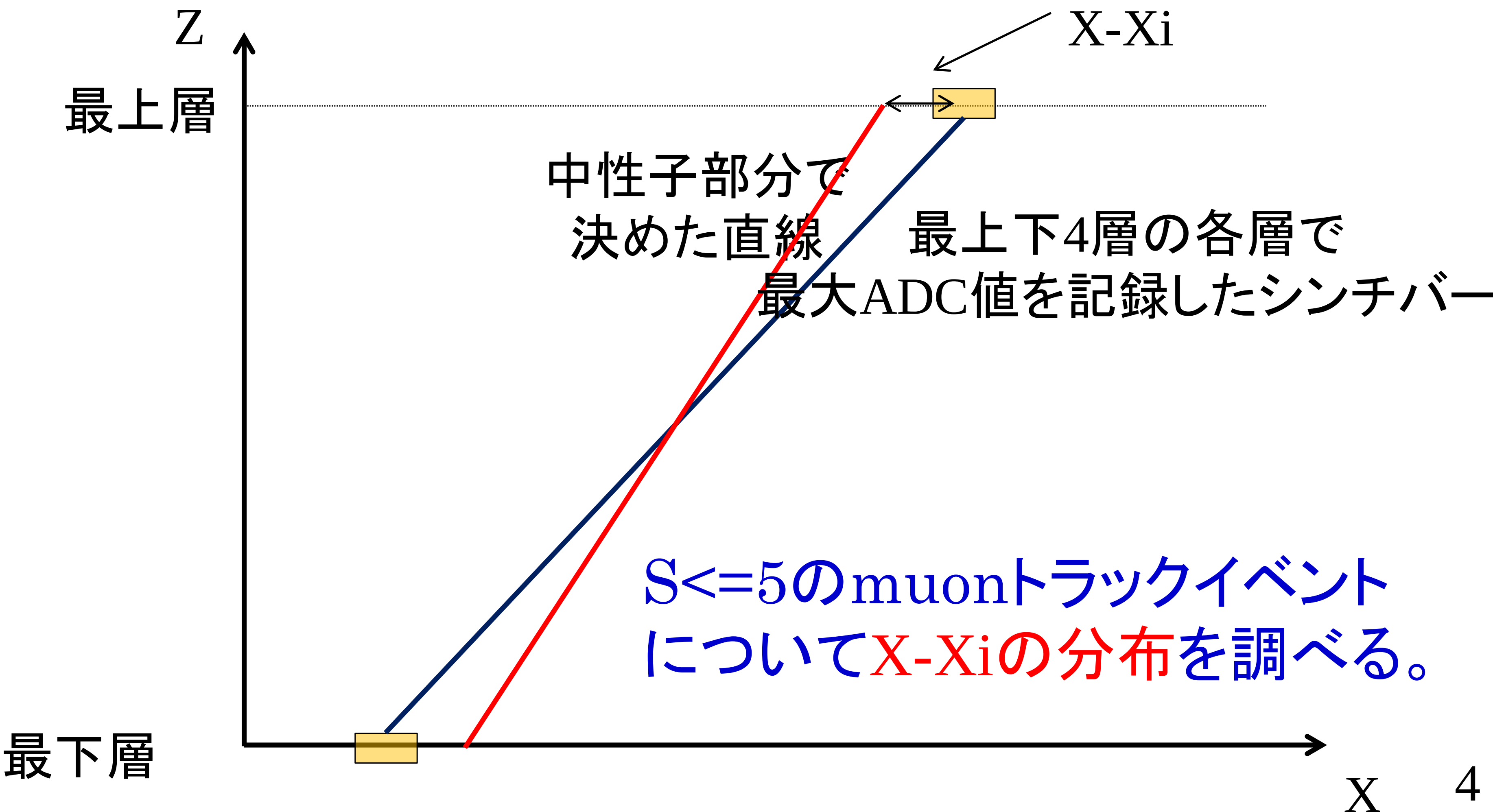


S<=5のmuonトラックイベントについてX-Xiの分布を調べる。

# 4 fold coin.による入射方向決定（2/2）

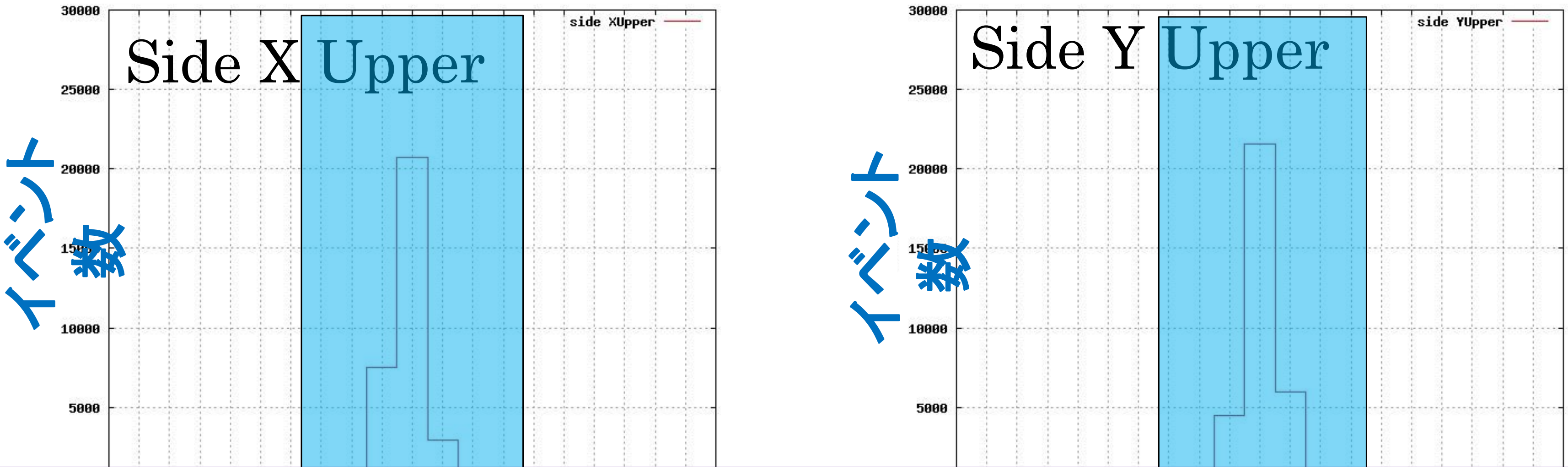


muonイベントに占める|X-Xi|<=3.5の割合は

94.84%

$\Delta\theta = \tan^{-1}(3.5\times2.5\mathrm{cm}/170\mathrm{cm}) \simeq \pm3°$

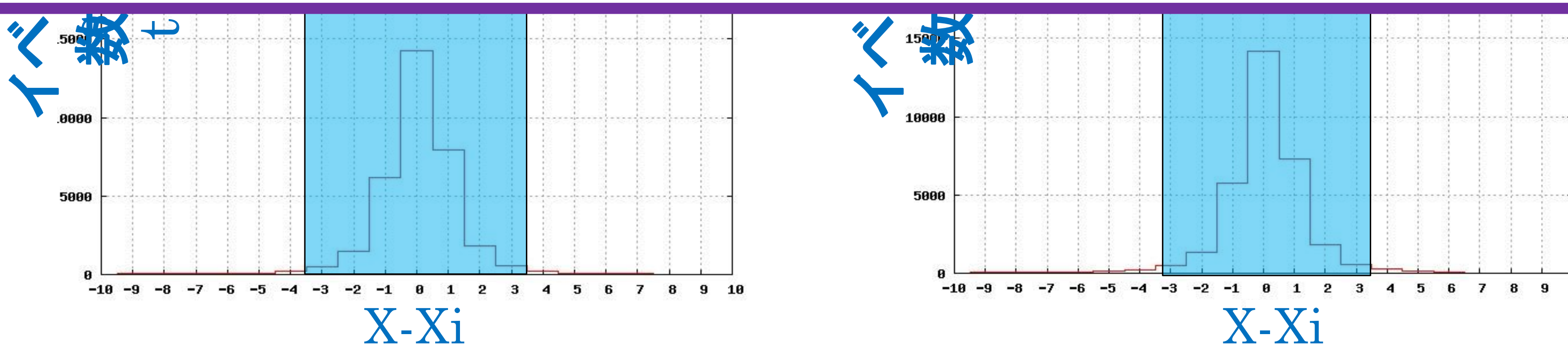

# 解析結果

| | イベント数 | 割合 I | 割合 II |
|---|---|---|---|
| **4-fold** | 40,000 | 100[%] | |
| **Muon event (S<=5)** | 36,790 | **91.98**[%] | 100[%] |
| **Track agreed (\|X-Xi\|<=3.5)** | 34,881 | 87.20[%] | **94.81**[%] |

# S>5のイベント例１

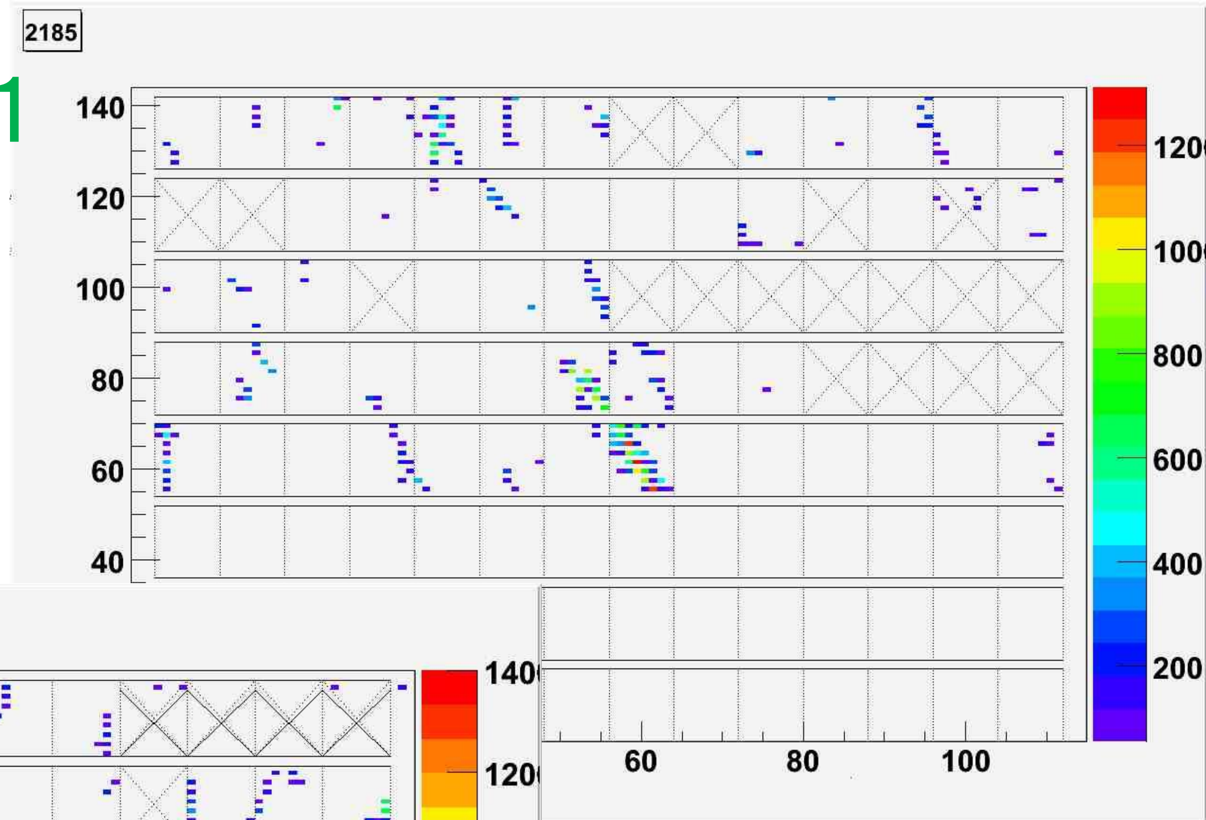


Side X

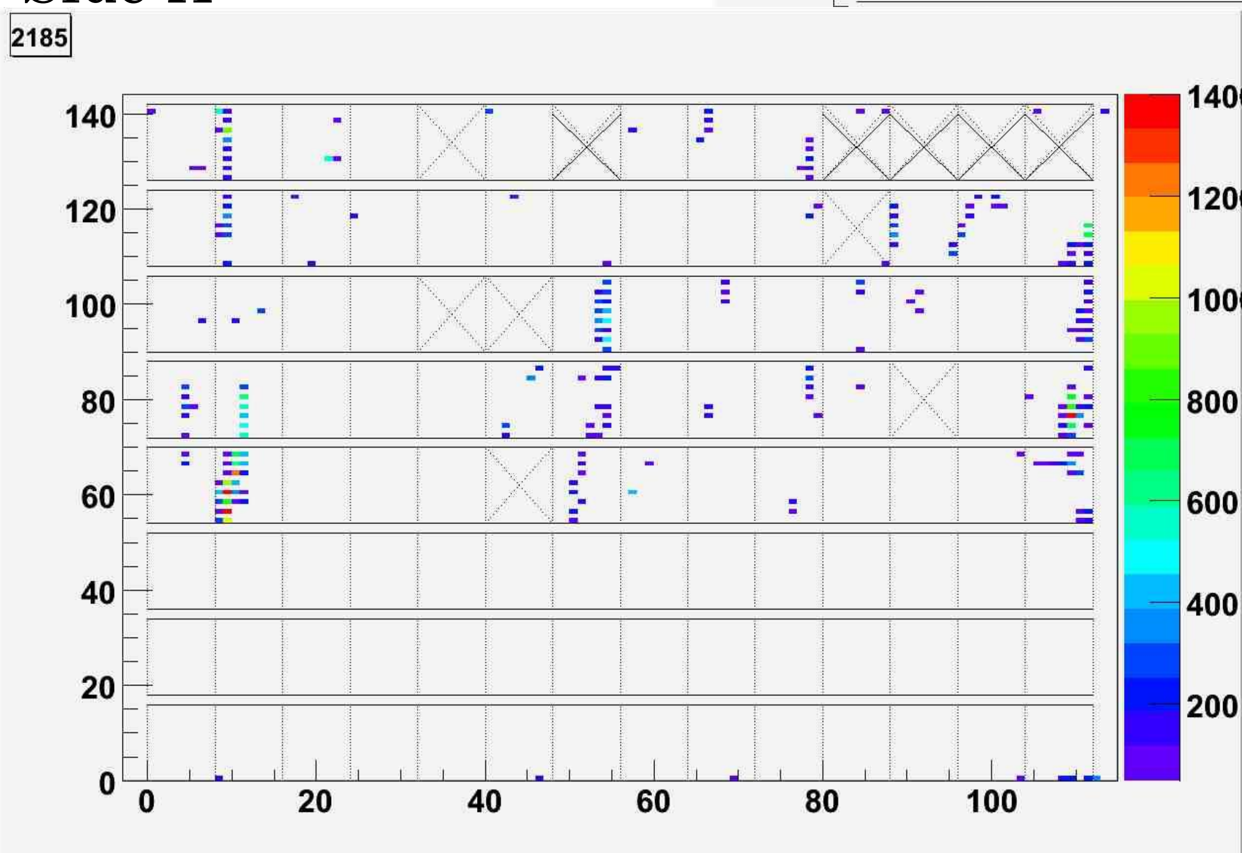


Side Y

# S>5のイベント例2

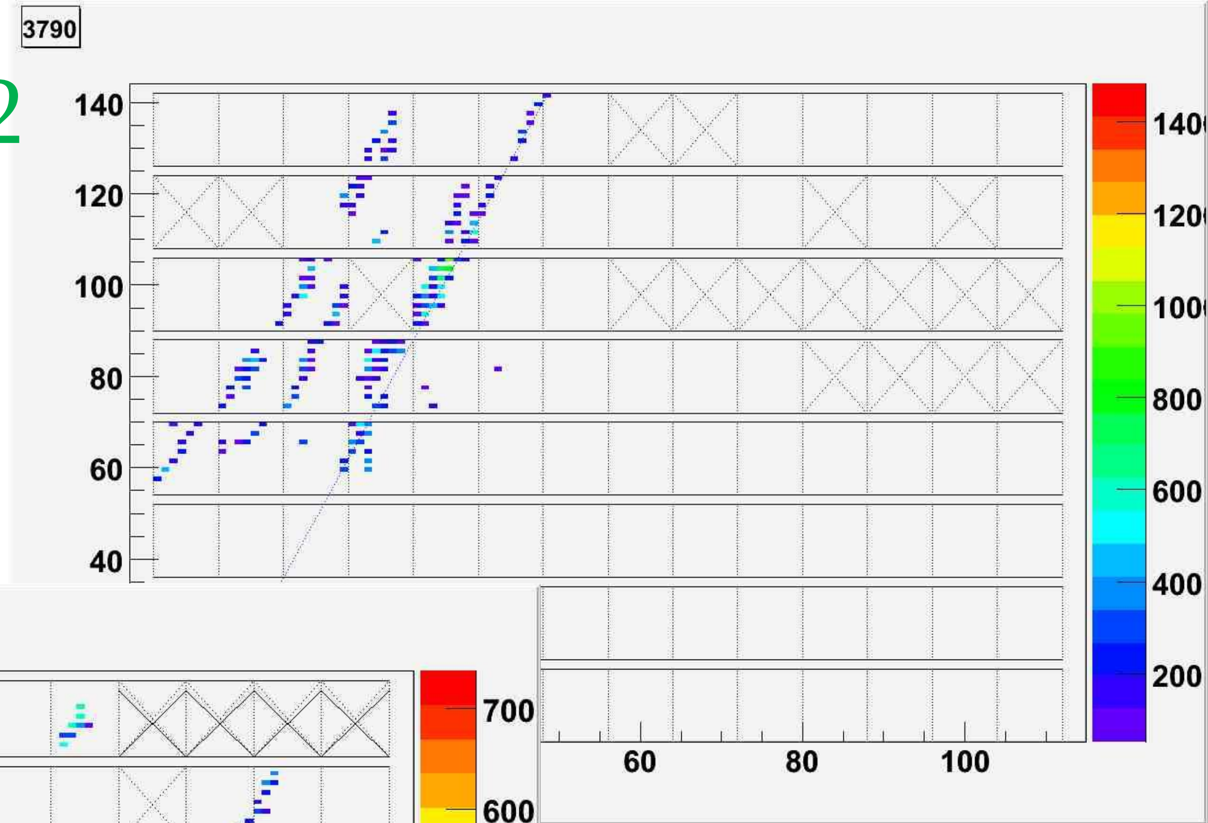


Side Y

Side X

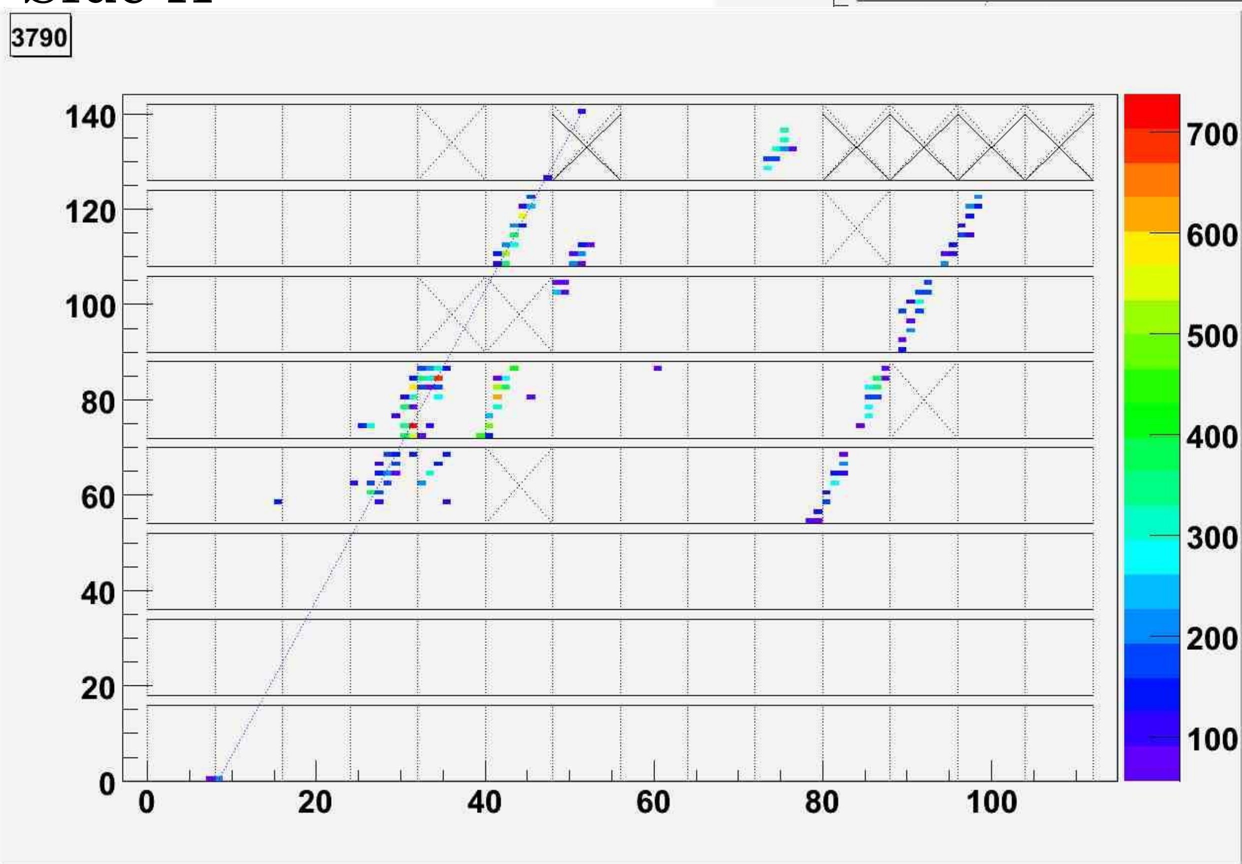

# 解析結果

| | イベント数 | 割合Ⅰ | 割合Ⅱ |
|---|---|---|---|
| **4-fold** | 40,000 | 100[%] | |
| **Muon event (S<=5)** | 36,790 | **91.98**[%] | 100[%] |
| **Track agreed (\|X-Xi\|<=3.5)** | 34,881 | 87.20[%] | **94.81**[%] |

| | イベント数 | 割合Ⅰ | 割合Ⅱ |
|---|---|---|---|
| **4-fold** | 40,000 | 100[%] | |
| **Muon event** | (+1,567)38,357 | **95.89**[%] | 100[%] |
| **Track agreed (\|X-Xi\|<=3.5)** | (+1,035)35,916 | 89.79[%] | **93.64**[%] |

# まとめ

- 最大ADC値を記録したchを選択することにより、4 fold coincidenceの約96%のイベントでmuonトラックが確認できた。
- muonトラックが確認できたイベントの約94%（4 fold coincidence全体の約90%）で、入射方向をmuon部分のみで精度よく決定できていた。
- muon入射方向の決定精度は±3°程度であった。

# 今後の課題

dead time（約20ms/イベント）の影響により、中性子部分も用いる今回の解析ではmuon rateや天頂角分布を評価できない。

⇒ 今回の結果をもとに、本観測と同様にmuon部分のみ（dead time約1ms/イベント）を用いた観測データの解析を行い、ミューオン計としての性能評価を行う

# Data of test run at INAOE